Oskar Johan Engberg

Impact of Lipid-Lipid Interactions on Lateral Segregation in Bilayers

Åbo Akademi University
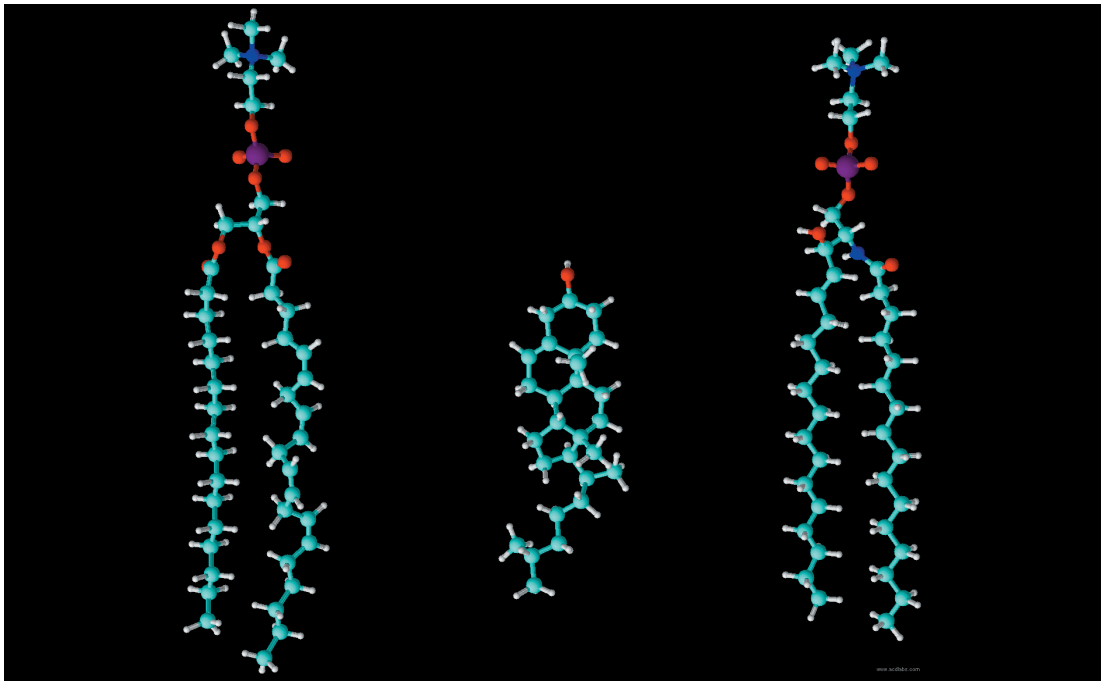
Oskar Johan Engberg

OSKAR ENGBERG was born on May 24, 1988 in Kyrkslätt, Finland. He graduated from Åbo Akademi University in January 2014 as a Master of Science in Biochemistry. This PhD thesis project in Biochemistry has taken place from February 2014 to May 2018 under the supervision of Professor J. Peter Slotte and Dr. Thomas Nyholm at the Faculty of Science and Engineering.

IMPACT OF LIPID-LIPID INTERACTIONS ON LATERAL SEGREGATION IN BILAYERS

Oskar Johan Engberg

Åbo Akademi University

Biochemistry, Faculty of Science and Engineering
Åbo Akademi University
Turku, Finland

2018

Supervised by:

Professor J. Peter Slotte

Biochemistry, Faculty of Science and Engineering
Åbo Akademi University
Turku, Finland

Dr. Thomas. K.M. Nyholm

Biochemistry, Faculty of Science and Engineering
Åbo Akademi University
Turku, Finland

Reviewed by:

Dr. Pentti Somerharju

Institute of Biomedicine/Biochemistry
Biomedicum, University of Helsinki
Helsinki, Finland

Professor Vesa Olkkonen

Minerva Foundation Institute for Medical Research
Biomedicum and University of Helsinki
Helsinki, Finland

Opponent:

Professor Daniel Huster

Faculty of Medicine, Institute of Medical Physics and Biophysics
Universität Leipzig
Leipzig, Germany

To my family

Table of Contents

LIST OF ORGINAL PUBLICATIONS

The thesis is based on the following original publications referred to by the Roman numerals I-III throughout the thesis. The original publications have been reprinted with the permission of the copyright holders.

I.   Engberg, O., H. Nurmi, T. K. M. Nyholm, and J. P. Slotte. **2015**. **Effects of cholesterol and saturated sphingolipids on acyl chain order in 1-palmitoyl-2-oleoyl-*sn*-glycero-3-phosphocholine bilayers-a comparative study with phase-selective fluorophores.** *Langmuir* 31: 4255-4263.

II.   Engberg, O., T. Yasuda, V. Hautala, N. Matsumori, T. K. M. Nyholm, M. Murata, and J. P. Slotte. **2016**. **Lipid Interactions and Organization in Complex Bilayer Membranes**. *Biophys. J.* 110: 1563-1573.

III.   Engberg, O., V. Hautala, T. Yasuda, H. Dehio, M. Murata, J. P. Slotte, and T. K. M. Nyholm. **2016**. **The Affinity of Cholesterol for Different Phospholipids Affects Lateral Segregation in Bilayers.** *Biophys. J.* 111: 546-556.

CONTRIBUTIONS OF THE AUTHORS

I.   The author designed experiments together with supervisors. Experiments were carried out by the author, helped by Mr. Henrik Nurmi under his supervision. Dr. Thomas. K. M. Nyholm performed partitioning experiments with the fluorescent probes. Professor Slotte synthesized the fluorescent probes. The author contributed to the manuscript writing together with Professor Slotte.

II. The author designed experiments together with supervisors, and Professor Michio Murata. The author performed the fluorescence experimental work together with Mr. Victor Hautala, under the authors supervision. Dr. Tomokazu Yasuda performed NMR experiments under the supervision of Professor Murata Osaka, Japan. Professor Slotte made the fluorescent and deuterated lipids. The author wrote the manuscript together with both supervisors and professor Murata.

III. The author designed experiments together with supervisors, and professor Murata. The author performed the fluorescence experimental work together with Mr. Hautala. Mrs. Henrike Delio performed some of the calorimetric and fluorescent experiments. Both Mrs. Delio and Mr. Hautala were supervised by the author. The author and Dr. Yasuda performed NMR experiments under the supervision of Professor Murata in Osaka, Japan. Professor Slotte prepared the fluorescent and deuterated lipids. The author write the manuscript together with both supervisors and Professor Murata.

ADDITIONAL PUBLICATIONS NOT INCLUDED IN THE THESIS

Lönnfors, M., O. Engberg, B. R. Peterson, and J. P. Slotte. **2012**. **Interaction of 3beta-amino-5-cholestene with phospholipids in binary and ternary bilayer membranes.** *Langmuir* 28: 648-655.

Sergelius, C., S. Yamaguchi, T. Yamamoto, O. Engberg, S. Katsumura, and J. P. Slotte. **2012**. **Cholesterol's interactions with serine phospholipids - A comparison of N-palmitoyl ceramide phosphoserine with dipalmitoyl phosphatidylserine.** *Biochim. Biophys. Acta* 1828: 785-791.

Gerhold, J. M., S. Cansiz-Arda, M. Lohmus, O. Engberg, A. Reyes, R. H. van, A. Sanz, I. J. Holt, H. M. Cooper, and J. N. Spelbrink. **2015**. **Human Mitochondrial DNA-Protein Complexes Attach to a Cholesterol-Rich Membrane Structure.** *Sci. Rep*. 5: 15292.

Slotte, J. P., T. Yasuda, O. Engberg, M. A. Al Sazzad, V. Hautala, T. K. M. Nyholm, and M. Murata. **2017**. **Bilayer Interactions among Unsaturated Phospholipids, Sterols, and Ceramide.** *Biophys. J* 112: 1673-1681.

ACKNOWLEDGEMENTS

Oskar Engberg
Åbo 9.4.2018

ABBREVIATIONS

18:1-DPH-PC	1-oleoyl-2-propionyl-1,3.5-hexatrienol-*sn*-glycero-3-phosphocholine
CTL	Cholestratrienol
DLPC	1,2-dilinoleoyl-*sn*-glycero-3-phosphocholine
DOPC	1,2-dioleoyl-*sn*-glycero-3-phosphocholine
DPH	1,6-diphenyl-1,3.5-hexatrienol
DPPC	1,2-dipalmitoyl-*sn*-glycero-3-phosphocholine
DSC	Differential scanning calorimetry
DSPC	1,2-distearoyl-*sn*-glycero-3-phosphocholine
FRET	Förster resonance energy transfer
GPL	Glycerophospholipid
GPMV	Giant plasma membrane vesicles
GUV	Giant unilamellar vesicles
$\mathbf{K_R}$	Relative partitioning coefficient
$\mathbf{K_x}$	Partitioning coefficient
Ld	Liquid-disordered
Lo	Liquid-ordered
LUV	Large unilamellar vesicle
$\mathbf{M_1}$	First spectral moment
MLV	Multilamellar vesicle
MβCD	Methyl-beta-cyclodextrin
NBD	N-(7-Nitrobenz-2-Oxa-1,3-Diazol-4-yl)
NMR	Nuclear magnetic resonance
O-tPA-PC	1-oleoyl-2-tPA-*sn*-3-glycero-phosphatidylcholine
PAPC	1-palmitoyl-2-arachidonoyl-*sn*-glycero-3-phosphocholine
PCer	Palmitoyl-ceramide
PDPC	1-palmitoyl-2-docosahexaenoyl-*sn*-glycero-3-phosphocholine
PE	Phosphatidylethanolamine
PL	Phospholipid
PLPC	1-palmitoyl-2-linoleoyl-*sn*-glycero-3-phosphocholine
POPC	1-palmitoyl-2-oleoyl-*sn*-glycero-3-phosphocholine
PS	Phosphatidylserine
PSM	N-palmitoyl-D-*erythro*-sphingosylphosphorylcholine
SSM	N-stearoyl-D-*erythro*-sphingosylphosphorylcholine
$\mathbf{T_m}$	Gel-to-liquid crystalline phase transition temperature
tPA	*trans*-parinaric acid
tPA-SM	N-tPA-sphingosylphosphorylcholine

ABSTRACT

The vast diversity of lipid species found in cells suggests that structural variation of lipids is essential for the normal function of the cell. One essential reason could be the formation of lateral heterogeneity in cell membranes, first associated with the polarized transport of membrane proteins in the intestinal epithelia. To learn more on the lipid-lipid interactions governing this lateral heterogeneity, different techniques have been utilized to study lipid interactions in both simple and more complex model membranes. Small structural nuances in the lipids can lead to very different lipid interactions. In the papers of this thesis, we have studied the connection between phospholipid (PL)-PL and cholesterol-PL interactions and how these interactions affect phase separation and likely also nanodomain formation in biological membranes.

In paper I, we have studied how sphingolipids with different head groups induced lateral segregation and altered acyl chain order in unsaturated fluid phosphatidylcholine (PC) bilayers. This was achieved by using different phase-selective probes. The size of the head group on the sphingolipid determined the miscibility of the sphingolipid. When temperature was raised so that the miscibility of the sphingolipids was higher, an increase in sphingolipid concentration increased acyl chain order in the fluid phase, as cholesterol did at all temperatures.

In paper II, deuterated PLs and fluorescent lipid-analog probes were utilized to understand cholesterol interactions in complex bilayers containing N-palmitoyl-sphingomyelin (PSM) and glycerophospholipids (GPLs) with different head groups. Cholesterol-induced ordering of PLs and the effect of cholesterol on ordered domain thermostability were examined. Cholesterol seemed to have more favorable interactions with PSM even in the presence of the other GPLs, while it did not favor any particular GPLs over the others, at least at the lipid compositions examined.

In paper III, we investigated the effects of unsaturation in PCs and the difference between saturated PC and SMs on lateral segregation. It was found that the number of double bonds in the unsaturated PL had larger impact on lateral segregation in the presence of cholesterol. This was related to the sterol affinity for unsaturated PL. In addition, the different sterol affinities of saturated di-palmitoyl-PC (DPPC) and PSM resulted in strongly promoted phase separation with PSM but only slight promotion with DPPC, especially in bilayers containing polyunsaturated PC. This was explained by the relative sterol affinity difference between saturated and unsaturated PLs. The experimental setup with sterol partitioning experiments and lateral segregation measurements with fluorescence spectroscopy could possibly be used to estimate in which cells and organelles nanodomains are most likely to form.

1.   INTRODUCTION

Lipids, in the form of triglycerides and fatty acids, have an important role in metabolic functions as immediate or stored energy for the cells. In addition, lipids are essential building blocks of life, and as cell signaling molecules. Lipid membranes isolate the interior of the cells from the more hostile and chaotic exterior environment. This isolation enables the cells to fine tune biochemical reactions. The membrane is also selective, enabling important small molecules like oxygen to enter freely while larger, charged molecules require protein-mediated transport. The fluid nature of membranes and non-covalent interactions between lipids enable proteins to insert in the membrane. Proteins found in the membrane regulate several important functions of life, *e.g.* photosynthesis, nutrient transport, and cell-cell communication (1). In addition, the membrane is a two-dimensional surface, helping cytosolic and exterior proteins to bind and interact with each other in a more regulated fashion than in the three-dimensional cytosol.

While only one lipid species is required to make a bilayer, even a single cell synthesizes thousands of different lipid species (2). The diversity of lipids have probably coincided with evolution of life. To enable a fluid bilayer in hot microenvironments, like close to undersea volcanoes, lipids have longer and saturated hydrocarbon chains (3). In contrast, in cold sea water, fish have evolved polyunsaturated PLs to enable fluid bilayers (4). Another way to regulate fluidity is methyl-branching of the acyl chains, which has similar fluidizing effect as unsaturation (5). While the cell membrane has several functions, different structural lipid variants are often used for the same function in different environments. These structural varieties of building blocks of life has enabled life in very diverse environments.

In eukaryotic organisms, there is a requirement to separate biochemical reactions to an even higher degree than in prokaryotes. This gave rise to membrane compartmentalization to several organelles and later to multicellular organisms (6). DNA analyses of mitochondria have indicated a prokaryotic origin, suggesting that eukaryotic cells engulfed a simpler prokaryotic organism for endosymbiosis and later as an organelle (7). These new functions of the cells gave rise to lipid molecules with new functions, such as membrane anchors for proteins and as receptors, ligands and second messengers (8). Glycolipids in the exterior leaflet enabled easier communication between cells in multicellular organisms. These new functions led to

an even larger variety of lipids. Viruses started to use the glycolipids as receptors, to infect cells, while the immune systems started to use lipoproteins to target pathogens (9). Evolution of eukaryotes led to the synthesis of sterols (10). Cholesterol, the major mammalian sterol, is distributed unevenly between different organelles. In early research, correlations were found between SM, and cholesterol content in different organelles (11). It also became clear that lipids could laterally segregate from each other both in the presence and absence of cholesterol (12, 13). In addition, it was found out that the interactions of cholesterol with PLs are of great importance to understand lateral segregation. In this thesis, we have studied the relationship between PL-cholesterol interactions and lateral segregation. By using several fluorescent probes and ^{2}H nuclear magnetic resonance (NMR), new information was found about the intrinsic properties of common biological GPLs and sphingolipids to laterally segregate and how they are affected by cholesterol.

2. REVIEW OF THE LITERATURE

2.1. Biological membranes

In the 19th century, it was discovered that plants had an osmotic barrier called plasma membrane (14). Later, through usage of a Langmuir monolayer, Gorter and Grendel proposed that biological membranes were bilayers. They also proposed that the bilayer consisted of amphiphilic molecules with the hydrophilic head group oriented to the aqueous phase on both sides of the membrane, and the hydrophobic tails oriented to the interior of the membrane (15). The invention of the electron microscope led to proposals by Danielli, Dawson, and Robertson that proteins adhere to the membrane, forming a protein layer on top of both sides of the bilayer (16). In 1972, Singer and Nicholson introduced "the fluid mosaic model" (17). In this model, the membrane is fluid and acts as a "solvent" for proteins that can diffuse laterally in the plane of the membrane. As shown in figure 1, the proteins can be embedded in the membrane as integral proteins, as peripheral proteins that bind to the membrane, only partially embedded in the membrane or attached to the membrane through a lipid molecule. Proteins can also function as transporters and channels for ions, sugars, metabolites and other molecules in the membranes, or membrane bound enzymes. In addition, proteins and lipids can be modified with carbohydrates, to glycol-lipids and -proteins. It was also discovered that lipids and proteins are asymmetrically distributed in the plasma membrane (18, 19).
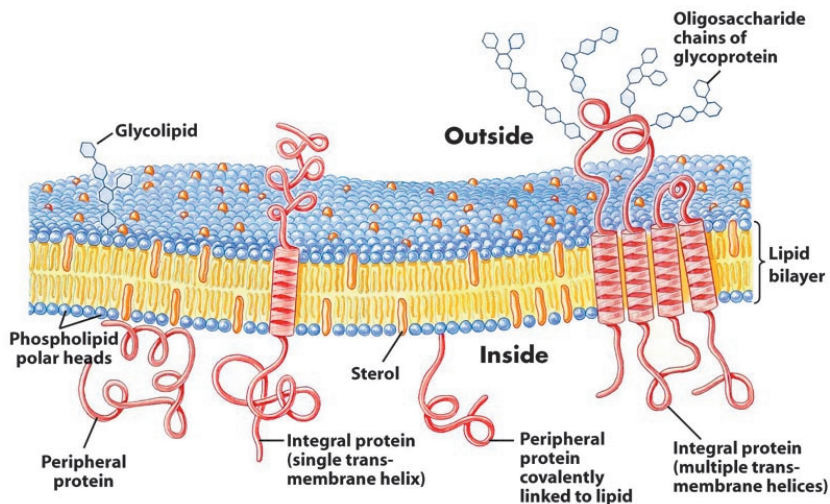
Figure 1. *The fluid-mosaic model. Shows a fluid lipid bilayer with several different kinds of proteins and oligosaccharides. Taken from (1).*

Later, Mouritsen and Bloom proposed in their "mattress model" that integral peptides and lipids are matched in their hydrophobic length, possibly leading to lateral heterogeneities (20). Simons and van Meer later refined the idea of lateral heterogeneities in the 1980s (21, 22). This led to the lipid raft hypothesis and numerous studies of the nanodomains or "rafts" in biological and model membranes (13, 23).

2.1.1. Lipid rafts in cells

The first indication of lipid rafts was observed in a study of lipid and protein sorting in epithelial cells (22). Those cells are polarized, meaning that they have an apical side oriented to the lumen of the intestine and a basolateral side that connects the rest of the cell to the body and circulation. In these cells, the membrane protein composition is different in the apical and basal membranes; some sorting mechanism must maintain this polarized membrane protein distribution (24). Polarized transport to the apical membrane was first shown with fluorescent (N-(7-Nitrobenz-2-Oxa-1,3-Diazol-4-yl) (NBD)-ceramide that was metabolized into NBD-glucosylceramide and transported asymmetrically to the apical plasma membrane (22). The lipid raft hypothesis proposed that sphingolipids and apical proteins associate with each other to form transport carriers that will be systematically delivered to the apical membrane (21). A method utilizing detergent-resistant membranes was one of the methods used to understand the lipid raft phenomenon. Addition of the detergent Triton X-100 to membranes led to an insoluble and soluble fraction that could be separated by ultracentrifugation (25). SMs and glycosphingolipids were enriched in the insoluble fraction while the other lipids were found in the soluble fraction (25). The enrichment of glycosylphosphatidyl- inositol-anchored proteins (GPI-AP) together with sphingolipids was the base lead to the proposed glycolipid sorting from trans-Golgi network (TGN) to the plasma membrane (26). In addition, cholesterol or SM depletion by genetic manipulations led to higher solubility of proteins originally associated with the detergent-resistant membrane fractions (27). It was also found that proteins localized to immune-isolated apical vesicles (caveolin or caveolin-associated proteins) were in the detergent-resistant membrane fraction (28). However, with time it became clear that a direct correlation between lipid rafts and detergent-resistant membranes could not be made (29). Because solubilization of membranes is dependent on temperature, and low temperatures were used in the Triton X-100 experiments, the observed insolubility does not prove lipid rafts at physiological temperatures. In addition, concerns were raised that some membrane solubilization experiments with Triton X-100 were not run to equilibrium, causing false interpretations (29).

Nevertheless, the study of detergent-resistant membranes lead to further research into lipid rafts (28, 30).

Lipid raft formation was also studied by manipulating of cholesterol level using cyclodextrin (a cyclic glucose oligosaccharide that binds sterols) (31), lipidomics and toxin binding to lipid raft proteins or lipids (28). It was discovered that the transport of the influenza protein hemagglutinin to the apical membrane was disrupted by depletion of the cellular cholesterol content by cyclodextrin (32). However, the use of cyclodextrin on cells poses problems due to possible disruption of the cytoskeleton, as well as PL and cholesterol distribution between internal membranes (33). Studies that used antibody and toxin binding to the ganglioside GM1 showed clustering of raft lipids (34, 35). In addition, caveolae, small invaginations of the plasma membrane were linked to the existence of lipid rafts (36). However, it was found that lipid raft markers segregate from non-lipid raft markers in a cholesterol-dependent manner even in caveolae-free membranes (37).

In T-cell activation, many proteins cluster in a non-random way to form a supramolecular structure called the immunological synapse that transmits signals into the interior of the cell (38). Crosslinking of GPI-APs led to the suggestion that lipid rafts were involved in the activation of the immunological synapse in the T-cell (39). Lipid analysis showed enrichment of sphingolipids, saturated PLs and cholesterol in the immunological synapse, suggesting that the lipid raft formation was cholesterol-dependent (40, 41).

2.1.2. Giant plasma membrane vesicles for studying lipid rafts

Cells are dynamic systems and the macroscopic phase separation observed in model membranes could not be directly observed in live cell membranes (42). A cell-like model membrane, the giant plasma membrane vesicles (GPMV), were prepared in the 1970s but were used to understand lipid raft formation only later (43, 44). GPMVs are produced by adding dithiothreitol (DTT) and paraformaldehyde (PFA) to cells that leads to blebbing of plasma membrane to produce large vesicles (44). The vesicles are devoid of the cytoskeleton and have only partial lipid asymmetry but have similar lipid profile as the plasma membrane and contain the proteins found in the plasma membrane (45). Interestingly, they phase separate when studied with the fluorescence microscope, although they do so only below the physiological temperatures (44). The membrane order as measured by C-laurdan, reports a very small difference in order

between the coexisting phases, in contrast to artificial giant unilamellar vesicles (GUVs) (46, 47). This macroscopic phase separation made it possible to test lipid raft affinity of membrane proteins (48). It was found that palmitoylated proteins and GPI-APs partition to the lipid-raft - phase while other proteins, especially the transmembrane proteins, partition to the non-lipid-raft - phase. Recently, it was proposed that the lipid raft affinity of proteins is based on the hydrophobic surface area and length of the hydrophobic transmembrane domains and palmitoylation of the protein (49, 50). However, GPMVs have their drawbacks. Addition of DTT removes protein palmitoylation (47), while PFA crosslinks lipids and proteins leading to phase separation up to 15 degrees higher than without crosslinking (51). The absence of the cytoskeleton in GPMVs helps studying lipid-lipid and lipid-protein interactions for lipid raft formation (44). However, the role of the cytoskeleton in the formation of lipid rafts could be important. The actin scaffold segregates the membranes into lateral compartments that limit lateral diffusion of both lipids and proteins (52). Actin could also affect phase separation in membranes. For example, if saturated PLs are coupled to actin, they will stabilize lipid raft-domains but prevent macroscopic phase separation (53, 54). It has been theorized that GPI-AP clustering in the outer leaflet in the plasma membrane could be orchestrated from the inner leaflet by nanoscopic contractible assemblies of actinomyosin termed asters (55).

2.1.3. Novel techniques and model organisms to study lipid rafts

Recent research has used new technologies to study nanodomains in cells (30). Using stimulated emission depletion (STED) microscopy with fluorescence correlation spectroscopy in live cells, the diffusion of an SM probe displayed transient immobilization in contrast to other PL probes (56). Other super-resolution microscopy techniques have further been used to understand heterogeneities in cell membranes (57). However, there are some limitations to the probes used in the STED study, which call into question the interpretation *i.e* the trapped diffusion indicates the presence of lipid rafts in the traditional sense (58). New mass spectrometry techniques have provided even more controversial results, suggesting that SMs form domains but cholesterol is evenly distributed in the plasma membranes (59, 60). It was also found that cyclodextrin-induced cholesterol depletion decreased SM-rich domains but cytoskeleton disruption totally eliminated them, highlighting the possible role of the cytoskeleton over cholesterol in lipid raft formation (59).

Different model organisms have also been used to study lipid raft phenomena. It was recently found that when yeast is stressed, macroscopic gel phases formed in the vacuole membrane (61). Even the bacterium *Borrelia burgdorferi*, can form lipid rafts by acquiring cholesterol and other lipid building blocks from mammalians cells (62). Altogether, while the results are often very difficult to interpret in biological membranes, evidence suggests that membrane heterogeneities and nanodomains probably exist in biological membranes. In addition to lipid raft studies in cells and GPMVs, lateral segregation has been investigated in model membranes (30). In my thesis, model membrane systems have been used throughout to understand the role of lipid-lipid interactions in lateral segregation.

2.2. Lipid structures

Lipids are amphiphilic molecules with vastly diverse structural features. In cell membranes, there are more than a thousand different lipid species (63), even if only one is required to make a lipid bilayer. The major lipid classes in mammalian membranes are glycerophospholipids, sphingolipids and sterols. Examples of all the groups are shown in figure 2. Cells also contain *e.g.* triglycerides, diacylglycerides, and fatty acids. Triglycerides functions as storage of energy, diacylglycerol has an important role in cell signaling, and fatty acids acts mainly as metabolites (1).

The head group, while varying in size, is polar and oriented towards the aqueous phase. The head group is attached with an ester-linkage to either a glycerol moiety in the GPLs or a long-chain base as in the sphingolipids. GPLs have two ester linked acyl chains or ether linked alkyl chains. Sphingolipids have a long-chain base and a N-linked acyl chain. These acyl chains can either be saturated chains or contain 1-6 *cis*-double bonds, and the chain length is often between 16-24 carbons (64, 65). In some organism acyl chains can be methyl-branched (66). Sterols are also a lipid class found in eukaryotic cells (67). The distribution of the different lipids in the cell is shown schematically in figure 3.
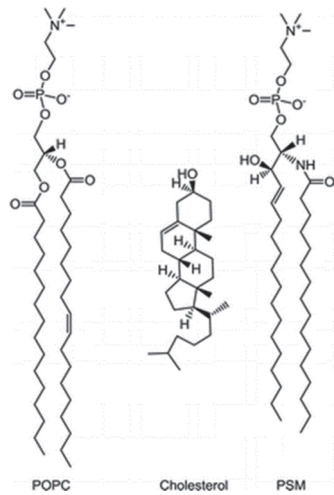
Figure 2. *Chemical structures of lipids from different lipid classes. From left to right, structure of 1-Palmitoyl-2-oleoyl-sn-glycero-3-phosphocholine (a GPL), cholesterol (a sterol), and N-palmitoyl-D-erythro-sphingosyl-phosphoryl-choline (a sphingolipid).*
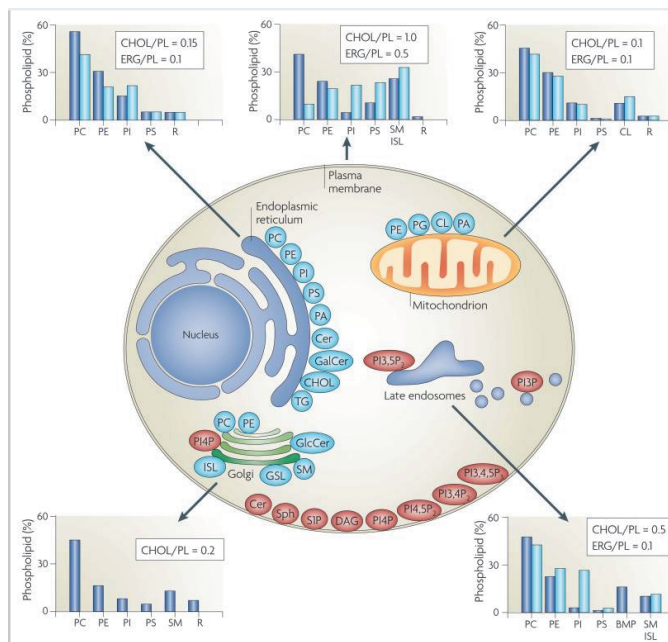
Figure 3. *Distribution in an eukaryotic cell of lipids according to head group and backbone structure (63). Cer = ceramide, CHOL = cholesterol, DAG = diacylglycerol, ERG = ergosterol, GlcCer = glucosyl-ceramide, GSL = glycosphingolipids, ISL = yeast inositol sphingolipid, R = remaining lipids, S1P = sphingosine-1-phosphate, Sph = sphingomyelin, TG = triacylglycerol.*

2.2.1. Glycerophospholipids

GPLs are the most abundant lipid class in mammalian membranes (63). GPLs share a common backbone of an L-glycerophosphate. The glycerol backbone in GPLs has three hydroxyl groups, which are denoted as *sn-1*, *sn*-2 and *sn-3*. The polar headgroup is coupled to the *sn-3* position. Two acyl or alkyl chains are coupled to the *sn-1* and *sn-2* positions through an ester or an ether linkage (68). The *sn*-1 coupled acyl chain is often saturated while the *sn*-2 coupled acyl chain is often mono- or polyunsaturated; such PLs are commonly referred to as asymmetric or hybrid PLs (69). When the acyl chains are identical in the *sn*-1 and *sn*-2 positions, the PLs are commonly referred to as symmetrical PLs.

The GPLs in biological membranes are classified by their head group. The most abundant ones are PC, phosphatidylserine (PS), phosphatidyl-ethanolamine (PE), phosphatidylglycerol (PG), phosphatic acid (PA), phosphatidylinositol (PI), and cardiolipins (CL). Different organelles have different compositions of the GPLs, some GPLs like CL are only found in the mitochondria (Fig. 3 and (63)). In the plasma membrane and the Golgi apparatus the GPLs are also asymmetrically distributed with PE and PS mainly in the inner leaflet (18). This asymmetry is strictly regulated by energy-dependent translocases that translocate aminophospholipids from the outer leaflet to the inner leaflet (70). The different GPL classes may have different charge, with PC and PE being zwitter-ionic while PI, PS, PA, PG, and CL are negatively charged. The charge is of great biological importance because many proteins have cationic surfaces that can bind the negatively charged PLs (71). In the case of PI, the number of phosphate groups attached to the head group can be modified in vivo and this has great importance for cell signaling and vesicle transport in the cell (72).

2.2.2. Sphingolipids

Sphingolipids contain an amino alcohol long-chain base. The most abundant long chain base is ((2S,3R,4E)-2-amino-4-ocatdecane-1,3-diol), also called sphingosine, which has a *trans* double bond between C4 and C5. Another less abundant long chain base is ((2S,3R)-2-amino-1,3-ocatadecanediol), also called sphinganine, which lacks the *trans* double bond (73). While there can be further modifications of this long-chain base, sphingolipids are classified mainly by their head group structure. The SMs have a PC head group, ceramides have one hydroxyl group and neutral glycolipids have one or several sugar moieties attached to the long-chain base. The most complex sphingolipids are the gangliosides, which contain one or more sialic acid moieties linked to a sugar head group. These sphingolipids contain a saturated acyl chain and

if they contain double bonds these are often located further down in the acyl chain such as in 24:1$^{\Delta 15}$-SM (74). Many sphingolipids have longer N-acyl chains than the long-chain base (74). This can lead to chains extending into the other leaflet, called interdigitation, and observed in both symmetric (75) and asymmetric bilayers (76, 77). The long-chain base is also positioned so that the effective chain length is approximately two methylene shorter than the N-acyl chain (78, 79).

Ceramide is both a precursor for other sphingolipids and a metabolically active biomolecule (80). Because of the small hydroxyl head group ceramides are very hydrophobic and pack very tightly (81). Ceramide is normally found in low concentrations in the cellular membranes but its concentration can be increased locally by sphingomyelinase that can be activated though several factors, like viral infections, heat, radiation, and cell signaling cascades (82, 83).

SMs are mostly found in the outer leaflet of the plasma membrane where they, depending on animal species, can represent up to 50 mol% of total PLs (84). It has been reported that SMs exist in the nuclear envelope membrane (85) and chromatin (86) where they could participate in cell signaling (87). SMs are also found in the mitochondria and could be used for ceramide generation for induction of apoptosis (88, 89). SMs are known for their favorable interactions with cholesterol (90) and their propensity to contribute to lipid raft domains (23). The unique structure of sphingolipids compared to GPLs enables sphingolipids to act both as a hydrogen bond donors and acceptors, while PC can only act as a hydrogen bond acceptor (91).

2.2.3. Sterols

Sterols are important lipids in eukaryotic cells. Sterol structure consists of a tetracyclic hydrocarbon ring, a 3β-hydroxyl group and an aliphatic side chain (92). The sterol rings are all-*trans* and rigid while the side chain is more flexible (92). In mammalian cells, cholesterol (structure shown in figure 2) is the predominant sterol. The 3β-hydroxyl group is oriented towards the aqueous phase while the side chain is oriented to the bilayer interior. The sterol have a slight tilt vs the bilayer normal, **,** *e.g.* α_0 = 16° reported for cholesterol in DMPC bilayers (93). Because of the small polar group, cholesterol cannot form bilayers on its own (94). However, if a synthetic cholesterol molecule is synthesized with a PC head group it can form bilayers (95).

2.2.3.1. Membrane properties of cholesterol

Cholesterol is a modulator of membrane properties (92). Cholesterol has a condensing effect on acyl chains, *i.e* it reduces the total area of lipids to less than the sum of the area of the individual components as shown for monolayers (96). This has also been demonstrated in bilayers by ^{2}H NMR (97). Even small change in the rings or the isooctyl side chain of cholesterol markedly weakens the condensation effect (98, 99). Interestingly, the side chain accounts for 40-60 % of the condensation effect (100, 101). Cholesterol orders the hydrocarbon chains of fluid PLs, resulting in more *trans*-isomers in the hydrocarbon chains and thereby leading to more extended acyl chains (102).

Because cholesterol is very important for lipid raft formation (23), the association of cholesterol with different PLs has been investigated (90, 103). The all-*trans*-configuration of the cholesterol leads to favorable interactions of cholesterol's ring system with saturated PLs (92). Cholesterol can more easily form van der Waals interactions with saturated PLs than with unsaturated PLs. This can be observed in sterol partitioning experiments between cyclodextrin and monolayers (91) or bilayers (103). For example spin-labeled cholesterol (3β-doxyl-5α-cholestane), reported only half the affinity for 1-palmiotyl-2-docosahexaenoic-PC (PDPC) bilayers compared to 1-palmitoyl-2-oleoyl-PC (POPC) bilayers. This is likely due to the 6 double bonds in PDPC vs one in POPC (104). Sterols affinities for di-oleoyl-PC (DOPC) was similar to PDPC, even if DOPC has only 2 double bonds. This probably reflects the much thinner bilayer created by two unsaturated acyl chains compared to one polyunsaturated acyl chain (up to 6 double bonds). Preference of cholesterol for saturated PLs over unsaturated PLs has also been shown with differential scanning calorimetry (DSC) (105) and isothermal titration calorimetry (ITC) (106). Polyunsaturated acyl chains are especially abundant in PE lipids (107).

The association of cholesterol with different PLs probably has an effect on cholesterol's solubility in bilayers. Studies with different GPLs showed that the cholesterol solubility was different between PC (66 mol%) and PE (51%) bilayers (108). The hypothesis derived from the cholesterol solubility experiments in different bilayers, *i.e* 'the umbrella hypothesis', proposes that because the smaller head group of PE cannot shield cholesterol as efficiently from water as the larger head group of PC (94). Alternatively, the super lattice model proposes that other factors contribute, *e.g.* maximization of head group rotational entropy, minimization of steric strain, *etc* (109, 110). Increasing the amount of double bonds in hybrid PLs had a stronger effect

on the solubility of cholesterol in PE than in PC bilayers (111). Cholesterol solubility is even lower in both symmetric di-unsaturated PCs and PEs bilayers (112).

There are also differences in sterol affinity between different saturated PLs. Cholesterol efflux to methyl-beta-cyclodextrin (MβCD) is slower from SM vs acyl chain-matched PC monolayers (113, 114). In addition, cholesterol is less exposed to cholesterol oxidase in SM than PC monolayers (115) or bilayers (116). Later, it was found that the affinity of the cholesterol analog cholestratrienol (CTL) for MβCD vs bilayer correlated well with acyl chain order of the PLs in the bilayers (117). SM has a higher acyl chain order than saturated PC at the same temperature (90, 118), even, when the acyl chain order was matched the sterol preferred SM (90). A higher acyl chain order of SMs is not the only reason for the high affinity of sterol for SM, but other factors must contribute. One obvious difference between SM and PC is that the SM backbone has both hydrogen bond acceptor and donor groups compared to PC, which only has acceptor groups (119). It was suggested that SM and cholesterol could form intermolecular hydrogen bonds (120). However, it now seems more likely that intra- and intermolecular hydrogen bonds between SMs facilitate the interaction with cholesterol (119). Other differences between PCs and SMs could be a different head group tilt (121), hydration (122), cholesterol depth (123), and possible interdigitation of the acyl chains (76).

In partitioning studies, the sterol affinity was always highest for SM and lowest for PE. Whether sterol has higher affinity for unsaturated PC vs PS varies between studies (91, 103, 105, 124). If the differences between sterol affinity for GPLs are because of the chosen method or the membranes chosen is not clear. The reduction of the head group size of PSM to palmitoyl-ceramide-PE or of DPPC to dipalmitoyl-PE (DPPE) led to a lower sterol affinity, in agreement with the umbrella hypothesis (125). One factor possibly contributing to differences between the studies is the choice of sterol, as small changes in sterol structure can lead to dramatically different effects (99, 126, 127). We have chosen CTL for the papers included in this thesis, because its better usability vs radiolabeled cholesterol and its similar properties as cholesterol (128).

2.3. The hydrophobic effect
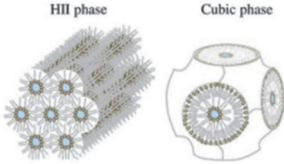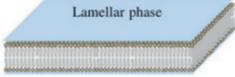
The hydrophobic effect causes the lipids to form aggregates in water. The monomeric lipid molecules disrupt the tight hydrogen bond network between water molecules. In addition, the lipid molecules order the water molecules, decreasing the entropy of

the system, which is thermodynamically unfavorable. When lipids segregate into a different phase, the entropy is increased and more of the water molecules maintain their hydrogen bond network.

2.3.1. Different lipid aggregates

The lipid aggregates that form in water depend on many factors, *e.g.* temperature, pH and ions, but most importantly is the shape of the lipid molecules (129). The packing parameter (PP) can be calculated to predict which aggregate is formed for differently shaped lipids, as described in equation 1 and shown in figure 4.

$$PP = \frac{v}{al_c}$$ (Eq 1)

Lipids	Shape	Parameter	Phase structure
PE, ceramide, cardiolipin		> 1	HII phase / Cubic phase
PC, PS, SM,		~1	Lamellar phase
Lysolipids, detergents		<1	HI phase

Figure 4. *How the geometrical shape and packing parameter describe which type of lipid aggregate the lipids form. Structure of the phases are modified from (129).*

Where v stands for the hydrophobic volume, a for the cross sectional area of head group and l_c stands for acyl chain length. Lipids with cylindrical shapes, *e.g.* SM and PC, have a PP of approximately 1, and thus form bilayers. Some lipids form non-lamellar aggregates. These lipids are cone-shaped, and form different lipid aggregates depending on if they are cones or inverted cones. Inverted cone shaped lipids have large head groups compared to their acyl chains, *e.g.* lysophospholipids and gangliosides. These have a packing parameter of less than one. They form micellar structures or hexagonal phase I, where the hexagonal tubular structures have the head group

13

oriented towards the outside and the lipid tails oriented towards the inside, as shown in figure 4. Cone-shaped lipids like PE, CL and ceramide have a packing parameter higher than one. These lipids are prone to form inverted micellar structures or the hexagonal II phase. Hexagonal II phase also forms tubular structures, where the head groups orient to form an inner water-filled cavity and the lipid tails point in the opposite direction, as in inverted micelles (130). If cone-shaped lipids are found in lower concentrations in a mixture of cylindrical lipids they induce negative or positive membrane curvature, which can *e.g* affect enzyme function and lipid fusion (129, 131).

2.3.2. *Lamellar phases*

Some lipids can exist in many different kinds of lamellar phases. Many factors regulate transition between the different phases, such as temperature, pressure, hydration, and pH. The factor that has been studied the most is temperature. Phase transitions can be observed in thermograms of DPPC (Fig. 5). DSC heats up a sample cell and a solvent reference cell and detects the energy required to increase the temperature (132). With lipid bilayers that undergo a phase transition, extra energy is required for the phase transition compared to the reference cell. In this way, the phase transitions can be detected by DSC (132). Different phases affect the properties of the lipids, *e.g.* hydration, rotational mobility, lateral diffusion, flip-flop and *trans-gauche* isomerization of the hydrocarbon chains (133).

At low temperatures the lipids are in a crystalline phase (L_c) where all lipid acyl chains are in the all-*trans* configuration. In this phase state, lipid bilayers are so tightly packed that they are not separated by a water layer and there is very low rotational mobility of the lipids. As the temperature increases, a so called subtransition (T_s) is observed. This occurs when the crystalline phase is converted into a gel phase, also called the solid-ordered phase (So). In the gel phase, the bilayers are separated by water and slow rotational motion occurs about their long axis. Characteristics for the gel phase is slow lipid diffusion, and that most acyl chains are in the all *trans*-configuration. Lipids are often also tilted in respect to the bilayer normal. As further increased temperatures, the gel phase is transformed to a ripple phase (pre-transition [T_P]), consisting of partially melted lipids. In the ripple phase, the lipids are much more free to rotate even although hydration does not change (133).

At higher temperatures yet, the lipids undergo a transition to the liquid crystalline phase ($L_{\alpha'}$), also called liquid-disordered phase (Ld). Upon this transition, the lipid

hydrocarbons increase their cross sectional area and reduce their effective chain length. This results in a thinner and more fluid bilayer. In the Ld phase lateral diffusion is high, and more *gauche* orientations of the acyl chains are observed. An increase in hydration is also observed, probably because polar groups such as the carbonyl group are more exposed to the aqueous environment as compared to the gel phase. The gel-to-liquid crystalline phase transition temperature is (T_m), indicates the mid-point in transition. In the case of DPPC, this transition occurs over a very narrow temperature range, showing cooperative melting of the lipids (133).
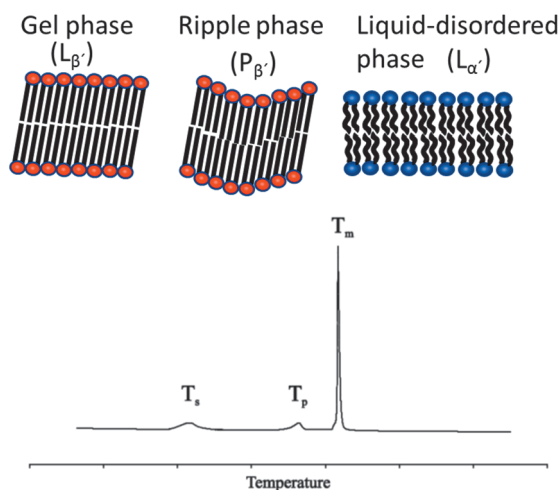
Figure 5. *Phase transitions in a DSC thermogram of DPPC bilayers. Schematic pictures of different phases over the DSC thermogram. T_s = sub-transition and T_p = pre-transition, T_m = mid-point in transition.*

2.3.3. Correlation of lipid structure with phase behavior

The molecular shape of lipids determines which type of aggregates most likely forms. The structure of the lipids also affects the phase behavior and properties. There is a correlation between chain length in di-saturated PCs and T_m. T_m increases with acyl chain length, although the trend is not linear (134). For SMs, the T_m also increases with acyl chain length, but the asymmetric nature of SM changes the slope of T_m increase (135). The long-chain base length is nearly constant; it has a greater effect on T_m than the N-acyl chain length, at least in ceramides (136). The consequences of chain asymmetry in di-saturated and hybrid PC and PE have been thoroughly reviewed in (137). The size of the head group also has a clear effect on T_m. A 16-carbon PC and SM

have a T_m of ~41 °C, while T_m of glycosphingolipids are ~85°C (138) and T_m of ceramides are ~90 °C (139). Systematically decreasing the size of the head group, by taking away methyl groups in a PC towards a PE head group, exemplifies the increase in T_m (125). Decreasing head group size leads to tighter packing and increased ability for the acyl chains to form interlipid van der Waals forces, but can also lead to curvature stress and formation of non-lamellar phases (129).

Biological membranes contain mainly PLs, with a saturated *sn-1* acyl chain and one mono- or polyunsaturated *sn-2* chain (65). DSC studies have shown that the inclusion of one double bond dramatically decreases the T_m for both symmetrical and hybrid PCs (140, 141). In addition, the position of the double bond has a clear effect on T_m for PCs. A double bond between the 9 and 10th carbon has the strongest reduction in T_m (140, 142). Addition of a second double bond further decreases T_m (143). However, increasing number of double bonds (up to six) does not decrease the T_m further and can even increase T_m (143). The longer carbon chains of biological polyunsaturated PLs (20-22 vs 16-18 carbons) compared to common monounsaturated PLs can partially explain the effect on T_m. Still, the several double bonds in the polyunsaturated PLs leads to quicker *C-C* isomerization, because of the =CH–CH2– CH= unit. This results in that polyunsaturated PLs can be more flexible with more torsional states than a monounsaturated PL (144-146). Therefore, the polyunsaturated PLs can probably mitigate the T_m decrease expected from an increased number of double bonds. Methyl-branches of the acyl chains, *e.g.* in diphytanoyl-PLs also leads to similar decreases of T_m (5). Unsaturated PLs may have very broad and less co-operative transitions (143). Glycolipids display complex phase transitions, but the highest-temperature transition is thought to be the gel-Ld phase transition (138).

2.4. Lateral segregation and phase diagrams

If two or more lipids are immiscible, they can segregate laterally in a bilayer. This is thought to be the reason why lipid rafts exist in cells, although the role of proteins and the cytoskeleton is unclear (30). Mixing of two lipids can be ideal or, as in most cases, non-ideal. Non-ideal mixing occurs *e.g.* when there is hydrophobic mismatch between PLs, *e.g.* between a shorter (di-lauroyl-PC) and a longer PC (di-stearoyl-PC; DSPC) (147). However, two or four carbons in chain length mismatch do not create lateral segregation although cooperativity of chain melting decreases (148). Inclusions of unsaturated PLs like DOPC or methyl-branched lipids like diphytanoyl-PC with saturated PCs or SMs also induce lateral segregation (148, 149). Both unsaturated and

methyl-branched PCs are low T_m lipids, which often induce lateral segregation when mixed with high T_m lipids. Phase separation can also occur for PLs with different head groups (12). In addition, cholesterol can induce lateral segregation (91). To understand these complex phenomena, biophysicists have constructed phase diagrams for model membranes by correlating the lipid composition with detecting phase transitions (150).

2.4.1. Phase diagrams for binary bilayers consisting of low- and high-T_m lipids

Lateral segregation between two lipids can be described with a binary phase diagram. A binary phase diagram has temperature on the y-axis and the fraction of high-T_m lipid on the x-axis as shown in figure 6. The lines indicate a phase boundary. The simplest binary phase diagrams have a liquid phase (Ld) at high temperatures and low fractions of high-T_m lipid. When temperature is decreased or the high-T_m lipid fraction increased, phase separation can occur, leading to the coexistence of a liquid and a gel phase. At low temperatures and high concentration of high-T_m lipid, there is only a uniform gel phase. If an isothermal line is drawn from the onset of the phase coexistence to the offset of the phase coexistence, a tieline is obtained, as shown in figure 6. Along the tieline, the proportion of the different phases changes but the lipid composition in the phases is unchanged. The onset and the offset of the coexistence region gives the lipid composition in each phase. The onset of the gel phase gives the fraction of both low- and high-T_m lipid in the Ld phase. The offset of the gel phase gives the lipid fractions of low- and high-T_m lipids in the gel phase. It is also possible to calculate the concentrations of the different phases at different fractions of low- or high-T_m lipids with the Lever rule (Eq. 2).

$$\boldsymbol{f}_{gel} \;\; = \frac{X - X_{L_d}}{X_{gel} - X_{L_d}} \quad \boldsymbol{f}_{Ld} \;\; = \frac{X_{gel} - X}{X_{gel} - X_{Ld}} \tag{Eq 2}$$

The different fractions can be abbreviated as f for fraction, X is the fraction of high-T_m lipid at an arbitrary point on the tieline, X_{gel} is the fraction of high-T_m lipid in the gel phase (offset) and X_{Ld} is the fraction of high-T_m lipid in the Ld phase (onset). The wider the coexistent region, the more non-ideally the lipids do mix. In addition, the partitioning coefficient of a lipid into a phase (K_P), can be calculated when the onset and offset are known. It can also be used to calculate probe partitioning into different phases (151).
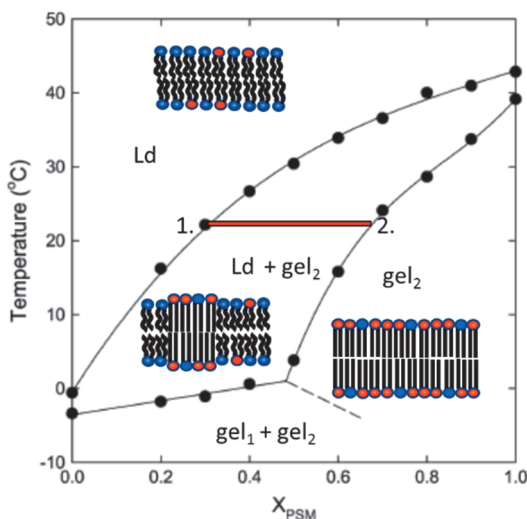
Figure 6. *Example binary phase diagram of POPC/PSM (low-/high-T$_m$ lipid), including schematic pictures of phases present. The tieline is shown as a red line that starts with 1) the onset of Ld and gel$_2$ phase coexistence and 2) offset of the same coexistence. The Lever rule can be applied at different points on the isothermal tieline. The two gel phases, indicate that the low- and high-T$_m$ lipid can phase-separate into two different gel phases. Modified phase diagram taken from (117).*

2.4.2. Impact of cholesterol on the phase behavior of mixed bilayers

Cholesterol can induce a liquid-ordered (Lo) phase (152, 153). It has been reported by DSC that cholesterol broadens and eventually abolishes the gel-Ld phase transition of saturated PCs (154). While there are some conflicting results, the general feature is that there are two different components of the DSC endotherms in saturated PC/cholesterol bilayers, *i.e.* one sharp component and a broad component. The sharp component displays a slightly reduced cooperativity and T$_m$ as compared to the pure saturated PL. The enthalpy of the sharp component also decreases linearly with cholesterol concentration until it disappears at 20-25 mol% of cholesterol. The enthalpy and T$_m$ of the broad component increases while the cooperativity decreases up to 20-25 mol% of cholesterol. Above 20-25 mol% cholesterol, the broad component decreases in enthalpy and its cooperativity continues to decrease. Eventually, at 50 mol% of cholesterol, the enthalpy reaches zero (154). These results have been interpreted to indicate that the sharp component is derived from melting of a cholesterol-poor phase, and the broad component from melting of the cholesterol-rich phase (133). When chain length homologs of di-saturated PCs were studied, it was

found that cholesterol affected the sharp component similarly independent of the chain length of the PCs. However, the change in T_m and cooperativity for the broad component varied upon addition of cholesterol. When the hydrocarbon chain length was 16 carbons or less, T_m of the broad component increased, while with ≥ 18 carbons the T_m of the broad component decreased. The shorter chain decreased the cooperativity of the broad component more than the longer chain PCs. Therefore it was concluded that the 17-carbon PC would optimally match the hydrophobic match to cholesterol (155). Cholesterol interaction with a SM may be different, but has not been studied to the same degree with DSC as saturated PCs (156, 157).

Several methods *e.g.* DSC, fluorescence spectroscopy and ^{2}H NMR have been used to construct binary phase diagrams to better understand the impact of cholesterol on lateral segregation (157). A binary cholesterol phase diagram has three phases: gel, Lo, and Ld phase (Fig. 7) Especially the liquid-liquid separation is of interest from the biological perspective. However, very few methods can directly show a liquid-liquid separation (157). ^{2}H NMR of DPPC-d$_{62}$/Chol bilayers showed Pake doublets from both the Lo and Ld phase in the spectra above the T_m of DPPC-d62, especially observable for the methyl groups (158). Electron-spin resonance (ESR) studies on spin-labeled lipids have also indicated liquid-liquid phase separation in DPPC/Chol and PSM/Chol bilayers (159, 160).
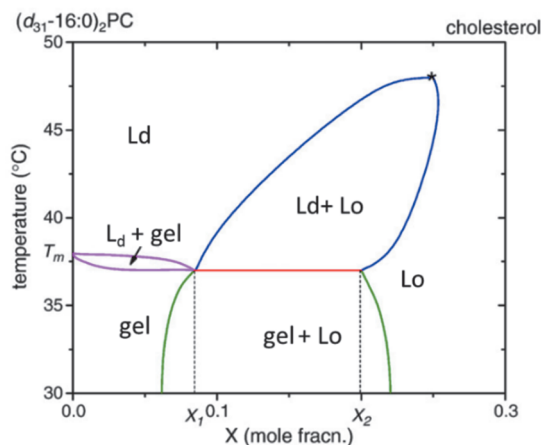
Figure 7. *Example of a binary cholesterol/saturated PL phase diagram. Modified from (157).*

2.4.3. Impact of cholesterol on phase behavior in more complex bilayers

The interest in the impact of cholesterol on phase behavior of bilayers has resulted in several ternary phase diagrams (161). The binary cholesterol/PL bilayers omit the low-T_m lipids even if they are abundant in biological membranes (63). In binary cholesterol/PL bilayers, ^{2}H NMR detected coexisting phases but fluorescence microscopy did not (162). In ternary bilayers, macroscopic phase separation is more common but is dependent on the lipid type (150).

Ternary phase diagrams have been constructed based on phase boundaries from ternary bilayers. A ternary phase diagram is most commonly represented as a Gibbs triangle, as shown in figure 8. The ternary phase diagram is isothermal as opposed to the binary phase diagram discussed above. Most ternary phase diagrams include a low-T_m lipid, a high-T_m lipid and cholesterol. Here, the liquid-liquid phase separation (Ld-Lo phase coexistence) is relevant for biological systems. Some researchers have even constructed quaternary phase diagrams by including different low-T_m lipids in the bilayer (163, 164). A quaternary phase diagram is represented as a three-dimensional pyramid (163).
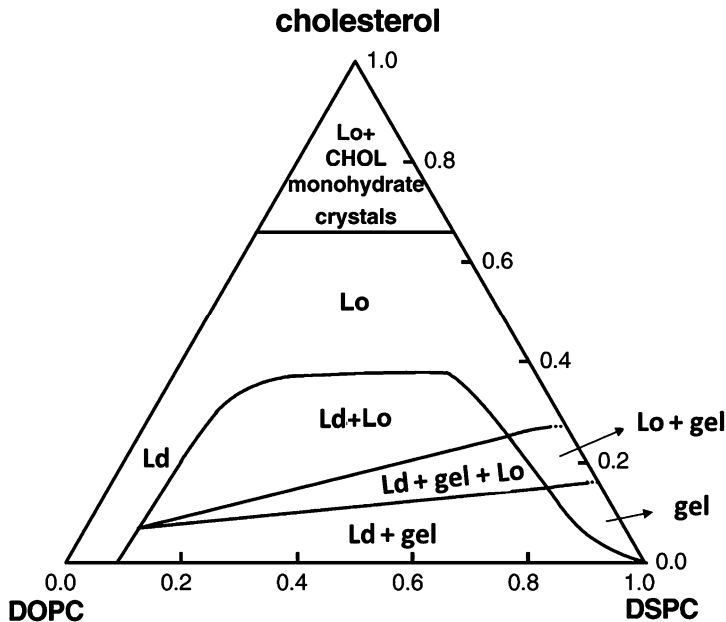
Figure 8. *A ternary phase diagram for DOPC/DSPC/Chol bilayers. Modified phase diagram from (165).*

20

Tielines can be very useful, since they allow one to calculate partitioning of lipids and proteins into different phases (166), and thereby to better understand cholesterol-PL interactions. However, it is more difficult to determine the tielines in ternary phase diagrams than for binary ones (161). To obtain the tielines, the end points of the tielines have to be determined. To determine the endpoints, a sample must include information about both the amount of phases and lipids in the coexisting phases (130). Although it is difficult, this has been achieved with several methods, *e.g.* with ^{2}H NMR (167), Förster resonance energy transfer (FRET) (168) or ESR (169). The tielines obtained indicate that cholesterol prefers the Lo phase (170, 171), as indicated in other studies (23, 153). Similarly to reported binary phase diagrams, most low-T_m lipids mainly partition into the Ld phase (172), with some exceptions (173). The high-T_m lipids are mostly found in the Lo phase (168). Partitioning of cholesterol into the Lo phase also dependens on the saturated PL studied. For example, the tielines for brain-SM/DOPC/Chol (168) and DOPC/SM/Chol (170) are much steeper than those for DOPC/DSPC/Chol (168), indicating that more cholesterol partitions into the Lo phase in bilayers containing SM vs saturated PCs.

2.5.   Methods to detect lateral segregation

While phase diagrams provide both qualitative and quantitative data, there are some discrepancies between different phase diagrams (161). Some phase diagrams lack some phase boundaries, *e.g.* the Lo-Ld phase coexistence region in saturated PL/Chol diagrams (157). Some phase diagrams indicate that unsaturated PLs together with cholesterol form Lo-Ld phase co-existence region without requiring a saturated PL (174, 175). In addition, the exact mole fractions of lipids at phase boundaries differ between studies (157, 161). There should be many reasons for such discrepancies *e.g.* due to different methods being used. Methods can vary in their capacity to detect coexisting phases; they can also differ in their spatial and temporal resolution. In addition, different methods can utilize different types of model membranes, which can affect the phase behavior. Furthermore, some methods use probes while others do not (30). A summary of differences between the methods used to detect phase behavior is shown in table 1.

Table 1. *Common outline of limitations and advantages of different methods for understanding phase behavior of lipid bilayers.*

Method	Directly detects co-existence of phases	Detects order of co-existing phases	Spatial and temporal resolution	Probe or probe-free	Model membrane system used
DSC	Yes/No	No	Medium	Probe-free	MLV
Fluorescence anisotropy	No	No**	Very High	Probes	MLV
Time-resolved fluorescence of tPA	Yes/No	Yes	Very High	Probes	MLV
FRET	Yes/No	No	High	Probes	LUV/MLV
Fluorescence microscopy	Yes/No	No*	Low	Probes	GUV
^{2}H NMR	Yes/No	Yes	Medium	Probes	MLV
AFM	Yes	Yes	Medium	Probe-free	SBL
ESR	Yes	Yes	Very High	Probes	MLV
SANS	Yes	Yes	High	Probes	LUV

AFM = atomic force microscopy, ESR = electron-spin resonance, FRET = Förster resonance energy transfer, LUV = large unilamellar vesicles, MLV = multilamellar vesicles, SANS = Small-Angle Neutron Scattering, tPA = trans-parinaric acid, * = possible with polarity-sensitive probes e.g. C-laurdan or with two probes.

Several methods may directly detect coexistence of phases, *e.g.* ^{2}H NMR can show a two-component spectra, and lipid order can be discerned from both Ld and Lo phase in liquid-liquid separation if the domains are large enough (176). ESR can also detect different phases and the order of the spin-labeled lipids in the different phases (130). AFM can detect coexisting phases based on different hydrophobic thicknesses of the phases (177). Fluorescence microscopy may also detect different phases, but is highly dependent on domain size. However, in fluorescence microscopy the order of the

phases can only be discerned by using special polarity-sensitive probes like laurdan (178). FRET that relies on probe separation may also detect phase coexistence but cannot indicate the lipid order in the different phases. DSC show the energies of phase transitions, indicating phase coexistence during the meltings (132).

Indirect methods of detecting phase co-existence often rely on changes in lipid acyl chain order or bulk membrane order. This can be measured by different fluorescence methods, like anisotropy and time-resolved fluorescence. These methods can detect phase transitions, because acyl chain order is often dramatically changed upon phase transitions (135, 179). However, in some cases, *e.g.* liquid-liquid separation in unsaturated PLs, acyl chain order is increased, although not always linearly, suggesting a phase transition (117). However, other methods *e.g.* FRET (180) and ^{2}H NMR (181) have not detected a phase transition (157). Some methods, like time-resolved fluorescence of tPA, reveal different lifetimes, which may indicate coexistence of phases.

Detection of a phase transition or phase coexistence depends on the method used (150). Such differences can occur because of the different spatial and temporal resolution of the method (130). In fluorescence spectroscopy, probes responds to nearest-neighbor interactions of the probe, therefore they allow one to detect extremely small domains (130). Depending on the lipids used, fluorescence imaging can detect phase separation in DSPC/Chol bilayers containing DOPC but not POPC (150). However, in both POPC- and DOPC-containing bilayers, phase separation was detected with FRET and ^{2}H NMR experiments (130). This is because different lipids form domains with different sizes (182). It has been proposed that phase diagrams with nanoscopic domains should be called type I phase diagrams and macroscopic phase diagrams are to be called type II (150). From a biological point of view, type I is more of interest, because lipid rafts are nanoscopic (30, 150).

Most methods use a probe to discern the phase transitions (130). A rely on the external probe could affect how the lipid components mix. Therefore, probe effects on bilayer properties have been investigated, *e.g.* by measuring the T_m of the lipids in the presence and absence of probes. There is also a difference in potential disruptiveness between probes; some probes are less disruptive than other ones. Among the less perturbing probes are deuterated lipids used in ^{2}H NMR and SANS. Perdeuterated acyl chains only cause a minor change in the T_m of the lipids (171). The change in T_m is dependent on the number of deuterium atoms, *i.e* site-specifically deuterated lipids

have a minimal effect on T_m compared to natural lipids. Fluorescent probes can have more perturbation (183); however, minimizing oxidation and using low probe/lipid ratios largely eliminates these artefacts (164). In addition, the phase-selectivity of the probes is also of importance, as shown in the result section.

The choice of a model membrane is important as it can bias the results. MLVs display more cooperative gel-Ld phase transition than LUVs and GUVs, as observed by DSC (184). These results suggest that lipids in the MLVs melt more cooperatively because the different bilayers are in register and not because of their lesser curvature than LUVs (184). Some methods, like X-ray diffraction, even rely on the bilayer-bilayer interaction for detection of lipid order and phase transitions (130).

Not all methods are equally suitable for detecting different phases and phase transitions. DSC can detect the decrease in cooperativity of a gel phase melting with addition of cholesterol, but fails to detect the low enthalpy in liquid-liquid phase transition (185). With ^{2}H NMR it is difficult to detect gel phase and when detected it is difficult to discern the hydrocarbon chain order (176). While fluorescence lifetimes lengths of tPA have been used to indicate in which phase the probe is inserted. (149, 175) Data interpretation becomes more difficult when comparing different lipid mixtures (179).

While the large discrepancies in phase boundaries detected on different methods can be discouraging at first, understanding of the advantages and limitations of the different methods can provide additional information on lipid-induced lateral segregation (182). However, the differences between methods could help to understand lateral segregation, especially in more complex systems, is still incomplete. The knowledge obtained from phase diagrams may help to plan new experiments.

3.   AIMS OF THE PRESENT STUDIES

The aims were to understand how cholesterol-PL and PL-PL interactions affect lateral segregation. This was achieved by measuring the impact of addition of high-T_m lipids and/or cholesterol to fluid low-T_m lipid bilayers, and the resulting effects on lateral segregation and acyl chain order. Fluorescent phase- and lipid-analog probes and deuterated lipids were used. In addition, sterol affinity for different PLs was investigated. The studies utilized both simple and complex bilayers containing up to 5 lipids.

In **paper I**, the aim was to understand how the acyl chain order was affected in the fluid phase by different sphingolipids. With different phase-selective probes, fluorescence anisotropy was compared when sphingolipids were added to a POPC bilayer. Cholesterol was included to compare how it ordered the bilayer compared to sphingolipids.

In **paper II**, the aim was to understand how different GPLs and SM interact with cholesterol in complex bilayers. ^{2}H NMR for different deuterated PLs and fluorescence lifetime of lipid-analog probes were used to compare the thermostability of ordered domains. Cholesterol-induced ordering of the different PLs was also investigated with ^{2}H NMR.

In **paper III**, the aim was to understand how formation of ordered phases is affected by different unsaturated and saturated PLs. Especially, the effects of cholesterol on formation of ordered phases were investigated. Fluorescence lifetimes of tPA were employed to detect formation of ordered phases. ^{2}H NMR was used to understand the properties of the coexisting phases. Sterol affinity experiments were performed to understand the influence of cholesterol-PL interaction on the formation of ordered phases.

4. MATERIALS & METHODS

Table 2. *Methods used in the papers*

Technique	Properties measured	I	II	III
^{2}H Nuclear magnetic resonance	Acyl chain-order, ordered domain thermostability		x	x
Fluorescence anisotropy	Acyl chain-order, ordered domain formation, probe partitioning	x		
Time-resolved fluorescence of tPa	Acyl chain-order, ordered domain thermostability and formation	x	x	x
Differential scanning calorimetry	Ordered domain thermostability			x
Sterol partitioning	Sterol affinity for PLs			x
Fluorescence quenching	Probe partitioning	x		

4.1. Materials

Lipid and lipid precursors were purchased from Avanti Polar Lipids (Alabaster, AL) or Sigma-Aldrich (St. Louis, MO). PSM was purified with high-performance liquid chromatography (HPLC) from egg-SM as described in (179). 9′,9′-d$_2$-PSM, 9′,9′-d$_2$-DPPC and PSM-d$_{31}$ were synthesized in-house according to (186). Diphenylhexatriene (DPH) was purchased from Molecular Probes (Leiden, Netherlands), TopFluor cholesterol (TF-Chol) and 1-palmitoyl-2-stearoyl-(7-doxyl)-PC (7SLPC) was purchased from Avanti Polar Lipids. The other fluorescent probes (CTL, 18:1-DPH-PC, tPA, O-tPA-PC and tPA-SM) were synthesized in the house, as described in (113, 186-190).

4.2. Vesicle preparation

Lipid vesicles were prepared from mixing lipids and fluorescent probes (max 1 mol%) in organic solvents and followed by evaporating at 40 °C under nitrogen flow. In

addition, ^{2}H NMR samples were dissolved in chloroform for a homogenous mixing and evaporated again under a nitrogen flow, followed by overnight in vacuum. The stock solutions of polyunsaturated PLs and fluorophores contained (butylated hydroxytoluene) to inhibit oxidation. The lipids were hydrated 30-60 min at a temperature above the lipid with the highest T_m. In papers I and II, a 50 mM Tris buffer with 140 mM NaCl was used for the fluorescence experiments, and argon-purged milli-Q H_2O was used in paper III and for ^{2}H NMR samples in paper II. Multilamellar vesicles (MLV) were produced for all studies except CTL and TF-Chol partitioning, which required large unilamellar vesicles (LUVs). The LUVs were extruded 11 times through either 100 or 200 nm polystyrene filters. To reduce light scattering in the fluorescence experiments, MLVs were bath sonicated 5 min at same temperature as hydration to reduce vesicle size. ^{2}H NMR samples were freeze-thawed three times after hydration followed by lyzophilization, rehydration to 50% (w/w) with deuterium-depleted H_2O, and again freeze-thawed. The samples were then transferred to 5 mm glass tubes (Wilmad, Vineland, NJ, U.S.A.) and sealed using epoxy glue.

4.3. Fluorescence spectroscopy

PTI QuantaMaster spectrophotometers (Photon Technology International, Lawrencwill, NJ, USA) operating in T-format were used for steady-state fluorescence experiments. A FluoTime200 spectrophotometer with a PicoHarp300E time-correlated single photon-counting module (PicoQuant GmbH, Berlin, Germany) with a monochromator was used for time-resolved fluorescence decays in paper II. A FluoTime100 spectrophotometer from the same company with a 350 or 395 nm cutoff filter was used in paper I and III, respectively.

4.3.1. Fluorescence anisotropy and quenching

MLVs were produced at 0.05 mM lipid concentration plus 1 mol% probe. The excitation and emission wavelengths for DPH and 18:1-DPH-PC were 360/430 nm, and 305/405 nm for trans-parinaric acid (tPA). A G-factor was measured before the emission intensity was measured as a function of temperature with a gradient of 2 °C/min. Anisotropy was calculated with the PTI-Felix32 software according to Lakowicz (191).

27

4.3.2. Time-resolved fluorescence of tPA

MLVs were prepared at varying lipid concentrations depending on the lipids and probe used. A ~0.05 mM concentration was used in paper I, 0.1-0.2 mM in paper II and 0.1 mM in paper III. 1 mol% probe was used in all samples. The excitation and emission wavelengths for tPA and tPA-derived probes were 305/405 nm. The FluoFit Pro software provided by PicoQuant was used for analysis of lifetime decays.

4.3.3. Sterol partitioning

Sterol partitioning was determined in two ways with two different cholesterol analogs, CTL or TF-Chol. The equilibrium partitioning of CTL (2 or 3 mol%) between pure PL LUVs (0.04 mM) and MβCD was measured at 50 °C. The reason for the high temperature was the requirement for fluid PL bilayers. By varying the concentration of MβCD (0-1 mM) and detecting the changing anisotropy of CTL (ex/em wavelength 324/390 nm), the molar fraction partitioning coefficient (K_x) could be calculated (128). Equilibrium partitioning of TF-Chol was between donor and acceptor LUVs. The donor LUVs contained 0.5 mol% DPH-PC and TF-Chol. FRET efficiency after equilibrium was calculated to obtain the relative partitioning coefficient (K_R).

4.4. Differential scanning calorimetry

MLVs were produced at a lipid concentration at 1 mM. A high sensitivity Micro-Cal VPDSC-instrument (MicroCal, Northampton, MA, USA) was used to acquire the data. For analysis, ORIGIN software (Originlab, Northampton, MA, USA) was used. At least four consecutive heating and cooling scans with a temperature gradient of 1 °C/min were performed.

4.5. ²H NMR experiments

Deuterium-labeled lipids were either 9',9'-d_2 –PSM (paper II and III) or 9',9'-d_2 –DPPC (paper III), or perdeuterated in the N-palmitoyl chain (PSM-d_{31}) and the unsaturated lipids had a perdeuterated palmitoyl chain in the *sn*-1 position (POPC-d_{31}, POPE-d_{31}, POPS-d_{31}). ²H measurements were recorded on a 300-MHz CMX spectrometer

(Chemagnetics, Agilent, Palo Alto, CA, U.S.A.) using a quadrupole echo sequence and 5-mm ^{2}H static probe (Otsuka Electronics, Osaka, Japan). The 90° pulse width was 2 μs, the repetition rate was 0.5 s and the interpulse delay was 30 μs. The number of scans was approximately 100 000 and sweep width was 200 kHz. The NMR data was analyzed with TopSpin software (Bruker) and ≥ 300 Hz of line broadening was used. The first spectral moment (M_1) was calculated for each ^{2}H spectrum using the following equation:

$$M_1 = \frac{\int_{-\infty}^{\infty} |\omega| f(\omega) d\omega}{\int_{-\infty}^{\infty} f(\omega) d\omega} \qquad \text{(Eq 3)}$$

where ω is the frequency with respect to the central Larmor frequency $\omega 0$, and $f(\omega)$ is the line shape (192). For some samples, the spectra were fast Fourier transform dePaked to enhance the resolution and give spectra similar to a planar membrane of single alignment (193).

5. RESULTS

5.1. Acyl chain order in the fluid phase (paper I)

There exists a wide variety of sphingolipids (194). They readily form gel phases with high thermostability (74, 195, 196). In addition, they could have an important role in affecting the bulk acyl chain order. In this paper, we studied how the acyl chain order of a POPC bilayer was affected by including different sphingolipids with varying head groups and compared the effect with that of cholesterol. Structures of the lipids that were used in the study are shown in figure 9. We used three phase-selective probes to acquire information about acyl chain order in both the fluid and gel phase. In addition, we compared how ceramide and cholesterol affected acyl chain order in a bilayer without phase separation. Because both ceramide and cholesterol lack a large head group, they could have similar effects on the acyl chain order in the fluid phase, as earlier reported (197).
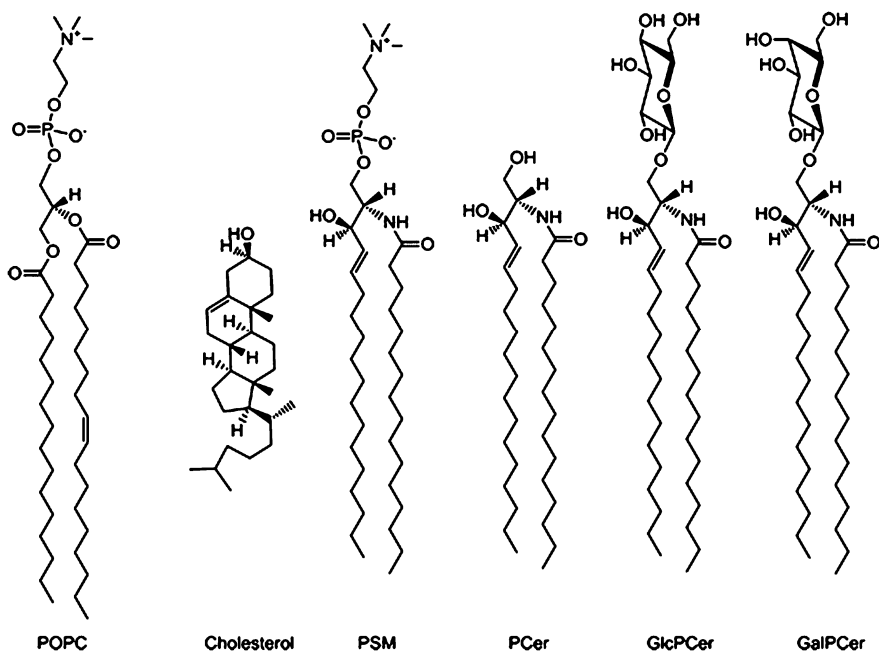
Figure 9. *Lipids used in the study. POPC was the bulk lipid, and cholesterol or sphingolipids with varying head groups were added. The figure is adapted from paper I with the permission of ACS Publications. GalPCer = galactosylpalmitoyl-ceramide. GlcPCer = glucosyl-palmitoyl-ceramide.*

5.1.1. Anisotropy with different phase-selective probes
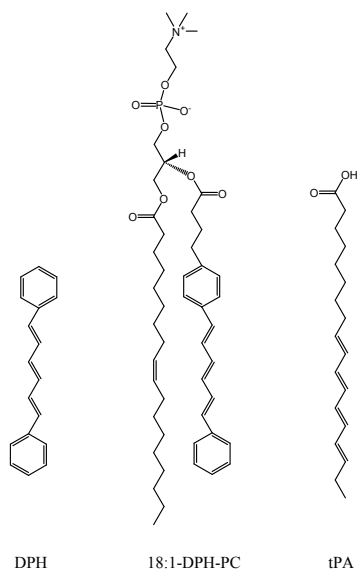
Figure 10. *Structures of the phase-selective probes used in the study. The figure is adapted from paper I with the permission of ACS Publications.*

The probes we used were diphenylhexatriene (DPH), 18:1-DPH-PC and tPA (Fig. 10). DPH partitions equally between Ld and Lo phase (198) and between Ld and gel phase in POPC/PSM bilayers (Fig S1 in paper I). However, it has been reported that DPH is excluded from ceramide gel phases (199). 18:1-DPH-PC has very low affinity for the gel phase in POPC/PSM bilayers ($K_p^{gel/Ld} \approx 0.31$) probably because of the unsaturated *sn*-1 acyl chain (Fig. S1 in paper I) and the DPH moiety. tPA, on the other hand, prefers the gel phase with $K_p^{gel/Ld}$ between 2 and 6.3 depending on the lipid composition (199-201).

 Anisotropy was measured in fluid POPC bilayers with increasing amounts of sphingolipid (PSM, PCer, PGalCer or PGlcCer) or cholesterol. If a sigmoidal or exponential shaped anisotropy curve is detected, it probably indicates that the probe is able to detect the newly formed phase. If a linear increase in anisotropy is found, it is difficult to interpret if a new phase has formed or if it merely reflects a general increase in acyl chain order. If the anisotropy is constant, a new phase is not detected or formed. Increasing cholesterol concentration led to an increase in anisotropy, as was reported by all three probes (Fig. 11). The initial and final anisotropies and the change in anisotropy were different for each probe.
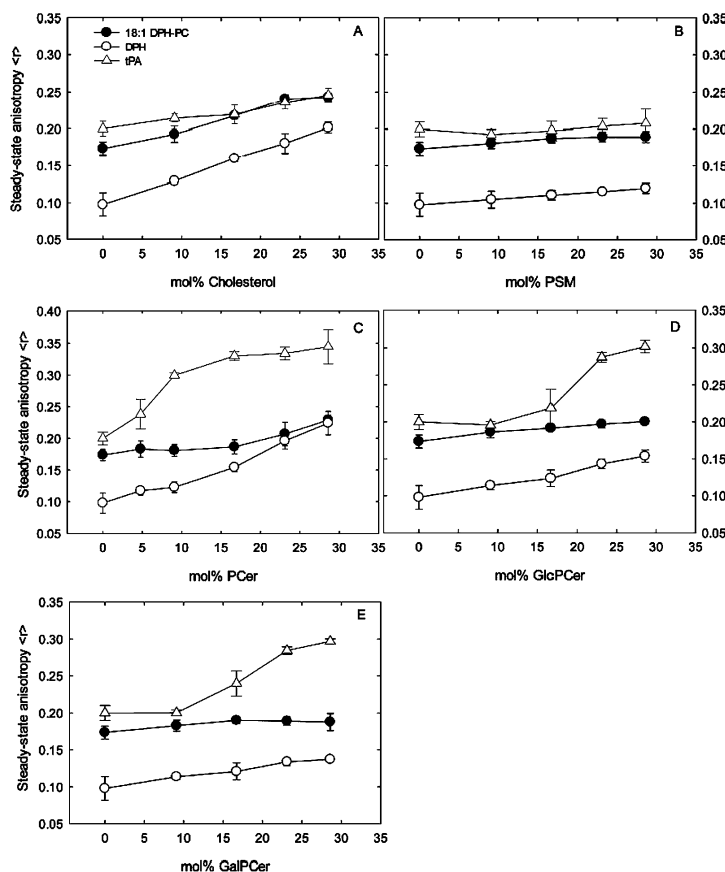
Figure 11. *Steady state anisotropy measurements with three phase-selective probes. The panels shows addition of A) cholesterol, B) PSM, C) PCer, D) GlcPCer or E) GalPCer to a fluid POPC bilayer. Each value is an average of n ≥ 3 ±SD. The figure is adapted from paper I with the permission of ACS Publications.*

DPH reported the largest change between initial and final anisotropies, probably because its more hydrophobic structure gives it more freedom to move than the other probes. Addition of PSM to fluid POPC bilayers led to a modest increase in the anisotropy, as reported by all probes. This probably occurred because the gel phase formation of PSM in POPC bilayer has been reported to occur at a higher PSM mol% than the measured concentration range (0-28 mol%) in this study (179). Addition of PCer to a fluid POPC bilayer led to sigmoidal tPA anisotropy vs PCer concentration curve. In contrast, PCer had almost no effect on 18:1-DPH-PC anisotropy in fluid POPC bilayers until going above 16 mol% PCer. A PCer gel phase is reported to form at very low concentrations of PCer (136, 199) and this agreed with the measured tPA anisotropy, where a clear discontinuity of the anisotropy was observed at low

concentrations of PCer, indicating phase separation. With DPH, the anisotropy increased linearly with PCer content, suggesting that DPH was partially incorporated in the gel phase, in contrast to earlier reports (202). For the glycosphingolipids, tPA reported gel phase formation at ~16 mol% glycosphingolipids, DPH reported a small increase in anisotropy while 18:1-DPH-PC anisotropy was mostly unaffected by the glycosphingolipids. Overall, tPA and to some degree DPH reported that lower concentrations of sphingolipids were required for gel phase formation if the head group size of the sphingolipid was smaller. tPA anisotropy data agreed well with the measurements of tPA lifetimes (Fig. 1 in paper I). All probes reported higher acyl chain order with cholesterol addition to the bilayers (Fig. 11).

5.1.2. Determining the phase-selectivity of the probes

To ensure that the probes reported from expected phases, fluorescence quenching experiments were performed (Fig. 12). If the probes partition into the gel phase, they are protected from the quencher 7SLPC that prefers the fluid phase (203). When temperature is increased in the quencher-containing sample (F), probe emission intensity will be lower compared to the quencher-free sample (F_0) when the gel phase melts. This occurs because the gel phase lipids melt and encounter the quencher. If there is a large change in F/F_0 with increasing temperature, it indicates that the probes have partitioned into the gel phase. We chose the sample POPC/PCer (10/4) because it is known to have a thermostable gel phase (199). In the tPA-quenching experiments, a large difference in F/F_0 was observed at the temperature reported for the PCer melting (Fig. 12), indicating preferable partitioning into the gel phase. DPH displayed a very small difference in F/F_0 with increasing temperature, especially compared to tPA, indicating predominantly a low partitioning into the gel phase. F/F_0 was essentially unchanged for 18:1-DPH-PC, indicating that it did not partition into the gel phase. These results agreed with the partitioning data and confirmed the phase selectivity of the different probes (Fig. S1 in paper I).
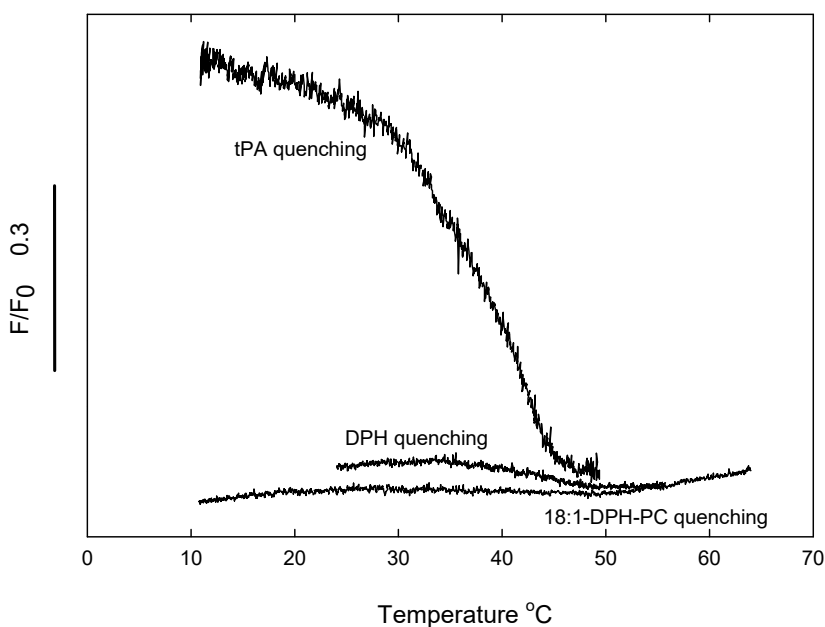
Figure 12. *Fluorescence quenching experiments to explore phase-selectivity of the fluorescent probes used. The composition was POPC/PCer 100/40 for the F_0 sample and POPC/7SLPC/PCer 70/30/40 for the F sample. Each value is an average of $n \geq 3$ ±SD. The figure is adapted from paper I with the permission of ACS Publications.*

5.1.3. Acyl chain ordering by cholesterol and sphingolipids in a fluid bilayer

At 23 °C, there was a coexistence of two-phases at some lipid compositions. To compare the acyl chain ordering of a fluid bilayer by cholesterol or PCer, a binary bilayer without phase separation was required. This was obtained by increasing the temperature to 50 °C. Increasing the concentration of either cholesterol or PCer in a POPC bilayer at 50 °C, both increased the bulk acyl chain order (Fig. 13). However, GlcPCer failed to do so at the concentration range tested. These results suggest that the lack of a large head group increased the ability of the lipids to increase the bulk acyl chain order. The difference between cholesterol and PCer is that PCer segregates laterally and therefore fails to increase the acyl chain order in the fluid phase at lower temperatures (Fig. 11). These results agree with the ^{2}H NMR results that PCer increases acyl chain order for POPC-d_{31} in a fluid bilayer (197). In conclusion, the size of the head group affects the bulk acyl chain ordering in the fluid phase, as long as the lipid does not create an ordered phase.

34
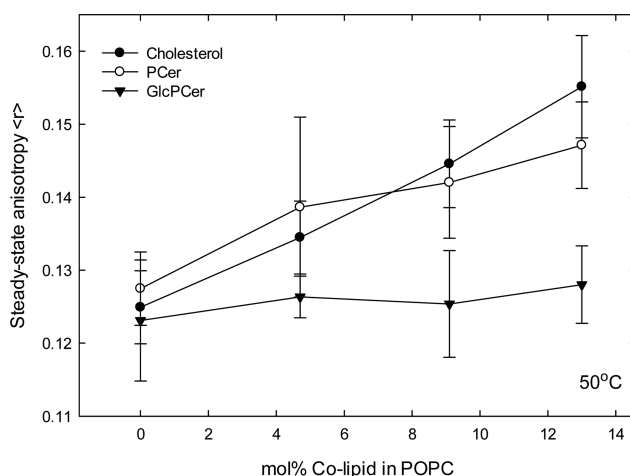
Figure 13. *Comparison of different sphingolipids and cholesterol, and how they affect the steady-state anisotropy of 18:1-DPH-PC in a fluid non-segregated bilayer. Measurements were carried out at 50 °C to ensure bilayer fluidity. Each value is an average of n ≥ 3 ±SD. The figure is adapted from paper I with the permission of ACS Publications.*

5.2.   Lipid interactions in complex bilayers (paper II)

Cholesterol is known to affect the acyl chain order in fluid bilayers, as was also shown in paper I and elsewhere (204, 205). The preference of cholesterol for different PLs has been studied (103, 104, 117). However, the observed sterol affinity for GPLs with different head groups varies between studies. In addition, the sterol affinity is often studied in a single-lipid bilayer, though sterol-PL interactions are likely affected by the several different PLs present in a complex bilayer. Favorable sterol-SM interactions have been demonstrated (74), but the competing interaction of other PLs with cholesterol could complicate the SM-cholesterol interaction. Therefore, we studied how cholesterol and temperature affected acyl chain order in complex bilayers consisting of perdeuterated palmitoyl chain in PSM (PSM-d_{31}), POPC (POPC-d_{31}), POPE (POPE-d_{31}), and POPS (POPSd_{31}). We also examined how the acyl chain order of PSM was affected by inclusion of the different GPLs in ternary bilayers, and compared it to binary bilayers. In paper I, phase-selective probes were used while in this study we used lipid-analog probes for both ^{2}H NMR and time-resolved fluorescence measurements.

5.2.1. Fluorescence lifetimes of tPA with lipid-analog probes

tPA partitions preferentially into the gel phase (199, 200). However, probe partitioning can be affected by attaching a fluorophore to a lipid, which has different affinity for a phase than the free probe (206). This was found out in paper I, where 18:1-DPH-PC had much lower affinity for the gel phase than free DPH. In paper II, we used the same approach but attached tPA to lyso-18:1-PC or lyso-SM. The oleoyl-tPA-PC (O-tPA-PC) has much lower affinity for the gel phase ($K_p^{gel/Ld}$ 0.35, Fig. S1 in paper II) than tPA-SM (($K_p^{gel/Ld}$ ~1.7 (201)).
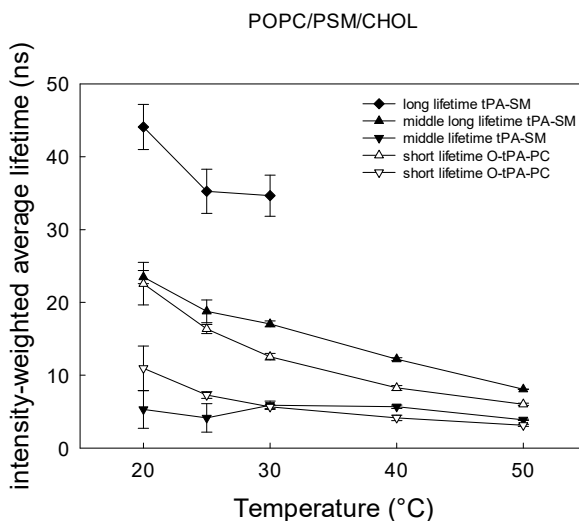
Figure 14. *Lifetime components of tPA-PLs in POPC/PSM/Chol bilayers. One mol% O-tPA-PC (partitions to Ld phase) or tPA-SM (partitions to Lo phase) was included in POPC/PSM/Chol (34.5/34.5/30 mol%) bilayers. Each value is an average of n ≥ 3 ±SD. The figure is adapted from paper II with the permission from Cell Press.*

The fluorescent decays of tPA are typically multiexponential (174). In POPC/PSM/Chol (34.5/34.5/30 mol%) bilayers, a clear difference was observed between O-tPA-PC and tPA-SM (Fig. 14). tPA-SM reported a third fluorescence lifetime component at low temperatures, while O-tPA-PC did not. The interpretation was that O-tPA-PC did not partition into the Lo-domains found in the bilayer while tPA-SM did. The other two lifetime components of O-tPA-PC had shorter lifetimes than tPA-SM, indicating that the probe preferred a more fluid environment.

36

5.2.2. 2H NMR data of of labeled PSM in binary and ternary lipid bilayers
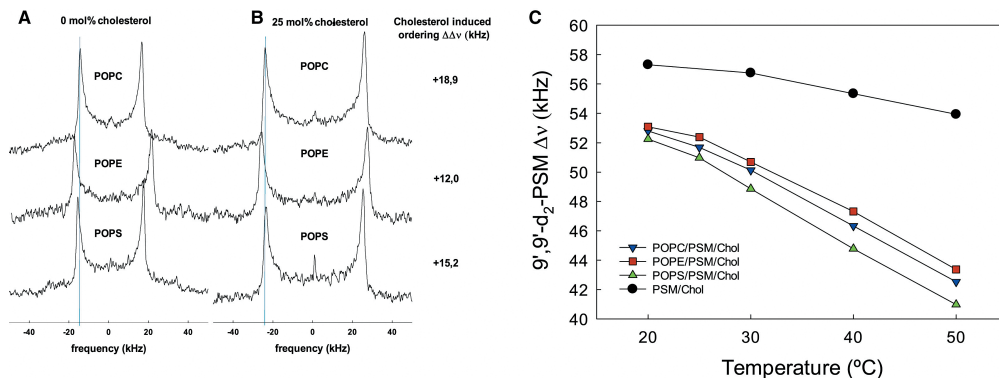
Figure 15. *2H NMR spectra and Δv for 9´,9´-d2-PSM, incorporated in monounsaturated GPLs and cholesterol bilayers. Panel A shows 2H NMR spectra of 9´,9´-d2-PSM in the absence of cholesterol and panel B in the presence of cholesterol. A vertical line was added to guide the eye. In panel B, the cholesterol induced ordering ΔΔv of 9´,9´-d2-PSM was calculated taking Δv of 9´,9´-d2-PSM in the presence minus the Δv in the absence of cholesterol. Panel C shows Δv of 9´,9´-d2-PSM at different temperatures in both binary and ternary bilayers. Composition were 9´,9´-d2-POPX/PSM (2/1) and PSM/Chol (1/1) for the binary bilayers and 9´,9´-d2-PSM/POPX/Chol (2/1/1) for the ternary bilayers. The figure is adapted from paper II with the permission of Cell Press.*

PSM interacts favorably with cholesterol and readily forms cholesterol-rich domains with high thermostability in both binary and ternary bilayers (161). However, the effect of the unsaturated GPLs on the ability of PSM to form ordered domains, and on ordered domain thermostability, is less clear. Therefore, we studied how PSM acyl chain order and domain thermostability was affected by exchanging POPC for POPE or POPS. *9´,9´-d2-PSM* was chosen, because the 9th acyl chain carbon seemed to be most affected by cholesterol in an earlier study (78). In the absence of cholesterol, the quadrupolar splittings of the Pake doublet of 9´,9´-d2-PSM was largest with POPE, followed by POPS and POPC as co-lipid (Fig. 15A). The addition of cholesterol increased Δv most with POPC as co-lipid followed by POPS and POPE (Fig. 15B). However, Δv of 9´,9´-d2-PSM in cholesterol-containing bilayers with different GPLs was very similar, especially at lower temperatures. Compared to binary PSM/Chol bilayers, Δv of 9´,9´-d2-PSM in ternary bilayers was clearly lower (Fig. 15C), in agreement with previous studies (207). Δv of 9´,9´-d2-PSM in binary bilayers was only slightly affected by temperature in contrast to the ternary bilayers. In conclusion, this

37

suggests that the cholesterol-PSM interaction was reduced by inclusion of GPLs independent of the head group in the GPLs, at least at low temperatures.

5.2.3. Cholesterol-induced ordering of different PLs in complex bilayers
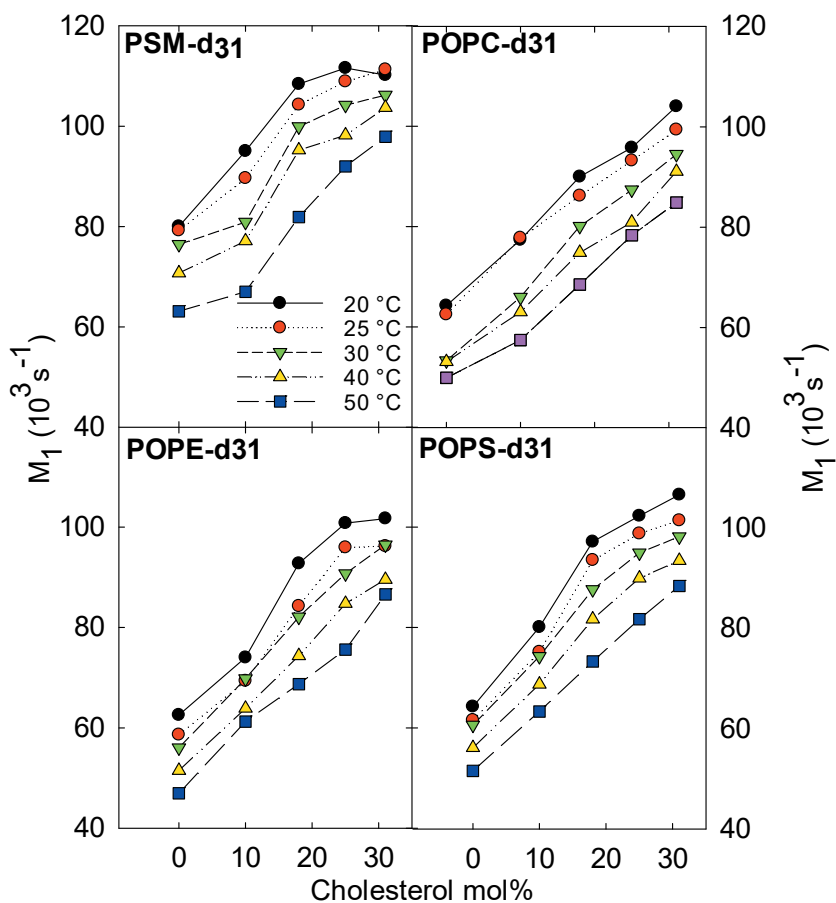
Figure 16. *Ordering of perdeuterated acyl chain of PLs by cholesterol concentrations in PSM/POPC/POPE/POPS (22/44/17/17) bilayers. The figure is adapted from paper II with the permission from Cell Press.*

We investigated how cholesterol concentrations affected different PLs in a bilayer consisting of (PSM/POPC/POPE/POPS, 22/44/17/17). This composition was chosen to mimic the plasma membrane lipid composition (63). ^{2}H NMR spectra was measured for perdeuterated PSM-d31, POPC-d31, POPE-d31, and POPSd31. First, only a single Pake doublet was observed at each carbon (Fig. S4 in paper II), indicating that if coexisting phases existed, the lipid diffusion between the phases is so fast that only

an average-weighted spectrum from both phases could be observed (176). The first spectral moment (M_1) was calculated for all spectra, because the parameter is proportional to the average acyl chain order (192). A linear increase in the acyl chain order with increasing cholesterol content was observed at 50 °C for all PLs. At 20-40 °C, the M_1 plateaued for PSM-d_{31} ≥ 18 mol% cholesterol (Fig. 16). For POPE-d_{31}, and POPSd$_{31}$ at lower temperatures, the M_1 plateaued after 18 and 25 mol% cholesterol respectively, but not to the same degree as PSM-d_{31}. For POPC-d_{31}, no plateau in M_1 was observed with cholesterol addition at any temperature. At all temperatures, PSM-d_{31} had a much larger M_1 than the other perdeuterated PLs. This indicated that in this complex bilayer, cholesterol interacted more favorably with PSM than the GPLs, while cholesterol-induced ordering did not differ substantially between the different GPLs.

5.2.4. Effect of temperature on complex bilayers

Next, we investigated how temperature (20-50 °C) affected the M_1 of the different PLs in complex bilayers at different cholesterol concentrations by replotting the data from figure 16 (Fig. 17). M_1 decreased linearly for all perdeuterated PLs with increasing temperature. The slope of the line increased with cholesterol content. Interestingly, at 10 mol% cholesterol, PSM has a much steeper line than the other PLs. This could indicate a stronger interaction of PSM at low cholesterol concentrations than other PLs have. It could also indicate formation of a cholesterol-rich domain, which then melts. Earlier, slope lines from ^{2}H NMR were interpreted to indicate domain melting in POPC/PSM/Chol bilayers (207). Overall, PSM had a favorable cholesterol interaction than the GPLs. First, indicated by a higher acyl chain order in the presence of cholesterol. Second, by the acyl order of PSM reaching a plateau value at lower cholesterol concentration. Third, that PSM was more affected by cholesterol at lower cholesterol concentrations, than the other GPLs. . The data was inconclusive for determining which GPL cholesterol preferred.
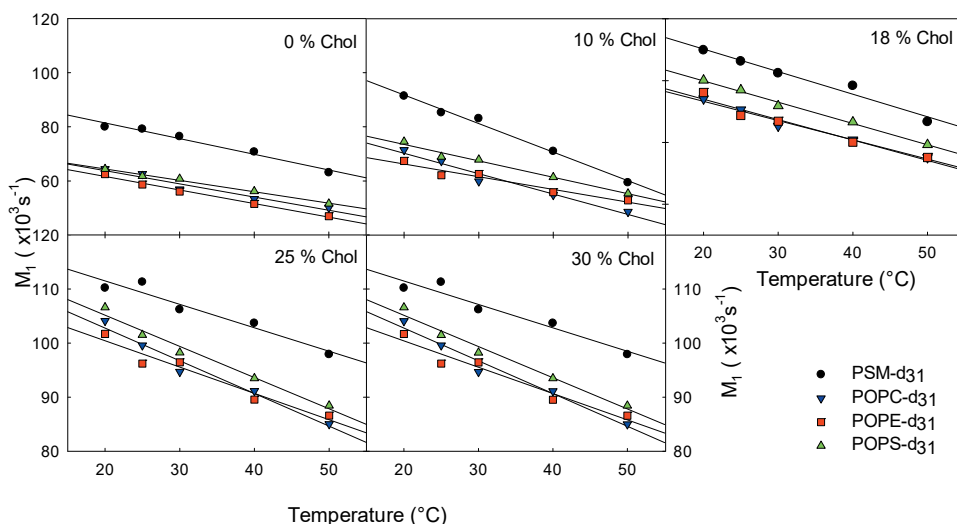
Figure 17. *Effect of temperature on the perdeuterated PLs in complex bilayers. Acyl chain ordering was measured from the first spectral moment (M_1). The bilayer consisted of PSM/POPC/POPE/POPS (22/44/17/17) and cholesterol concentration varied from 0 to 31 mol%. The figure is adapted from paper II with the permission of Cell Press.*

5.3. Cholesterol-PL affinity and lateral segregation (paper III)

It has long been known that cholesterol has higher affinity for saturated PLs than mono- or poly-unsaturated PLs (103, 105). Polyunsaturated PLs are found in all cells but are enriched in certain cells and compartments, *e.g.* synaptic termini in neurons, sperm, and retinal rod outer membrane segments (208). In this study, we compared how different unsaturated PCs affected lateral domain formation both in the presence and absence of cholesterol. We varied the number of double bonds in the *sn*-2 chains (hybrid PLs) and in both chains (symmetrical PLs). We also varied the saturated PLs by including either PSM or DPPC. All structures are shown in figure 18.

We used time-resolved fluorescence of tPA since it is known to have high spatial and temporal resolution to detect lateral segregation (209). When an unsaturated PL was replaced for a saturated PL, the fluorescence lifetime increased linearly but modestly. When lateral segregation occurs, tPA partitions into the ordered phase. In

40
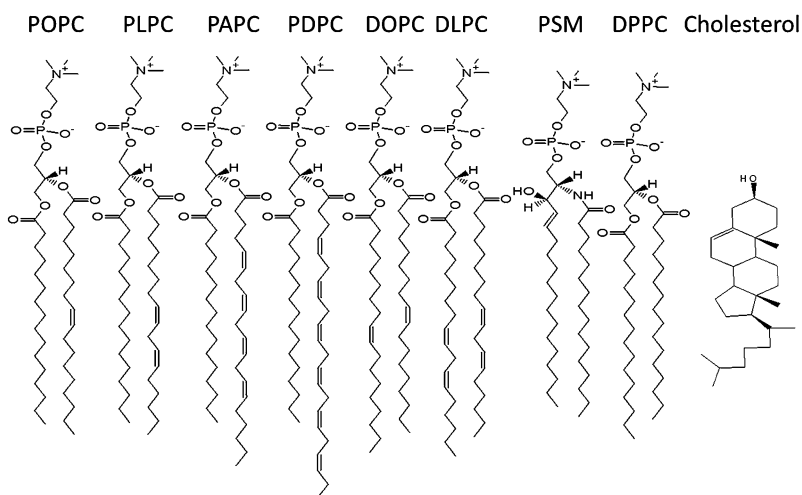
Figure 18. *Lipids used in the study. The four lipids on the left are hybrid PLs with varying number of double bonds. The next two are di-unsaturated PCs. The last three lipids are the two saturated PLs and cholesterol. DLPC = 1,2-dilinoleoyl-PC, PAPC = 1-palmitoyl-2-arachidonoyl-PC, PLPC = 1-palmitoyl-2-linoleoyl-PC.*

the ordered phase, tPA has higher quantum yield and longer lifetime and appeared as kink in the curve (149, 209). The discontinuity or kink in the increase in fluorescence lifetime of tPA vs composition indicates a phase boundary and the mol% of the saturated PL required for lateral segregation to occur. By taking an average of several individual measurements of the trend series, the amount of saturated PL required for formation of ordered domains can be determined for both the gel and Lo phase formation. An example can be seen in figure 19, where 20 mol% of PSM was required to form Lo phase in POPC/PSM/Chol bilayers. Cholesterol concentration was 20 mol% because most phase diagrams indicate liquid-liquid separation at that cholesterol concentration at 23 °C (161, 168). 20 mol% PSM is significantly less than the ~30 mol% required to form ordered domains in the absence of cholesterol (179). The lower amount of PSM required to form an ordered domain in the presence of cholesterol suggests that cholesterol-PSM interactions are of importance for lateral segregation.
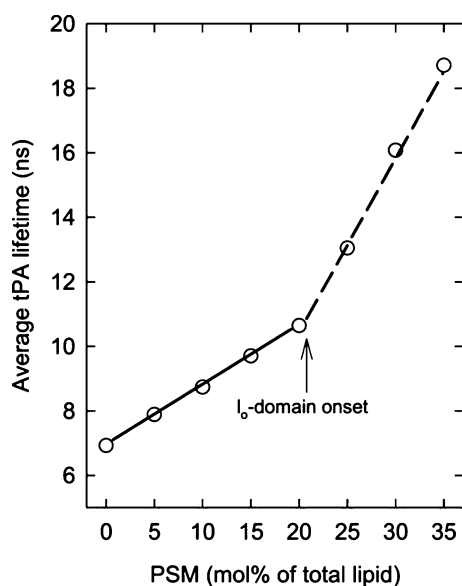
Figure 19. *Detection of lateral segregation based on time-resolved fluorescence of tPA. Initially the bilayer consisted of a fluid POPC bilayer with 20 mol% cholesterol. When POPC was gradually replaced for PSM until a kink in the average lifetime was observed. This kink is assumed to be the onset of Ld-Lo phase coexistence. The figure is adapted from paper III with the permission of Cell Press.*

5.3.1. Effect of cholesterol and polyunsaturated PLs on the formation of ordered domains

It has been suggested that polyunsaturated PLs could promote Lo phase formation (210). The disordered acyl chains of polyunsaturated PLs make the cholesterol-PL interaction unfavorable (211). We tested this by replacing the POPC by PCs with an increasing number of double bonds. We observed that an increasing number of double bonds in hybrid PCs did not change the amount of PSM required to form a gel phase, in an earlier study, (179) and also shown in figure 20. Only di-unsaturated PCs with more than one double bond in each acyl chain lowered the amount of PSM required to form a gel phase (179). However, in cholesterol-containing samples, there was a large difference in the ability to promote lateral segregation between the different unsaturated PCs (Fig. 20). By increasing the number of double bonds from one (POPC) to six (PDPC), the amount of PSM required for lateral segregation decreased from ~20 to ~8 mol%. In conclusion, only in the presence of cholesterol did polyunsaturated hybrid PLs promote formation of ordered domains. This indicates that aversion of cholesterol for polyunsaturated PLs could be the driving force.

42
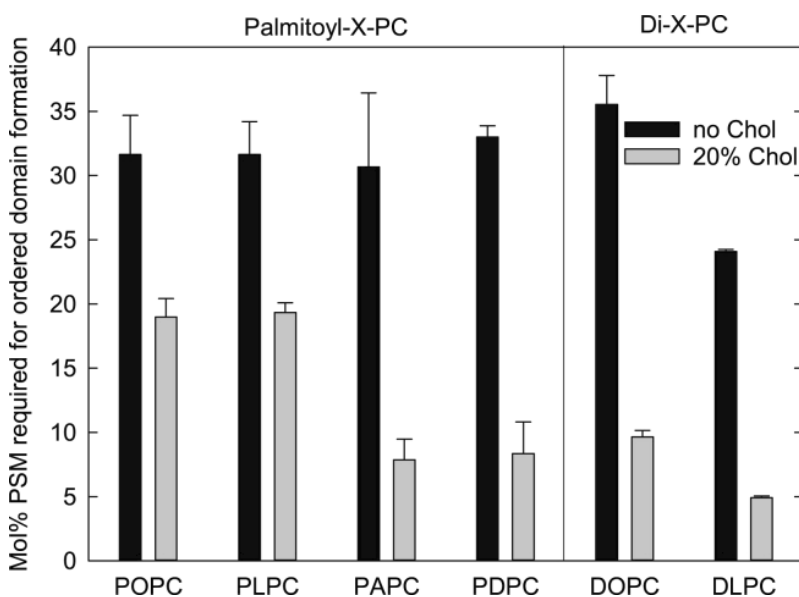
Figure 20. *Mol% PSM required to form ordered domains with different unsaturated PCs in the presence or absence of 20 mol% cholesterol. The onset point was calculated from individual measurements (see Fig. 19). and an average was calculated from n ≥ 3 ±SD at 23 °C. Some values were taken from (179). The figure is adapted from paper III with the permission of Cell Press.*

5.3.2. Sterol affinity for PSM vs DPPC

To investigate whether the aversion between cholesterol and polyunsaturated PLs was the only driving force to promote formation of ordered domains, we examined the impact of replacing SM with a saturated PC. Sterol affinity of saturated PCs has systematically been lower than for SMs, even if the T_m of the lipids are similar (90, 105). We chose DPPC because it has a similar T_m, and therefore is unfortunately widely used a SM substitute (161). To confirm the different sterol affinities, two sterol partitioning assays were used: one where the cholesterol analog CTL will equilibrate between MβCD and LUVs (128), and one relying on partitioning of TF-Chol between donor and acceptor LUVs. When the donor LUVs composed of POPC and acceptor LUVs of POPC and increasing amount of DPPC, K_R (relative partitioning value) increased from one to 1.5 for pure DPPC acceptor LUVs (Fig. 21). In contrast, exchange of POPC for PSM in the acceptor LUVs increased K_R 4-fold. PSM had roughly 2.7 times higher K_R than DPPC, in agreement with the CTL partitioning results (Fig. 21 insert).
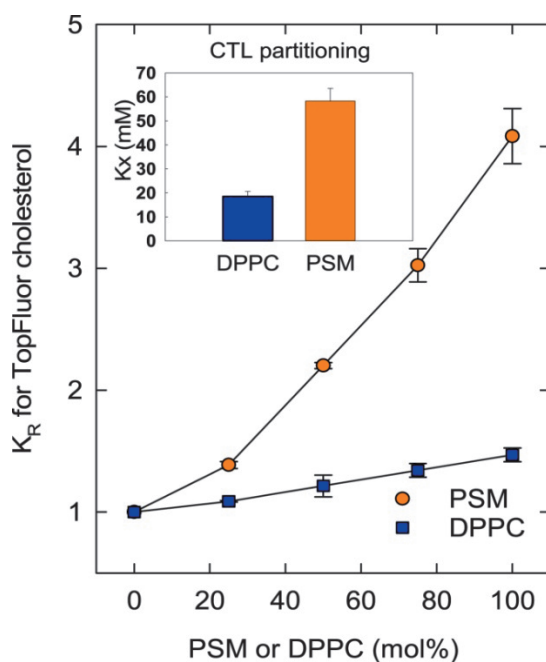
Figure 21. *Equilibrium partitioning of TF-Chol between donor and acceptor LUVs. The acceptor LUVs consisted of POPC and increasing amounts of PSM or DPPC (up to 100%). Donor LUVs contained the probes: DPH-PC (0.5 mol%) and TF-Chol (0.5 mol%). FRET efficiency was calculated to obtain the relative partitioning coefficient (K_R). A partitioning coefficient (K_x), as shown in the insert, was calculated from CTL partitioning between MβCD and PSM or DPPC LUVs. To ensure bilayer fluidity, the experiments were performed at 50 °C. The figure is adapted from paper III with the permission of Cell Press.*

If aversion between cholesterol and polyunsaturated PLs would be the only driver for Lo domain formation, replacement of PSM by DPPC should not substantially change the effect of cholesterol addition on ordered domain formation. While DPPC segregated at lower mol% in unsaturated PL bilayers than PSM (179), effect of cholesterol on lateral segregation was weaker with DPPC vs PSM (Fig. 22). Only when the unsaturated PC had four double bonds did DPPC laterally segregate at a lower concentration in the presence of cholesterol when compared to cholesterol-free bilayers. The data clearly indicates that the lower sterol affinity for DPPC than PSM reduced the impact of including polyunsaturated PLs on lateral segregation.
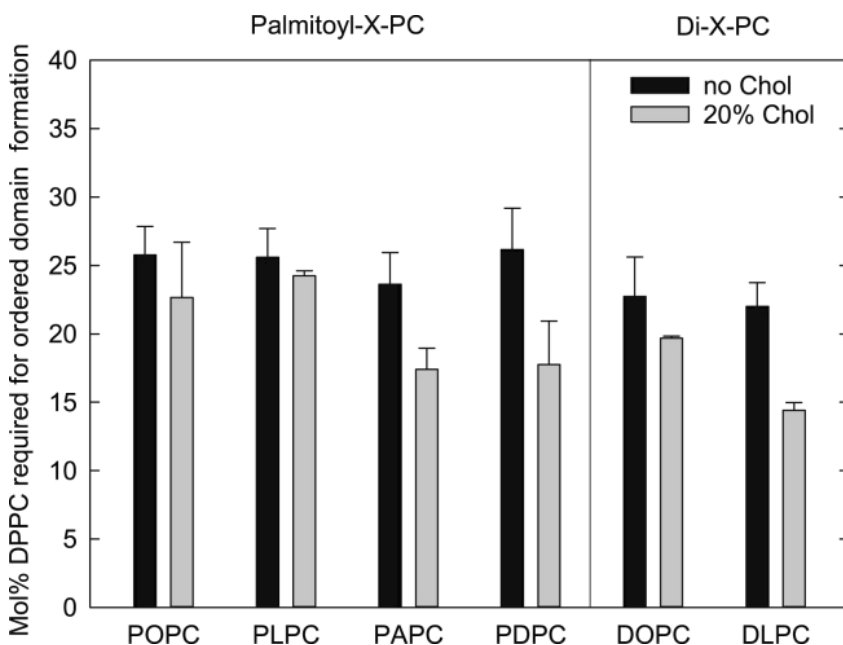
Figure 22. *Mol% of DPPC required for ordered domain formation with different unsaturated PCs in the presence and absence of 20 mol% cholesterol. The onset point was obtained from as shown in figure 19. Some values were taken from (179) Data is of n ≥ 3 measurements ±SD at 23 °C. The figure is adapted from paper III with the permission of Cell Press.*

5.3.3. Impact of polyunsaturated PLs on the acyl chain order of PSM and DPPC as measured with ^{2}H NMR

To acquire information about the properties of the formed ordered domains, ^{2}H NMR spectra of 9′,9′-d$_2$-PSM and 9′,9′-d$_2$-DPPC containing bilayers were recorded. If the spectrum shows two Pake doublets, the lipid order can be determined for both Ld/Lo phases (176). This approach has been applied before for both perdeuterated lipids (212, 213) and site-specifically deuterated lipids (167). For the 9′,9′-d$_2$-PSM spectra, two Pake doublets were detected in ternary bilayers which included a different unsaturated PLs (POPC, PLPC, PAPC or DOPC)(Fig. S6 in paper III). In the case of 9′,9′-d$_2$-DPPC, two Pake doublets were only detected for PAPC and DOPC containing bilayers (Fig. S6 in paper III). However, the Δv for 9′,9′-d$_2$-DPPC, was still relatively high in POPC and PLPC bilayers, suggesting that an average of Δv from two phases was observed (Fig. 23). Δv for 9′,9′-d$_2$-PSM in the Lo phase increased with increasing number of double bonds in the PCs, especially at 28 °C. For 9′,9′-d$_2$-PSM in the Ld phase there was a substantial decrease with increasing number of double bonds.

45

Overall, PSM had higher order in the Lo phase than DPPC. The unsaturated PLs mostly affected the order of labeled PSM and DPPC in the fluid phase.
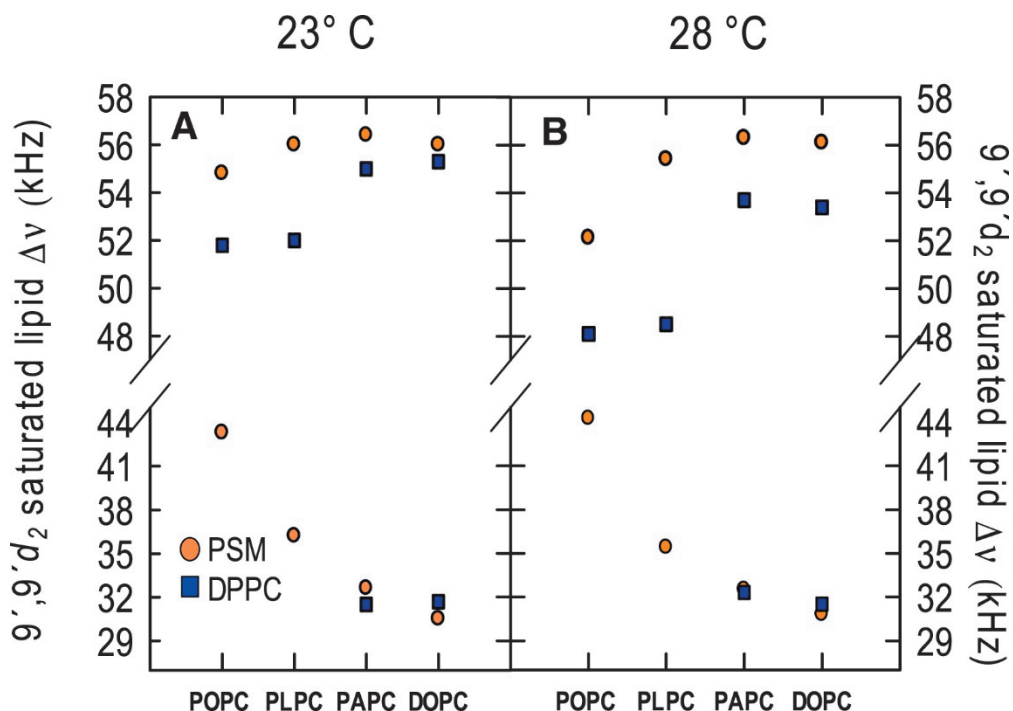
Figure 23. *Δv for site-specifically deuterated saturated PLs in either the Ld or Lo phase at 23 and 28 °C. The bilayers contained a saturated PL (9´,9´-d₂-PSM or 9´,9´-d₂-DPPC), an unsaturated PL (POPC, PLPC, PAPC or DOPC) and cholesterol (40/40/20). The figure is adapted from paper III with the permission of Cell Press.*

6. DISCUSSION

In paper I, the focus was on the size of PL head group and how it affected the acyl chain order in the fluid phase of a bilayer. In paper II, the focus was on the interactions of cholesterol with different PLs and the lipid complexity. Finally, in paper III the effect of unsaturation of PC acyl chains was explored, with the effect of cholesterol interaction with PLs on phase separation.

6.1. PL-PL interactions as studied by different probes

Probes are commonly used to study PL-PL interactions, especially for lateral segregation (206). In this thesis, several different fluorescent probes were used. In the ^{2}H NMR experiments, the probes were deuterium-labeled lipids. Understanding the phase-selectivity of the probes is of obviously important to understand the results.

6.1.1. Correlation between phase-selectivity and probes

Probes partitioning between the lipid phases will affect which environment the probes will report from. It has been observed that the structure of the probes affects their phase-selectivity (206). Most partitioning experiments have investigated the probe partitioning between gel and Ld phases (214, 215). Probes that partition selectively into the Lo phase have been more difficult to find than gel and Ld phase partitioning probes (46). For sensitive detection of Lo-phase we have used the fluorescent probe tPA. While the reported $K_P^{Lo/Ld}$ values for tPA vary between studies (216, 217), we have successfully used tPA to detect the formation of the Lo phase (Fig. 19, 20 and 22 and (149)).

Both the structure of the fluorophore and the molecule to which it is attached affect the phase-selectivity of the probe. In addition, the site of attachment of a fluorophore to a lipid also makes a difference, because polar or bulky fluorophores attached to the acyl chains (*e.g.* NBD or TopFluor) can disrupt acyl chain packing, and the probes may therefore not partition into the gel phase (206, 218). The probes that partition into the tightly packed gel phase often have their fluorophores attached closer to the terminal methyl groups, to the head group or further out in the aqueous phase linked through a long spacer, where the disruption of interactions between neighboring

lipids by the fluorophores is less. Some fluorophores like DPH partitions equally into gel and Ld phases, at least in commonly used lipid systems like POPC/PSM bilayers (Figure S1 in paper I). The attachment of propionyl-DPH to a palmitoyl-lyso-PC diminished the probes affinity for the gel phase compared to DPH itself (Fig. S1 in paper I). Probably the smaller size and possible distribution in the center of the bilayer of the DPH is the cause for the higher gel phase partitioning of DPH.

If the fluorophore is attached to a PL which contains an unsaturated acyl chain, the latter favors partitioning of the probe to the Ld phase, as was observed for both 18:1-DPH-PC (Fig. S1 in paper I) and O-tPA-PC (Fig. S1 in paper II). When NBD fluorophores were attached to the head group of PEs, acyl chain structure determined the probe's phase selectivity (219). Longer and saturated chains led to predominant partitioning into the gel phase, while shorter chains and a $\Delta 9$-*cis* unsaturated chains favored partitioning into Ld phase.

Parinaric acid, a fatty acid, which has four conjugated double bonds, shows different partitioning into the gel phase depending on the double bond isomers present. The *cis* double bonds in *cis*-parinaric acid, *e.g.* (*cis-trans-trans-cis*) favor Ld phase partitioning (220). The cis double bonds results in $K_p^{gel/Ld}$ of 0.6 for in *cis*-parinaric acid in PDPC/DPPC bilayers. However, with mostly *trans* double bonds as in tPA, the $K_p^{gel/Ld}$ is 3 in the same bilayers, and even higher in other high-T_m lipid -containing bilayers (Fig S1 in paper 1) and (199). The *trans* double bonds make the hydrocarbon chain more extended and straight, similar to acyl chains in gel phase lipids. Attaching a tPA to an SM molecule led to only marginally lower affinity for the SM-rich gel phase than observed for free tPA (201). Overall, smaller probes with long hydrocarbon chains with bulky fluorescent groups closer to the membrane interior or in the aqueous phase seem to be the key for high gel phase partitioning (206). In contrast, an unsaturated chain or a short saturated chain in combination with bulky fluorophores often leads to high partitioning into Ld phase.

6.1.2. *Experimental considerations with phase-selective probes*

Fluorescence anisotropy of a probe can be used to measure lateral segregation based on changes in acyl chain order (117, 199). When gradually replacing a low-T_m lipid with a high-T_m one, a gel phase may be formed. In paper I, there were quite small changes in the acyl chain order upon addition of different sphingolipids to fluid POPC bilayers at 23 °C (Fig. 11). However, a major increase in acyl chain order was

observed when a gel phase was formed. In this gel phase, the acyl chain order was dramatically different from the fluid phase (paper I). Therefore, if the probe partitions into the gel phase, changes in anisotropy are often clearly detected (221). This was for example indicated by fluorescence anisotropy of DPH in laterally segregated POPC/PSM bilayers but not with 18:1-DPH-PC (Fig. S1 in paper 1 and (201)). 18:1-DPH-PC did not detect the onset of the PSM gel phase in POPC/PSM bilayers (Fig S1 in paper I), because it shows very inefficient partitioning into the gel phase. However, at sufficiently high concentrations of PSM, sufficient fraction of 18:1-DPH-PC will partition into the gel phase and detect it. However, if 18:1-DPH-PC is used to detect gel phase onset it would become very difficult to determine the phase boundary. On the other hand, the gel-phase favoring probe tPA did not show a linear fluorescence anisotropy increase but a more sigmoidal one, suggesting formation of a gel phase (Fig. 11). This marked increase in fluorescence anisotropy of tPA upon gel or Lo phase formation, makes it a suitable for the detection of phase boundaries. In addition, using time-resolved fluorescence of tPA, similar change in acyl chain order can be observed (Fig. 19 and (179)).

Probe partitioning is often measured isothermally (*e.g.* 23 °C) and with specific lipid components. At a different temperature, the phase-selectivity of the probes could change. This is probably one of the reasons why a clear melting was not indicated by the average fluorescence lifetime of tPA-SM in POPX/PSM/Chol bilayers (Fig. 1 in paper II). Anisotropies of tPA and 18:1-DPH-PC were measured as a function of temperature in phase-separated bilayers containing POPC and different sphingolipids (Fig. 4 in paper I). Here, tPA reported clear melting of the gel phase, while 18:1-DPH-PC did not, demonstrating that the probes maintained similar phase-selectivity at higher temperature. Similar results were observed in the quenching experiments (Fig. 12).

Changing the lipid components could also affect the probe partitioning into the gel phase, *e.g.* because of different packing of the lipids in the gel phase. Both DPH and tPA reported the gel phase formation in POPC/PSM bilayers (117, 175, 179). In contrast, while tPA reported a non-linear increase in fluorescence anisotropy in POPC bilayers with increasing GlcPCer or GalPCer concentrations, DPH had a linear increase in anisotropy (Fig. 11). A linear increase in fluorescence anisotropy could indicate that no gel phase is formed. The non-linear increase in anisotropy and lifetimes of tPA confirms a phase separation, in agreement with the higher gel phase partitioning that has been reported with tPA vs DPH (200). In paper III and (179), an

unsaturated PL was exchanged gradually for PSM or DPPC to detect the formation of Lo or gel phases. Varying the number of double bonds in unsaturated PCs led to distinct non-linear increases of fluorescent lifetimes at the phase boundary. This was probably because the difference in the acyl chain order between the gel/Lo and Ld phase changed depending on PCs, but also because tPA probably had different partitioning into the different gel and Lo phases present. Still, reasonable fluorescence lifetimes of tPA trend curves were acquired in paper III.

Phase-selectivity of the probes can also be determined from FRET. When using fluorescent probes with different phase selectivity, they separate when new phases are formed, or the probes come in contact when phases melt. Both scenarios will affect the FRET efficiency, and therefore FRET can be used to detect phase boundaries (166). Several phase diagrams have been constructed with the FRET approach (168, 180).

6.1.3. Lipid-analogs as probes

It has long been a goal to selectively mimic lipid behavior to examine individual lipid species instead of using phase-selective probes alone (46). However, because lipids are small molecules, small modifications can easily bias the lipid′s behavior (222). Examples include cholesterol analogs, *e.g.* NBD fluorophore attachment to the side chain of cholesterol. This NBD turns the OH-group of cholesterol to the interior of the bilayer, and the sidechain/fluorophore to the surface (223). NBD-Chol also show different phase partitioning than cholesterol, making it very unsuitable to mimic cholesterol behavior (224). Other fluorescent or spin-labeled sterol analogs have the correct orientation, but can differ in their polarity, phase partitioning, membrane-water partitioning and ordering of PLs as compared to cholesterol (98). An example is TF-Chol which has similar relative partitioning coefficients between fluid DPPC and PSM (Fig. 21), as has CTL (98), TF-Chol also has similar Lo phase partitioning behavior as cholesterol (46), but does not induce cholesterol-like ordering of PLs (225). Thus, depending on the method used or parameter examined, a lipid-analog probe may or may not be suitable to measuring the parameter under investigation.

Lipid-analog probes can also be phase-selective, *e.g.* low-T_m lipid-analog probes, probably also show low partitioning to the gel phase. POPC has $K_p^{gel/Ld}$ of 0.5 (117) while O-tPA-PC has $K_p^{gel/Ld}$ at ~0.35 in POPC/PSM bilayers. The lower $K_p^{gel/Ld}$ of O-tPA-PC compared to POPC could be due to the four conjugated double bonds or that the oleoyl chain in O-tPA-PC is in the *sn*-1 instead of *sn*-2 chain. The different phase-

selectivity of O-tPA-PC and tPA-SM was indicated by an additional fluorescence lifetime component found for tPA-SM in the ternary POPC/PSM/Chol bilayers (Fig. 14). This probably has to do with tPA-SM partitioning into the Lo phase, while O-tPA-PC favored the Ld phase.

There also non-fluorescent lipid-analog probes, *e.g.* deuterated lipids. These are used for both ^{2}H NMR and SANS (130). Exchange of hydrogen to deuterium in the acyl chain is minimally disruptive on lipid behavior compared to other lipid-analogue probes, because only the molecular weight is increased slightly. However, perdeuteration decreases the T_m slightly, by around 2-3 °C (171). Site-specifically deuterated lipids are even less disruptive because only two hydrogens are exchanged for deuterium. In conclusion, lipids are best mimicked by deuterated lipids, but for certain practical purposes fluorescent lipid analogs can also be used. However, understanding probe's possible effect on phase behavior is very important so that one can draw biological conclusions.

6.2. Cholesterol-PL interactions

Cholesterol-PL interactions depend on several factors, *e,g.* PL structure, the phases present, complexity of the bilayer, and temperature. Sterol-PL interactions can be studied *e.g* by sterol partitioning, acyl chain ordering by cholesterol in both binary and more complex bilayers, and ordered domain thermostability. All of these approaches were used in the present study.

6.2.1. Effect of PL structure on cholesterol-PL interactions

Cholesterol interacts differently with saturated vs unsaturated PLs. Addition of cholesterol to a bilayer of a saturated PL leads to the formation of an Lo phase. However, the exact Ld-Lo or gel-Lo phase coexistence boundaries are composition- and temperature-dependent, and can thus be difficult to define (157). The results with unsaturated PLs/cholesterol bilayers are even less clear (157). In an unsaturated PL bilayer, inclusion of cholesterol leads to substantially higher acyl chain order (Fig. 11). The higher acyl chain order is indicative of Lo-phase, and has therefore led to an interpretation of Ld-Lo phase coexistence (117, 175). Lipid diffusion is also slowed down slightly with the addition of cholesterol to unsaturated PL bilayers, as would be expected with Lo phase formation (181, 226). However, coexistence of two phases

cannot be detected with ^{2}H NMR (181) or FRET (180, 227). Thus, a likely interpretation is that cholesterol slowly transforms the Ld phase into an Lo phase without any distinct phase transition. A pressure perturbation calorimetry study suggested that POPC and cholesterol form an intermediate state between random mixing and phase separation (228). Starting with a bilayer initially containing 20 mol% cholesterol and an unsaturated PXPC or DXPC and gradually replacing the unsaturated PC for DPPC or PSM led to a clear discontinuity in tPA fluorescence lifetime trend curves (paper III), indicative of a phase separation. If unsaturated PL/Chol bilayers would have two coexisting phases, the addition of a saturated PL would probably not lead to a marked separation at low SM concentrations (paper III). Therefore, we suggest that the Lo-Ld phase coexistence region forms after addition of sufficient amounts of a saturated PL. In agreement with published phase diagrams (149, 168, 229).

Effects of cholesterol is also affected by the structure of the saturated PLs. Formation of Lo phase differs between saturated PCs and SM (Fig. 20 and 22). The order parameter profiles of perdeuterated palmitoyl chains of DPPC or PSM in fluid bilayers shows that the acyl chain carbons closer to the water interface are more affected by cholesterol more than the carbons further away (102). When cholesterol was added to fluid bilayers containing site-specifically deuterated PSPC or SSM the spectra showed that the order profile of carbons in the acyl chain were highest in the middle and lower in both the beginning and end of the acyl chain (123).

In paper II, we found that unsaturated GPLs with different head groups in PSM–containing bilayers affected acyl chain order of PSM more in the absence than in the presence of cholesterol (Fig. 15). Previous studies on cholesterol's interaction with GPLs with different head groups showed varied results. In studies on sterol partitioning between bilayers and MβCD, cholesterol affinity decreased in the order of PS > PC > PE (103). In binary cholesterol-PL bilayers, cholesterol ordered the acyl chains of POPC more than that of POPE (230, 231). However, the final acyl chain order after addition of cholesterol was very similar between PE and PC bilayers. In ternary bilayers, ordered domain thermostability was highest when including POPE in POPX/PSM/Chol bilayers as measured with DPH quenching (231). One way to understand the sterol's interactions with GPLs with different head groups is to compare results obtained with saturated GPLs. DSC studies have shown that 50 mol% cholesterol does not completely abolish the gel-Ld phase transition enthalpy in di-steraoyl-PS and di-steraoyl-PE bilayers (232), contrary to what observed for saturated PCs and SMs (155, 233). CTL quenching has been used to detect if ordered domains

are enriched in CTL (234). When palmitoyl-ceramide-PS or di-palmitoyl-PS were included in POPC/XPS/Chol (6/3/1) bilayers, CTL-enriched domains were only found for palmitoyl-ceramide-PS (235). In another study, CTL-enriched domains were not found with palmitoyl-ceramide-PE or DPPE (236). In contrast to results with bilayers containing PSM or DPPC (125). These results suggested that the sphingosine backbone favored enrichment of CTL in the ordered domains but serine and amino phospholipid head group decreased the amount of CTL in the domains. Altogether, interactions of cholesterol with saturated PE and PS were much weaker as compared to saturated PCs or SMs. In paper II it was difficult to see clear differences between interactions of cholesterol with POPE vs POPS vs POPC. For example, the disappearance of a third long lifetime component of tPA-SM in POPC/XPX/Chol bilayers after 30 °C (Fig. 14), there was no difference in ordered domain thermostability between POPC, POPE and POPS. The high cholesterol concentration (~30 mol%) used in some experiments in paper II could make it more difficult to observe differences between the GPLs, because of the low SM/sterol ratio.

6.2.2. Other factors affecting cholesterol-PL interactions

Cholesterol-PL interactions have often been investigated by studying sterol partitioning between cyclodextrin and bilayers (106). However, interpretations of such studies is complicated upon the inclusion of higher amounts of sterol in the bilayer. With high concentrations of sterol in a saturated PL bilayer, phase separation could occur and sterol would not only partition between MβCD and bilayers, but also laterally between bilayer phases. If the sterol is present in the Ld or Lo phase it can dramatically alter the sterol affinity for the PL (237). Molecular dynamics (MD) simulations show that MβCD preferably extracts cholesterol from the Ld phase, because of the high energy cost of absorbing cholesterol from the Lo phase (238). However, in order to measure sterol affinity for pure PL bilayers in fluid non-segregated state, the temperature has to be above the T_m of the saturated PLs. Therefore, CTL and TF-Chol partitioning was performed at 50 °C and with a low sterol concentration (Fig. 21).

The number of lipid components in a bilayer and temperature will also affect cholesterol-PL interactions. In binary PL/Chol bilayers, cholesterol has no other choice but to interact with the PL present, even if the sterol affinity for that lipid would be low. Therefore, it is interesting to compare the acyl chain order in the binary PL/cholesterol bilayers to that of the Lo-phase in ternary bilayers with ^{2}H NMR

measurements (167, 239). When the number of double bonds in the PCs were varied in XXPC/9′,9′-d$_2$-PSM/Chol (4/4/2) bilayers, the largest changes in Δν were for the deuterated lipids in the fluid phase, not in the Lo-phase (Fig. 23A). This probably occurs because there is little of the unsaturated PLs in the Lo phase. In DOPC/SSM/Chol (1/1/1) bilayers, deuterated 10′,10′-d$_2$-SSM reported similar Δν in the Lo phase as 10′,10′-d$_2$-SSM in SSM/Chol (1/1) bilayers. In POPC/PSM/Chol (4/4/2) bilayers (Fig. 23), Δν of 9′,9′-d$_2$-PSM was similar to the Δν of 9′,9′-d$_2$-PSM in binary PSM/Chol (2:1) bilayers (Fig. 15C). In time-resolved fluorescence studies of different tPA-PLs, the Ld phase partitioning O-tPA-PC probe lacked a long third lifetime component, which was observed for the Lo phase partitioning tPA-SM probe (Fig. 14). In addition, tPA-SM reported similar average fluorescent lifetimes in binary and ternary bilayers, especially at lower temperatures (Fig. 1 in paper II). Therefore, the results suggest that SM and cholesterol interactions in the Lo-phase, and not the cholesterol or SM interactions with the unsaturated PLs, mostly determine the acyl order in the Lo phase. However, when only a single Pake doublet was observed in the ^{2}H NMR spectra, the 9′,9′-d$_2$-PSM had lower Δν in ternary bilayers compared to binary bilayers (Fig. 15A and C). Similar results were found for M$_1$ of perdeuterated PSM in another study (207). When no two-component spectrum was observed in ^{2}H NMR, either an average order of the different phases were observed or the bilayers were devoid of phase separation (176). This could explain why there was a difference in lipid order in the binary PL/Chol vs ternary bilayers. The relatively high acyl chain order for 9′,9′-d$_2$-PSM in POPX/Chol bilayers (Fig. 15C) suggests that phase separation occurred at the lower temperatures. With increased temperature difference in the acyl chain order between the binary and ternary bilayers increased (Fig. 15C), probably because the Lo-phase is less thermostable in ternary bilayers. In addition, the rigid cholesterol molecule is much less affected by temperature than unsaturated co-lipids (240).

6.3. Influence of sterol affinity of PLs on lateral segregation

In paper III, we started with a bilayer containing an unsaturated PC and cholesterol and gradually replaced the unsaturated PC for PSM or DPPC. With PSM, a lower concentration was required to form ordered domains in the presence of 20 mol% cholesterol than in the absence of cholesterol (~20 vs ~30 mol% PSM). While the ordered domains in the cholesterol-containing membranes would likely be Lo phase as indicated by previous phase diagrams (161), and the domains formed in absence

of cholesterol should be gel phase, they are both ordered domains that form in Ld phase bilayers. Less PSM was required when the number of double bonds increased in either hybrid or symmetrical PCs. It has been suggested that aversion of cholesterol for polyunsaturated PLs could promote formation of Lo-phase (241, 242). Still, in DPPC-containing bilayers increasing the unsaturation of PCs promoted much less formation of domains than in the PSM-containing bilayers (Fig. 24). When comparing effect how cholesterol promoted lateral segregation with the sterol-partitioning data in paper III, a clear correlation was observed (Fig 24A). The more cholesterol preferred the saturated PL to the unsaturated PLs, the more it promoted lateral domain formation. The difference amount of saturated PL required to form a gel vs Lo phase is the measure of how strongly cholesterol affected the lateral segregation, as shown on the y-axis (Fig. 24A). Preferences of cholesterol for PLs is indicated the relative partitioning coefficient K_R, which is the K_x of sterol analogs for high-T_m lipid bilayers, divided by the K_x for the low-T_m lipid bilayers. K_R is shown on the x-axis (Fig. 24A). In paper III, the low-T_m lipid was an unsaturated PC and the high-T_m lipid was PSM or DPPC. Based on this correlation, we developed a model to explain the phenomenon (Fig. 24B). In this model, a low sterol affinity of the unsaturated PL could lead to promoted formation of ordered domains, but only in the presence of saturated PL, for which the sterol has sufficiently high affinity (Fig. 24B). While sterol had low affinity for polyunsaturated PLs, its moderate affinity for DPPC, as compared to PSM, had only a slight effect on promoting formation of ordered domains. From a biological perspective, this is interesting, because cells have mostly saturated SMs and hardly any saturated PCs (243). Other studies have also found that cholesterol promotes formation of ordered domains (229, 244). However, no quantitative connection between K_R has not been made previously. Some phase diagrams have not shown cholesterol to promote formation of ordered domains, but in these often have been using different lipids, either a saturated PC (161) or a more complex SM mixture like brain-SM (168). In ternary bilayers the tielines are much steeper for SM than in saturated PC bilayers, indicating that K_R has an effect on the composition of the Lo-phase, and not only on promoting the formation of Lo-phase (168, 245). In conclusion, applying the model to different SMs and mixtures of SM would be an interesting aim for future studies.
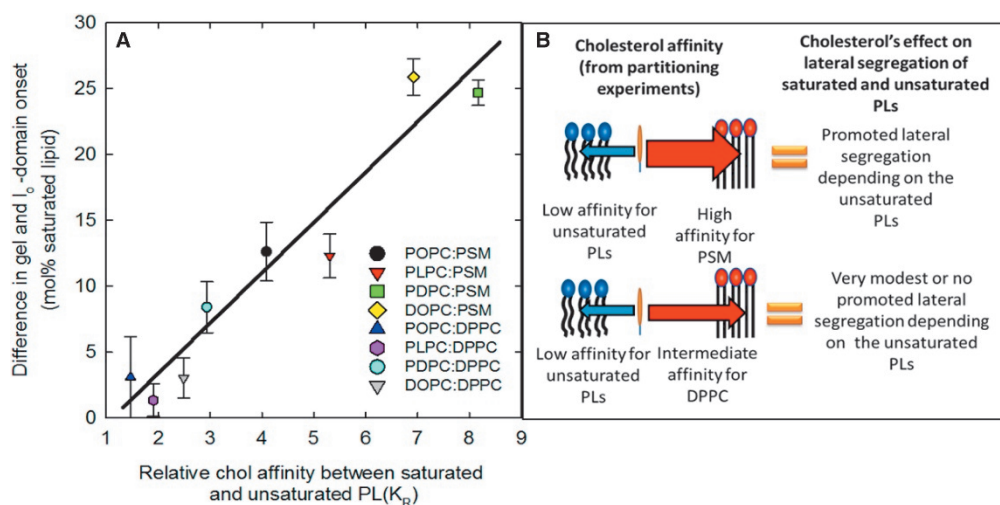
Figure 24. *The relative affinity of cholesterol between unsaturated and saturated PLs correlates with the cholesterol-promoted formation of ordered domains as measured by fluorescent tPA-lifetimes. Panel A shows the correlation and panel B shows a model of how the different parameters correlate. Some values were taken from (104). The figure is adapted from paper III with the permission of Cell Press.*

How sterol-PL affinity results in phase separation is still unclear, but it could be through clustering of fluid SMs, which could be facilitated by having cholesterol close by. Alternatively, the stability of the clusters could be increased by cholesterol. In a bilayer containing unsaturated PLs, cholesterol could be pushed closer to SMs, further promoting clustering and eventually domain formation. The "push/pull" effect of unsaturated PLs and saturated PLs has been calculated as 'unlike nearest-neighbor interaction free energies' (ωAB) between lipids, from various experiments (237, 241, 246, 247). Based on this parameter, the likelihood that sterol interacts with a certain PL can be compared. An example is provided by ultraviolet-crosslinking analogs for DPPC and cholesterol, whose interaction energy is $\omega AB = +12 \pm 19$ cal/mol in the Ld phase, indicating a slight push of the sterol by DPPC. However, the sterol-DPPC interaction is more favorable than the interactions of a sterol and a polyunsaturated PL. This was observed when DPPC was added to DOPC/Chol or PAPC/Chol bilayers (Fig. 22). In addition, in the Lo phase, the same lipids have an interaction energy of $\omega AB = -260 \pm 6.3$ cal/mol (247). In this case, the sterol was "pulled in" by DPPC in the Lo phase. The push/pull effect of sterol on unsaturated vs saturated PLs is even larger increase of SMs (237), in agreement with our model. The favorable interaction of SMs and cholesterol in the Lo-phase compared to the Ld phase could lead to promotion of the formation of Lo-phase. Possibly, ordering of nearby SMs by cholesterol could be

56

greater than the by saturated PCs. However, only a small difference was found in the cholesterol-induced ordering of fluid myristoyl-SM compared to DMPC bilayers (90). The hydrogen-bond network between SMs could affect SM clustering and how cholesterol affects this process (119). Hydrophobic mismatch between different PLs can lead to gel phase formation may also explain Lo phase formation and Lo phase thermostability (248, 249). The hydrophobic mismatch between domains create line tension. The thickening effect of cholesterol on bilayers can lead to line tension between the cholesterol-rich and -poor phase (213). In other studies, line tension had a larger effect on the domain size than phase boundaries (168, 182).Yet, others caution against drawing strong conclusions from single lipid composition samples (250). Hydrophobic mismatch does lead to lateral segregation but it is difficult to explain the difference of Lo phase formation between saturated PC and SM (paper III) only as the effect of hydrophobic mismatch. For example, the difference in Δv of $9',9'\text{-}d_2$-PSM between Ld and Lo-phase in PAPC/Chol bilayers were similar to difference of Δv $9',9'\text{-}d_2$-DPPC in a similar PAPC/Chol bilayer (Fig 23A). However, the effect of cholesterol on lateral segregation was that cholesterol reduction the concentration of saturated PL required for Lo-phase formation ~22 mol% for PSM to ~7 mol% for DPPC by cholesterol. Therefore, a model that includes sterol affinity (Fig. 24) could explain the promotion of ordered domains better than hydrophobic mismatch of lipids.

6.4. Biological implications

There are several parameters that need to be accounted for when extrapolating from model membranes to biological ones. Model membranes have been extensively utilized to understand the individual properties of lipid species. However, a diverse mixture of lipids is required in order to mimic biological membranes. In addition, biological membranes contain thousands of proteins as well as an attached cytoskeleton (63). However, simple model membranes have allowed one to understand how structural modifications modify the phase behavior. For example, PLs with longer and saturated acyl chains form more thermostable phases, and are more rigid compared to PLs with shorter and unsaturated acyl chains (137, 179). Most commonly, binary and ternary bilayers have been studied (157, 161), but also quaternary bilayers have been studied (163). In paper II we also included a five-component bilayer to try to better mimic biological membranes. However, the difficulty in finding nanodomains in live cells (30) reflects the very different nature of model bilayers vs complex biological membranes.

Plasma membrane derived bilayers (GPMVs) have been studied to better study the effects lipid components on lateral segregation. The polarity-sensitive probe, C-laurdan, reported that the calculated GP (indicating lipid order) difference between Lo and Ld phase in the GUVs was very large (46). However, in GPMVs GP between Ld and Lo phases was much smaller. Probably indicating that inclusion of more biologically relevant lipids and proteins leads to smaller differences in lipid order between Ld and Lo phase. From a biological point of view, large differences in acyl chain order are probably unfavorable because of the line tension between the interfaces and the macroscopic phase separation (182). When comparing phases between GUVs and GPMVs, it was observed that lipid-analog probes partitioned more favorably to the Lo phase in the GPMVs than in the GUVs (46). A limitation of light microscopy studies is the requirement of macroscopic phase separation (171), which often require including di-unsaturated low-T_m lipids. While some lipidomics studies suggest that biological membranes indeed contain di-unsaturated PLs (251), others show that most PLs have a saturated chain in the *sn*-1 position (243). It has also been shown that brain-SM forms smaller domains than PSM (168), suggesting that more complex mixtures of SMs could lead to more dynamic nanoscopic domains. Fluorescence spectroscopy methods, *e.g.* tPA fluorescence anisotropy and lifetime measurements are therefore suitable for detecting nanodomains in model membranes. However, because their excitation and emission wavelengths are in the ultraviolet range, they are not suitable for cell experiments because of low quantum yield and possible autofluorescence from the cells (252). Still, the results obtained with these methods and together with ^{2}H NMR experiments performed included in this thesis, may allow one to estimate in which cells and organelles biological nanodomains are most likely to form.

A major difference between the plasma membrane and most model membranes is the trans-bilayer PL asymmetry (253). In addition, cholesterol probably has an asymmetric distribution, but this is yet to be determined (254). The enrichment of SM in the outer leaflet of the plasma membrane indicates the enrichment of cholesterol in this leaflet (255). Trans-bilayer PL asymmetry of plasma membrane is partially retained in GPMVs, but it is not clear to what degree (44). Recently, asymmetric model membranes have been created both in vesicles (256) and supported bilayers (257). Molecular dynamics simulations have also started to simulate asymmetric membranes (77, 258). Because asymmetric membranes have leaflets with different lipid compositions, interleaflet coupling could probably enhance lateral segregation. While most studies suggest this, it is probably dependent very much on which lipids

and in which leaflet they are included (256, 259-261). Interleaflet coupling could also affect properties other than lateral segregation. For instance, 24:1-SM was in one leaflet affected the lateral diffusion of lipids in the other leaflet (76, 77). Despite the potential of asymmetric bilayers, the difficulty in controlling the specific lipid asymmetry hampers their use (262).

Results in paper III showed that cholesterol promotes ordered domain formation, so that lower concentrations of SMs are required for ordered domain formation. For example, less than 10 mol% SM was required for formation of ordered domains in PAPC/Chol bilayers at 23 °C (Fig. 20). The ability of SMs to form ordered domains even in bilayers containing POPS and POPE (paper II) suggests that it they are partially present in the inner leaflet, they could also form ordered domains. Polyunsaturated PLs may enhance the formation of ordered domains, at least in the presence of cholesterol. It seems that lateral segregation in PAPC/PSM/Chol bilayers is less affected by temperature than in POPC/PSM/Chol bilayers (Fig. 23). This would suggest that nanodomain formation is more likely at physiological temperatures if polyunsaturated PLs are present. In membranes of many neural cells, there is a high concentration of polyunsaturated PLs. Thus indicating that nanodomains could form therein (263).

7. CONCLUSIONS

Cholesterol plays an important role in many cellular membranes (92). One of its possible roles is to facilitate lipid raft formation (23). However, cholesterol does not form lipid rafts or nanodomains with all lipids, because its interaction differ dramatically depending on the PL. (103). Structurally different lipids often laterally segregate even in the absence of cholesterol (179). However, cholesterol changes the phase properties and promotes the formation of Lo-domains (97). The combination of cholesterol-PL interaction and PL-PL interactions and the effects on lateral segregation have been studied in the papers included in this thesis. Several major conclusions can be drawn from the results:

i)   Information about the acyl chain order from co-existing phases could be obtained with site-specifically deuterated PLs, and by both fluorescent phase-selective and lipid analog probes.

ii)   Acyl chain order in the Ld phase is affected by the miscibility of the high-T_m lipid in the Ld phase, and also by the size of the head group.

iii)   Lateral segregation in cholesterol-containing membranes was affected more by the number of double bonds in the low-T_m lipid acyl chains than the structure of the head group of the low-T_m lipid.

iv)   Cholesterol promotes formation of ordered domains. The effect depends on its affinity of the low- vs high-T_m lipid.

As demonstrated in this thesis, different structural features of lipids like head group size and number of double bonds in the acyl chain affect nanodomain formation. This knowledge of lipids could be used when synthesizing new phase-selective probes, as shown in paper I and II. Phase diagrams were used to plan more time effective studies where many different PLs could be compared systematically. The quantitative parameters like K_R can be used to estimate which lipids most readily form sterol-rich domains, possibly reducing the need to make complete phase diagrams. Eventually, by combining these results with experiments in biological membranes, a more detailed picture of the function and structure of nanodomains in cells could likely be generated.

8. REFERENCES

1. Nelson, D. L., and M. M. Cox. 2017. Lehninger, Principles of Biochemistry. Macmillan higher education, Houndmills, Basingstoke, England.

2. van, M. G. 2005. Cellular lipidomics. EMBO J. 24: 3159-3165.

3. Hanford, M. J., and T. L. Peeples. 2002. Archaeal tetraether lipids: unique structures and applications. Appl. Biochem. Biotechnol. 97: 45-62.

4. Bell, M. V., R. J. Henderson, and J. R. Sargent. 1986. The role of polyunsaturated fatty acids in fish. Comp Biochem. Physiol B 83: 711-719.

5. Poger, D., B. Caron, and A. E. Mark. 2014. Effect of methyl-branched fatty acids on the structure of lipid bilayers. J. Phys. Chem. B 118: 13838-13848.

6. Eme, L., A. Spang, J. Lombard, C. W. Stairs, and T. J. G. Ettema. 2017. Archaea and the origin of eukaryotes. Nat. Rev. Microbiol. 15: 711-723.

7. Ettema, T. J. 2016. Evolution: Mitochondria in the second act. Nature 531: 39-40.

8. Merrill, A. H., Jr., E. M. Schmelz, D. L. Dillehay, S. Spiegel, J. A. Shayman, J. J. Schroeder, R. T. Riley, K. A. Voss, and E. Wang. 1997. Sphingolipids--the enigmatic lipid class: biochemistry, physiology, and pathophysiology. Toxicol Appl Pharmacol 142: 208-25.

9. Chandler, C. E., and R. K. Ernst. 2017. Bacterial lipids: powerful modifiers of the innate immune response. F1000Res. 6.

10. Desmond, E., and S. Gribaldo. 2009. Phylogenomics of sterol synthesis: insights into the origin, evolution, and diversity of a key eukaryotic feature. Genome Biol. Evol. 1: 364-381.

11. Patton, S. 1970. Correlative relationship of cholesterol and sphingomyelin in cell membranes. J Theor Biol 29: 489-91.

12. Shimshick, E. J., and H. M. McConnell. 1973. Lateral phase separation in phospholipid membranes. Biochemistry 12: 2351-2360.

13. Simons, K., and E. Ikonen. 1997. Functional rafts in cell membranes. Nature 387: 569-72.

14. De, W. P. 2000. A century of thinking about cell membranes. Annu. Rev. Physiol 62: 919-926.

15. Gorter, E., and F. Grendel. 1925. on bimolecular layers of lipoids on the chromocytes of the blood. J. Exp. Med. 41: 439-443.

16. Robertson, J. D. 1957. New observations on the ultrastructure of the membranes of frog peripheral nerve fibers. J. Biophys. Biochem. Cytol. 3: 1043-1048.

17. Singer, S. J., and G. L. Nicolson. 1972. The fluid mosaic model of the structure of cell membranes. Science 175: 720-31.

18. Verkleij, A. J., R. F. Zwaal, B. Roelofsen, P. Comfurius, D. Kastelijn, and L. L. Van Deenen. 1973. The asymmetric distribution of phospholipids in the human red cell membrane. A combined study using phospholipases and freeze-etch electron microscopy. Biochim. Biophys. Acta 323: 178-193.

19. Evans, R. M., D. C. Ward, and L. M. Fink. 1979. Asymmetric distribution of plasma membrane proteins in mouse L-929 cells. Proc. Natl. Acad. Sci. U. S. A 76: 6235-6239.

20. Mouritsen, O. G., and M. Bloom. 1984. Mattress model of lipid-protein interactions in membranes. Biophys. J. 46: 141-153.

21. Simons, K., and G. van Meer. 1988. Lipid sorting in epithelial cells. Biochemistry 27: 6197-6202.

22. van, M. G., E. H. Stelzer, R. W. Wijnaendts-van-Resandt, and K. Simons. 1987. Sorting of sphingolipids in epithelial (Madin-Darby canine kidney) cells. J. Cell Biol. 105: 1623-1635.

23. Lingwood, D., and K. Simons. 2010. Lipid rafts as a membrane-organizing principle. Science 327: 46-50.

24. Duffield, A., M. J. Caplan, and T. R. Muth. 2008. Protein trafficking in polarized cells. Int. Rev. Cell Mol. Biol. 270: 145-179.

25. Yu, J., D. A. Fischman, and T. L. Steck. 1973. Selective solubilization of proteins and phospholipids from red blood cell membranes by nonionic detergents. J. Supramol. Struct. 1: 233-248.

26. Brown, D. A., and J. K. Rose. 1992. Sorting of GPI-anchored proteins to glycolipid-enriched membrane subdomains during transport to the apical cell surface. Cell 68: 533-44.

27. Hanada, K., M. Nishijima, Y. Akamatsu, and R. E. Pagano. 1995. Both sphingolipids and cholesterol participate in the detergent insolubility of alkaline phosphatase, a glycosylphosphatidylinositol-anchored protein, in mammalian membranes. J. Biol. Chem. 270: 6254-6260.

28. Coskun, U., and K. Simons. 2010. Membrane rafting: from apical sorting to phase segregation. FEBS Lett. 584: 1685-1693.

29. Lichtenberg, D., F. M. Goni, and H. Heerklotz. 2005. Detergent-resistant membranes should not be identified with membrane rafts. Trends Biochem. Sci. 30: 430-436.

30. Sezgin, E., I. Levental, S. Mayor, and C. Eggeling. 2017. The mystery of membrane organization: composition, regulation and roles of lipid rafts. Nat. Rev. Mol. Cell Biol.

31. Zidovetzki, R., and I. Levitan. 2007. Use of cyclodextrins to manipulate plasma membrane cholesterol content: evidence, misconceptions and control strategies. Biochim. Biophys. Acta 1768: 1311-1324.

32. Scheiffele, P., M. G. Roth, and K. Simons. 1997. Interaction of influenza virus haemagglutinin with sphingolipid- cholesterol membrane domains via its transmembrane domain. Embo J 16: 5501-8.

33. Hinzey, A. H., M. A. Kline, S. R. Kotha, S. M. Sliman, E. S. Butler, A. B. Shelton, T. R. Gurney, and N. L. Parinandi. 2012. Choice of cyclodextrin for cellular cholesterol depletion for vascular endothelial cell lipid raft studies: cell membrane alterations, cytoskeletal reorganization and cytotoxicity. Indian J. Biochem. Biophys. 49: 329-341.

34. Revesz, T., and M. Greaves. 1975. Ligand-induced redistribution of lymphocyte membrane ganglioside GM1. Nature 257: 103-106.

35. Spiegel, S., S. Kassis, M. Wilchek, and P. H. Fishman. 1984. Direct visualization of redistribution and capping of fluorescent gangliosides on lymphocytes. J. Cell Biol. 99: 1575-1581.

36. Harder, T., and K. Simons. 1997. Caveolae, DIGs, and the dynamics of sphingolipid-cholesterol microdomains. Curr Opin Cell Biol 9: 534-42.

37. Harder, T., P. Scheiffele, P. Verkade, and K. Simons. 1998. Lipid domain structure of the plasma membrane revealed by patching of membrane components. J Cell Biol 141: 929-42.

38. Monks, C. R., B. A. Freiberg, H. Kupfer, N. Sciaky, and A. Kupfer. 1998. Three-dimensional segregation of supramolecular activation clusters in T cells. Nature 395: 82-86.

39. Stefanova, I., V. Horejsi, I. J. Ansotegui, W. Knapp, and H. Stockinger. 1991. GPI-anchored cell-surface molecules complexed to protein tyrosine kinases. Science 254: 1016-1019.

40. Stulnig, T. M., M. Berger, T. Sigmund, H. Stockinger, V. Horejsi, and W. Waldhausl. 1997. Signal transduction via glycosyl phosphatidylinositol-anchored proteins in T cells is inhibited by lowering cellular cholesterol. J. Biol. Chem. 272: 19242-19247.

41. Zech, T., C. S. Ejsing, K. Gaus, W. B. de, A. Shevchenko, K. Simons, and T. Harder. 2009. Accumulation of raft lipids in T-cell plasma membrane domains engaged in TCR signalling. EMBO J. 28: 466-476.

42. Munro, S. 2003. Lipid rafts: elusive or illusive? Cell 115: 377-388.

43. Scott, R. E. 1976. Plasma membrane vesiculation: a new technique for isolation of plasma membranes. Science 194: 743-745.

44. Baumgart, T., A. T. Hammond, P. Sengupta, S. T. Hess, D. A. Holowka, B. A. Baird, and W. W. Webb. 2007. Large-scale fluid/fluid phase separation of proteins and lipids in giant plasma membrane vesicles. Proc. Natl. Acad. Sci. U. S. A 104: 3165-3170.

45. Levental, K. R., and I. Levental. 2015. Giant plasma membrane vesicles: models for understanding membrane organization. Curr. Top. Membr. 75: 25-57.

46. Sezgin, E., I. Levental, M. Grzybek, G. Schwarzmann, V. Mueller, A. Honigmann, V. N. Belov, C. Eggeling, U. Coskun, K. Simons, and P. Schwille. 2012. Partitioning, diffusion, and ligand binding of raft lipid analogs in model and cellular plasma membranes. Biochim. Biophys. Acta 1818: 1777-1784.

47. Levental, I., D. Lingwood, M. Grzybek, U. Coskun, and K. Simons. 2010. Palmitoylation regulates raft affinity for the majority of integral raft proteins. Proc. Natl. Acad. Sci. U. S. A 107: 22050-22054.

48. Sengupta, P., A. Hammond, D. Holowka, and B. Baird. 2008. Structural determinants for partitioning of lipids and proteins between coexisting fluid phases in giant plasma membrane vesicles. Biochim. Biophys. Acta 1778: 20-32.

49. Lorent, J. H., B. Diaz-Rohrer, X. Lin, K. Spring, A. A. Gorfe, K. R. Levental, and I. Levental. 2017. Structural determinants and functional consequences of protein affinity for membrane rafts. Nat. Commun. 8: 1219.

50. Diaz-Rohrer, B. B., K. R. Levental, K. Simons, and I. Levental. 2014. Membrane raft association is a determinant of plasma membrane localization. Proc. Natl. Acad. Sci. U. S. A 111: 8500-8505.

51. Levental, I., M. Grzybek, and K. Simons. 2011. Raft domains of variable properties and compositions in plasma membrane vesicles. Proc. Natl. Acad. Sci. U. S. A 108: 11411-11416.

52. Fujiwara, T., K. Ritchie, H. Murakoshi, K. Jacobson, and A. Kusumi. 2002. Phospholipids undergo hop diffusion in compartmentalized cell membrane. J. Cell Biol. 157: 1071-1081.

53. Liu, A. P., and D. A. Fletcher. 2006. Actin polymerization serves as a membrane domain switch in model lipid bilayers. Biophys. J. 91: 4064-4070.

54. Honigmann, A., S. Sadeghi, J. Keller, S. W. Hell, C. Eggeling, and R. Vink. 2014. A lipid bound actin meshwork organizes liquid phase separation in model membranes. Elife. 3: e01671.

55. Gowrishankar, K., S. Ghosh, S. Saha, C R, S. Mayor, and M. Rao. 2012. Active remodeling of cortical actin regulates spatiotemporal organization of cell surface molecules. Cell 149: 1353-1367.

56. Eggeling, C., C. Ringemann, R. Medda, G. Schwarzmann, K. Sandhoff, S. Polyakova, V. N. Belov, B. Hein, M. C. Von, A. Schonle, and S. W. Hell. 2009. Direct observation of the nanoscale dynamics of membrane lipids in a living cell. Nature 457: 1159-1162.

57. Sezgin, E. 2017. Super-resolution optical microscopy for studying membrane structure and dynamics. J. Phys. Condens. Matter 29: 273001.

58. Honigmann, A., V. Mueller, H. Ta, A. Schoenle, E. Sezgin, S. W. Hell, and C. Eggeling. 2014. Scanning STED-FCS reveals spatiotemporal heterogeneity of lipid interaction in the plasma membrane of living cells. Nat. Commun. 5: 5412.

59. Kraft, M. L. 2016. Sphingolipid Organization in the Plasma Membrane and the Mechanisms That Influence It. Front Cell Dev. Biol. 4: 154.

60. Kraft, M. L. 2013. Plasma membrane organization and function: moving past lipid rafts. Mol. Biol. Cell 24: 2765-2768.

61. Toulmay, A., and W. A. Prinz. 2013. Direct imaging reveals stable, micrometer-scale lipid domains that segregate proteins in live cells. J. Cell Biol. 202: 35-44.

62. LaRocca, T. J., J. T. Crowley, B. J. Cusack, P. Pathak, J. Benach, E. London, J. C. Garcia-Monco, and J. L. Benach. 2010. Cholesterol lipids of Borrelia burgdorferi form lipid rafts and are required for the bactericidal activity of a complement-independent antibody. Cell Host. Microbe 8: 331-342.

63. van, M. G., D. R. Voelker, and G. W. Feigenson. 2008. Membrane lipids: where they are and how they behave. Nat. Rev Mol. Cell Biol. 9: 112-124.

64. Barenholz, Y., and T. E. Thompson. 1999. Sphingomyelin: biophysical aspects. Chemistry and Physics of Lipids 102: 29-34.

65. Dougherty, R. M., C. Galli, A. Ferro-Luzzi, and J. M. Iacono. 1987. Lipid and phospholipid fatty acid composition of plasma, red blood cells, and platelets and how they are affected by dietary lipids: a study of normal subjects from Italy, Finland, and the USA. Am. J. Clin. Nutr. 45: 443-455.

66. Jackson, M., G. Stadthagen, and B. Gicquel. 2007. Long-chain multiple methyl-branched fatty acid-containing lipids of Mycobacterium tuberculosis: biosynthesis, transport, regulation and biological activities. Tuberculosis. (Edinb.) 87: 78-86.

67. Maxfield, F. R., and M. G. van. 2010. Cholesterol, the central lipid of mammalian cells. Curr. Opin. Cell Biol. 22: 422-429.

68. Dean, J. M., and I. J. Lodhi. 2017. Structural and functional roles of ether lipids. Protein Cell.

69. Dougherty, R. M., C. Galli, A. Ferro-Luzzi, and J. M. Iacono. 1987. Lipid and phospholipid fatty acid composition of plasma, red blood cells, and platelets and how they are affected by dietary lipids: a study of normal subjects from Italy, Finland, and the USA. Am. J. Clin. Nutr. 45: 443-455.

70. Sharom, F. J. 2011. Flipping and flopping--lipids on the move. IUBMB. Life 63: 736-746.

71. von, H. G. 1992. Membrane protein structure prediction. Hydrophobicity analysis and the positive-inside rule. J. Mol. Biol. 225: 487-494.

72. Marat, A. L., and V. Haucke. 2016. Phosphatidylinositol 3-phosphates-at the interface between cell signalling and membrane traffic. EMBO J. 35: 561-579.

73. Pruett, S. T., A. Bushnev, K. Hagedorn, M. Adiga, C. A. Haynes, M. C. Sullards, D. C. Liotta, and A. H. Merrill, Jr. 2008. Biodiversity of sphingoid bases ("sphingosines") and related amino alcohols. J. Lipid Res. 49: 1621-1639.

74. Slotte, J. P. 2013. Molecular properties of various structurally defined sphingomyelins - correlation of structure with function. Prog. Lipid. Res. 52: 206-219.

75. Levin, I. W., T. E. Thompson, Y. Barenholz, and C. Huang. 1985. Two types of hydrocarbon chain interdigitation in sphingomyelin bilayers. Biochemistry 24: 6282-6.

76. Chiantia, S., and E. London. 2012. Acyl chain length and saturation modulate inter-leaflet coupling in asymmetric bilayers: effects on dynamics and structural order. Biophys J 103: 2311-2319.

77. Rog, T., A. Orlowski, A. Llorente, T. Skotland, T. Sylvanne, D. Kauhanen, K. Ekroos, K. Sandvig, and I. Vattulainen. 2016. Interdigitation of long-chain sphingomyelin induces coupling of membrane leaflets in a cholesterol dependent manner. Biochim. Biophys. Acta 1858: 281-288.

78. MAtsumori, N., T. Yasuda, H. Okazaki, T. Suzuki, T. Yamaguchi, H. Tsuchikawa, M. Doi, T. Oishi, and M. Murata. 2012. Comprehensive molecular motion capture for sphingomyelin by site-specific deuterium labeling. Biochemistry 51: 8363-8370.

79. Slotte, J. P., T. Yasuda, O. Engberg, M. A. Al Sazzad, V. Hautala, T. K. M. Nyholm, and M. Murata. 2017. Bilayer Interactions among Unsaturated Phospholipids, Sterols, and Ceramide. Biophys. J. 112: 1673-1681.

80. Bartke, N., and Y. A. Hannun. 2009. Bioactive sphingolipids: metabolism and function. J Lipid Res. 50 Suppl: S91-S96.

81. Jendrasiak, G. L., and R. L. Smith. 2001. The effect of the choline head group on phospholipid hydration. Chem. Phys. Lipids 113: 55-66.

82. Gulbins, E., and R. Kolesnick. 2002. Acid sphingomyelinase-derived ceramide signaling in apoptosis. Subcell. Biochem. 36: 229-244.

83. Hannun, Y. A., and C. Luberto. 2000. Ceramide in the eukaryotic stress response. Trends Cell Biol. 10: 73-80.

84. Nelson, G. J. 1967. Lipid composition of erythrocytes in various mammalian species. Biochim. Biophys. Acta 144: 221-232.

85. Lucki, N. C., and M. B. Sewer. 2012. Nuclear sphingolipid metabolism. Annu. Rev. Physiol 74: 131-151.

86. Albi, E., M. Mersel, C. Leray, M. L. Tomassoni, and M. P. Viola-Magni. 1994. Rat liver chromatin phospholipids. Lipids 29: 715-719.

87. Scassellati, C., E. Albi, D. Cmarko, C. Tiberi, J. Cmarkova, C. Bouchet-Marquis, P. J. Verschure, R. Driel, M. V. Magni, and S. Fakan. 2010. Intranuclear sphingomyelin is associated with transcriptionally active chromatin and plays a role in nuclear integrity. Biol. Cell 102: 361-375.

88. Mullen, T. D., and L. M. Obeid. 2012. Ceramide and apoptosis: exploring the enigmatic connections between sphingolipid metabolism and programmed cell death. Anticancer Agents Med. Chem. 12: 340-363.

89. Birbes, H., C. Luberto, Y. T. Hsu, B. S. El, Y. A. Hannun, and L. M. Obeid. 2005. A mitochondrial pool of sphingomyelin is involved in TNFalpha-induced Bax translocation to mitochondria. Biochem. J. 386: 445-451.

90. Lönnfors, M., J. P. Doux, J. A. Killian, T. K. Nyholm, and J. P. Slotte. 2011. Sterols Have Higher Affinity for Sphingomyelin than for Phosphatidylcholine Bilayers even at Equal Acyl-Chain Order. Biophys. J. 100: 2633-2641.

91. Ohvo-Rekila, H., B. Ramstedt, P. Leppimaki, and J. P. Slotte. 2002. Cholesterol interactions with phospholipids in membranes. Prog. Lipid Res. 41: 66-97.

92. Yeagle, P. L. 1985. Cholesterol and the cell membrane. Biochim Biophys Acta 822: 267-87.

93. Marquardt, D., F. A. Heberle, D. V. Greathouse, R. E. Koeppe, R. F. Standaert, B. J. Van Oosten, T. A. Harroun, J. J. Kinnun, J. A. Williams, S. R. Wassall, and J. Katsaras. 2016. Lipid bilayer thickness determines cholesterol's location in model membranes. Soft. Matter 12: 9417-9428.

94. Huang, J., and G. W. Feigenson. 1999. A microscopic interaction model of maximum solubility of cholesterol in lipid bilayers. Biophys. J. 76: 2142-2157.

95. Lönnfors, M., O. Langvik, A. Björkbom, and J. P. Slotte. 2013. Cholesteryl Phosphocholine - A Study on Its Interactions with Ceramides and Other Membrane Lipids. Langmuir.

96. Demel, R. A., L. L. M. v. Deenen, and B. A. Pethica. 1967. Monolayer interactions of phospholipids and cholesterol. Biochim. Biophys. Acta 135: 11-19.

97. Ipsen, J. H., O. G. Mouritsen, and M. Bloom. 1990. Relationships between lipid membrane area, hydrophobic thickness, and acyl-chain orientational order. The effects of cholesterol. Biophys J 57: 405-12.

98. Scheidt, H. A., P. Muller, A. Herrmann, and D. Huster. 2003. The potential of fluorescent and spin-labeled steroid analogs to mimic natural cholesterol. J. Biol. Chem. 278: 45563-45569.

99. Slotte, J. P., M. Jungner, C. Vilcheze, and R. Bittman. 1994. Effect of sterol side-chain structure on sterol-phosphatidylcholine interactions in monolayers and small unilamellar vesicles. Biochim Biophys Acta 1190: 435-43.

100. Scheidt, H. A., T. Meyer, J. Nikolaus, D. J. Baek, I. Haralampiev, L. Thomas, R. Bittman, P. Muller, A. Herrmann, and D. Huster. 2013. Cholesterol's aliphatic side chain modulates membrane properties. Angew. Chem. Int. Ed Engl. 52: 12848-12851.

101. Meyer, T., D. J. Baek, R. Bittman, I. Haralampiev, P. Muller, A. Herrmann, D. Huster, and H. A. Scheidt. 2014. Membrane properties of cholesterol analogs with an unbranched aliphatic side chain. Chem. Phys. Lipids 184: 1-6.

102. Sankaram, M. B., and T. E. Thompson. 1990. Modulation of phospholipid acyl chain order by cholesterol A solid state 2H MNR study. Biochemistry 29: 10676-10684 -.

103. Niu, S. L., and B. J. Litman. 2002. Determination of membrane cholesterol partition coefficient using a lipid vesicle-cyclodextrin binary system: effect of phospholipid acyl chain unsaturation and headgroup composition. Biophys. J. 83: 3408-3415.

104. Williams, J. A., C. D. Wassall, M. D. Kemple, and S. R. Wassall. 2013. An electron paramagnetic resonance method for measuring the affinity of a spin-labeled analog of cholesterol for phospholipids. J. Membr. Biol. 246: 689-696.

105. Demel, R. A., J. W. C. M. Jansen, P. W. M. van Dijck, and L. L. M. van Deenen. 1977. The preferential interaction of cholesterol with different classes of phospholipids. Biochimica et Biophysica Acta 465: 1-10.

106. Tsamaloukas, A., H. Szadkowska, and H. Heerklotz. 2006. Thermodynamic comparison of the interactions of cholesterol with unsaturated phospholipid and sphingomyelins. Biophys. J. 90: 4479-4487.

107. Stubbs, C. D., and A. D. Smith. 1984. The modification of mammalian membrane polyunsaturated fatty acid composition in relation to membrane fluidity and function. Biochim Biophys Acta 779: 89-137.

108. Huang, J., J. T. Buboltz, and G. W. Feigenson. 1999. Maximum solubility of cholesterol in phosphatidylcholine and phosphatidylethanolamine bilayers. Biochim Biophys Acta 1417: 89-100.

109. Somerharju, P., J. A. Virtanen, and K. H. Cheng. 1999. Lateral organisation of membrane lipids. The superlattice view. Biochim Biophys Acta 1440: 32-48.

110. Somerharju, P., J. A. Virtanen, K. H. Cheng, and M. Hermansson. 2009. The superlattice model of lateral organization of membranes and its implications on membrane lipid homeostasis. Biochim. Biophys. Acta 1788: 12-23.

111. Shaikh, S. R., V. Cherezov, M. Caffrey, S. P. Soni, D. LoCascio, W. Stillwell, and S. R. Wassall. 2006. Molecular organization of cholesterol in unsaturated phosphatidylethanolamines: X-ray diffraction and solid state 2H NMR reveal differences with phosphatidylcholines. J. Am. Chem. Soc. 128: 5375-5383.

112. Brzustowicz, M. R., V. Cherezov, M. Zerouga, M. Caffrey, W. Stillwell, and S. R. Wassall. 2002. Controlling membrane cholesterol content. A role for polyunsaturated (docosahexaenoate) phospholipids. Biochemistry 41: 12509-12519.

113. Ramstedt, B., and J. P. Slotte. 1999. Interaction of cholesterol with sphingomyelins and acyl-chain-matched phosphatidylcholines: a comparative study of the effect of the chain length. Biophys J 76: 908-15

114. Ohvo, H., and J. P. Slotte. 1996. Cyclodextrin-mediated removal of sterols from monolayers: effects of sterol structure and phospholipids on desorption rate. Biochemistry 35: 8018-24.

115. Mattjus, P., and J. P. Slotte. 1996. Does cholesterol discriminate between sphingomyelin and phosphatidylcholine in mixed monolayers containing both phospholipids? Chem Phys Lipids 81: 69-80.

116. Leventis, R., and J. R. Silvius. 2001. Use of cyclodextrins to monitor transbilayer movement and differential lipid affinities of cholesterol. Biophys J 81: 2257-67.

117. Halling, K. K., B. Ramstedt, J. H. Nystrom, J. P. Slotte, and T. K. Nyholm. 2008. Cholesterol interactions with fluid-phase phospholipids: effect on the lateral organization of the bilayer. Biophys. J. 95: 3861-3871.

118. Mehnert, T., K. Jacob, R. Bittman, and K. Beyer. 2006. Structure and lipid interaction of N-palmitoylsphingomyelin in bilayer membranes as revealed by 2H-NMR spectroscopy. Biophys J 90: 939-946.

119. Slotte, J. P. 2016. The importance of hydrogen bonding in sphingomyelin's membrane interactions with co-lipids. Biochim. Biophys. Acta 1858: 304-310.

120. Ramstedt, B., and J. P. Slotte. 2002. Membrane properties of sphingomyelins. FEBS Letters 531: 33-37.

121. Siminovitch, D. J., and K. R. Jeffrey. 1981. Orientational order in the choline headgroup of sphingomyelin: A 14N-NMR study. Biochim Biophys Acta 645: 270-278.

122. Rog, T., and M. Pasenkiewicz-Gierula. 2006. Cholesterol-sphingomyelin interactions: a molecular dynamics simulation study. Biophys J. 91: 3756-3767.

123. Yasuda, T., M. Kinoshita, M. Murata, and N. MAtsumori. 2014. Detailed comparison of deuterium quadrupole profiles between sphingomyelin and phosphatidylcholine bilayers. Biophys. J. 106: 631-638.

124. Huster, D., K. Arnold, and K. Gawrisch. 1998. Influence of docosahexaenoic acid and cholesterol on lateral lipid organization in phospholipid mixtures. Biochemistry 37: 17299-17308.

125. Björkbom, A., T. Rog, K. Kaszuba, M. Kurita, S. Yamaguchi, M. Lönnfors, T. K. Nyholm, I. Vattulainen, S. Katsumura, and J. P. Slotte. 2010. Effect of Sphingomyelin Headgroup Size on Molecular Properties and Interactions with Cholesterol. Biophys J 99: 3300-3308.

126. Rog, T., I. Vattulainen, M. Jansen, E. Ikonen, and M. Karttunen. 2008. Comparison of cholesterol and its direct precursors along the biosynthetic pathway: effects of cholesterol, desmosterol and 7-dehydrocholesterol on saturated and unsaturated lipid bilayers. J Chem Phys 129: 154508.

127. Beattie, M. E., S. L. Veatch, B. L. Stottrup, and S. L. Keller. 2005. Sterol Structure Determines Miscibility versus Melting Transitions in Lipid Vesicles. Biophys J. 89: 1760-1768.

128. Nystrom, J. H., M. Lönnfors, and T. K. Nyholm. 2010. Transmembrane peptides influence the affinity of sterols for phospholipid bilayers. Biophys. J 99: 526-533.

129. Jouhet, J. 2013. Importance of the hexagonal lipid phase in biological membrane organization. Front Plant Sci. 4: 494.

130. Pabst, G., N. Kucerka, M. P. Nieh, and J. Katsaras. 2014. Liposomes, Lipid Bilayers and Model membranes. CRC press, Broca Rotan, Florida.

131. Stiasny, K., and F. X. Heinz. 2004. Effect of membrane curvature-modifying lipids on membrane fusion by tick-borne encephalitis virus. J. Virol. 78: 8536-8542.

132. Chiu, M. H., and E. J. Prenner. 2011. Differential scanning calorimetry: An invaluable tool for a detailed thermodynamic characterization of macromolecules and their interactions. J. Pharm. Bioallied. Sci. 3: 39-59.

133. Yeagle, P. L. 2005. The structure of biological membranes. CRC Press LLC, Boca Raton, Florida.

134. Lewis, R. N., N. Mak, and R. N. McElhaney. 1987. A differential scanning calorimetric study of the thermotropic phase behavior of model membranes composed of phosphatidylcholines containing linear saturated fatty acyl chains. Biochemistry 26: 6118-6126.

135. Jaikishan, S., and J. P. Slotte. 2011. Effect of hydrophobic mismatch and interdigitation on sterol/sphingomyelin interaction in ternary bilayer membranes. Biochim. Biophys. Acta 1808: 1940-1945.

136. Al Sazzad, M. A., T. Yasuda, M. Murata, and J. P. Slotte. 2017. The Long-Chain Sphingoid Base of Ceramides Determines Their Propensity for Lateral Segregation. Biophys. J. 112: 976-983.

137. Huang, C., and S. Li. 1999. Calorimetric and molecular mechanics studies of the thermotropic phase behavior of membrane phospholipids. Biochim Biophys Acta 1422: 273-307.

138. Saxena, K., R. I. Duclos, P. Zimmermann, R. R. Schmidt, and G. G. Shipley. 1999. Structure and properties of totally synthetic galacto- and gluco-cerebrosides. J Lipid Res. 40: 839-849.

139. Shah, J., J. M. Atienza, R. I. Duclos, Jr., A. V. Rawlings, Z. Dong, and G. G. Shipley. 1995. Structural and thermotropic properties of synthetic C16:0 (palmitoyl) ceramide: effect of hydration. J Lipid Res. 36: 1936-1944.

140. Barton, P. G., and F. D. Gunstone. 1975. Hydrocarbon chain packing and molecular motion in phospholipid bilayers formed from unsaturated lecithins. Synthesis and properties of sixteen positional isomers of 1,2-dioctadecenoyl-sn-glycero-3-phosphorylcholine. J. Biol. Chem. 250: 4470-4476.

141. Wang, Z. Q., H. N. Lin, S. Li, and C. H. Huang. 1995. Phase transition behavior and molecular structures of monounsaturated phosphatidylcholines. Calorimetric studies and molecular mechanics simulations. J. Biol. Chem. 270: 2014-2023.

142. Wassall, S. R., M. A. McCabe, C. D. Wassall, R. O. Adlof, and S. E. Feller. 2010. Solid-state (2)H NMR and MD simulations of positional isomers of a monounsaturated phospholipid membrane: structural implications of double bond location. J. Phys. Chem. B 114: 11474-11483.

143. Niebylski, C. D., and N. Salem, Jr. 1994. A calorimetric investigation of a series of mixed-chain polyunsaturated phosphatidylcholines: effect of sn-2 chain length and degree of unsaturation. Biophys. J. 67: 2387-2393.

144. Feller, S. E. 2008. Acyl chain conformations in phospholipid bilayers: a comparative study of docosahexaenoic acid and saturated fatty acids. Chem. Phys. Lipids 153: 76-80.

145. Soubias, O., and K. Gawrisch. 2007. Docosahexaenoyl chains isomerize on the sub-nanosecond time scale. J. Am. Chem. Soc. 129: 6678-6679.

146. Mihailescu, M., O. Soubias, D. Worcester, S. H. White, and K. Gawrisch. 2011. Structure and dynamics of cholesterol-containing polyunsaturated lipid membranes studied by neutron diffraction and NMR. J. Membr. Biol. 239: 63-71.

147. Mabrey, S., and J. M. Sturtevant. 1976. Investigation of phase transitions of lipids and lipid mixtures by sensitivity differential scanning calorimetry. Proc Natl Acad Sci U S A 73: 3862-6.

148. Phillips, M. C., B. D. Ladbrooke, and D. Chapman. 1970. Molecular interactions in mixed lecithin systems. Biochim. Biophys. Acta 196: 35-44.

149. Nyholm, T. K., D. Lindroos, B. Westerlund, and J. P. Slotte. 2011. Construction of a DOPC/PSM/Cholesterol Phase Diagram Based on the Fluorescence Properties of trans-Parinaric Acid. Langmuir 27: 8339-8350.

150. Feigenson, G. W. 2009. Phase diagrams and lipid domains in multicomponent lipid bilayer mixtures. Biochim. Biophys. Acta 1788: 47-52.

151. Silvius, J. R. 2005. Partitioning of membrane molecules between raft and non-raft domains: insights from model-membrane studies. Biochim. Biophys. Acta 1746: 193-202.

152. Ipsen, J. H., G. Karlstrom, O. G. Mouritsen, H. Wennerstrom, and M. J. Zuckermann. 1987. Phase equilibria in the phosphatidylcholine-cholesterol system. Biochim Biophys Acta 905: 162-72.

153. Quinn, P. J., and C. Wolf. 2009. The liquid-ordered phase in membranes. Biochim. Biophys. Acta 1788: 33-46.

154. Mannock, D. A., R. N. Lewis, T. P. McMullen, and R. N. McElhaney. 2010. The effect of variations in phospholipid and sterol structure on the nature of lipid-sterol interactions in lipid bilayer model membranes. Chem. Phys. Lipids 163: 403-448.

155. McMullen, T. P., R. N. Lewis, and R. N. McElhaney. 1993. Differential scanning calorimetric study of the effect of cholesterol on the thermotropic phase behavior of a homologous series of linear saturated phosphatidylcholines. Biochemistry 32: 516-22.

156. Nyholm, T. K. M., M. Nylund, and J. P. Slotte. 2003. A calorimetric study of binary mixtures of dihydrosphingomyelin and sterols, sphingomyelin, or phosphatidylcholine. Biophysical Journal 84: 3138-3146.

157. Marsh, D. 2010. Liquid-ordered phases induced by cholesterol: a compendium of binary phase diagrams. Biochim. Biophys. Acta 1798: 688-699.

158. Davis, J. H., J. J. Clair, and J. Juhasz. 2009. Phase equilibria in DOPC/DPPC-d62/cholesterol mixtures. Biophys. J. 96: 521-539.

159. Sankaram, M. B., and T. E. Thompson. 1991. Cholesterol-induced fluid-phase immiscibility in membranes. Proc. Natl. Acad. Sci. U. S. A 88: 8686-8690.

160. Collado, M. I., F. M. Goni, A. Alonso, and D. Marsh. 2005. Domain formation in sphingomyelin/cholesterol mixed membranes studied by spin-label electron spin resonance spectroscopy. Biochemistry 44: 4911-4918.

161. Marsh, D. 2009. Cholesterol-induced fluid membrane domains: a compendium of lipid-raft ternary phase diagrams. Biochim. Biophys. Acta 1788: 2114-2123.

162. Veatch, S. L., and S. L. Keller. 2005. Seeing spots: Complex phase behavior in simple membranes. Biochim Biophys Acta.

163. Konyakhina, T. M., J. Wu, J. D. Mastroianni, F. A. Heberle, and G. W. Feigenson. 2013. Phase diagram of a 4-component lipid mixture: DSPC/DOPC/POPC/chol. Biochim. Biophys. Acta 1828: 2204-2214.

164. Konyakhina, T. M., and G. W. Feigenson. 2016. Phase diagram of a polyunsaturated lipid mixture: Brain sphingomyelin/1-stearoyl-2-docosahexaenoyl-sn-glycero-3-phosphocholine/cholestero l. Biochim. Biophys. Acta 1858: 153-161.

165. Zhao, J., J. Wu, F. A. Heberle, T. T. Mills, P. Klawitter, G. Huang, G. Costanza, and G. W. Feigenson. 2007. Phase studies of model biomembranes: complex behavior of DSPC/DOPC/cholesterol. Biochim. Biophys. Acta 1768: 2764-2776.

166. Loura, L. M., R. F. de Almeida, L. C. Silva, and M. Prieto. 2009. FRET analysis of domain formation and properties in complex membrane systems. Biochim. Biophys. Acta 1788: 209-224.

167. Yasuda, T., H. Tsuchikawa, M. Murata, and N. Matsumori. 2015. Deuterium NMR of raft model membranes reveals domain-specific order profiles and compositional distribution. Biophys. J. 108: 2502-2506.

168. Petruzielo, R. S., F. A. Heberle, P. Drazba, J. Katsaras, and G. W. Feigenson. 2013. Phase behavior and domain size in sphingomyelin-containing lipid bilayers. Biochim. Biophys. Acta 1828: 1302-1313.

169. Chiang, Y. W., J. Zhao, J. Wu, Y. Shimoyama, J. H. Freed, and G. W. Feigenson. 2005. New method for determining tie-lines in coexisting membrane phases using spin-label ESR. Biochim. Biophys. Acta 1668: 99-105.

170. Farkas, E. R., and W. W. Webb. 2010. Precise and millidegree stable temperature control for fluorescence imaging: application to phase transitions in lipid membranes. Rev. Sci. Instrum. 81: 093704.

171. Veatch, S. L., I. V. Polozov, K. Gawrisch, and S. L. Keller. 2004. Liquid domains in vesicles investigated by NMR and fluorescence microscopy. Biophys. J. 86: 2910-2922.

172. Bezlyepkina, N., R. S. Gracia, P. Shchelokovskyy, R. Lipowsky, and R. Dimova. 2013. Phase diagram and tie-line determination for the ternary mixture DOPC/eSM/cholesterol. Biophys. J. 104: 1456-1464.

173. Kinnun, J. J., R. Bittman, S. R. Shaikh, and S. R. Wassall. 2018. DHA Modifies the Size and Composition of Raftlike Domains: A Solid-State (2)H NMR Study. Biophys. J. 114: 380-391.

174. Reyes Mateo, C., A. Ulises Acuna, and J. C. Brochon. 1995. Liquid-crystalline phases of cholesterol/lipid bilayers as revealed by the fluorescence of trans-parinaric acid. Biophys J 68: 978-87.

175. de Almeida, R. F., A. Fedorov, and M. Prieto. 2003. Sphingomyelin/phosphatidylcholine/cholesterol phase diagram: boundaries and composition of lipid rafts. Biophys J 85: 2406-2416.

176. Molugu, T. R., S. Lee, and M. F. Brown. 2017. Concepts and Methods of Solid-State NMR Spectroscopy Applied to Biomembranes. Chem. Rev. 117: 12087-12132.

177. El, K. K., S. Morandat, and Y. F. Dufrene. 2010. Nanoscale analysis of supported lipid bilayers using atomic force microscopy. Biochim. Biophys. Acta 1798: 750-765.

178. Kim, H. M., H. J. Choo, S. Y. Jung, Y. G. Ko, W. H. Park, S. J. Jeon, C. H. Kim, T. Joo, and B. R. Cho. 2007. A two-photon fluorescent probe for lipid raft imaging: C-laurdan. Chembiochem. 8: 553-559.

179. Kullberg, A., O. O. Ekholm, and J. P. Slotte. 2015. Miscibility of Sphingomyelins and Phosphatidylcholines in Unsaturated Phosphatidylcholine Bilayers. Biophys. J. 109: 1907-1916.

180. Feigenson, G. W., and J. T. Buboltz. 2001. Ternary phase diagram of dipalmitoyl-pc/dilauroyl-pc/cholesterol: nanoscopic domain formation driven by cholesterol. Biophys J 80: 2775-88.

181. Filippov, A., G. Oradd, and G. Lindblom. 2003. The effect of cholesterol on the lateral diffusion of phospholipids in oriented bilayers. Biophys. J. 84: 3079-3086.

182. Usery, R. D., T. A. Enoki, S. P. Wickramasinghe, M. D. Weiner, W. C. Tsai, M. B. Kim, S. Wang, T. L. Torng, D. G. Ackerman, F. A. Heberle, J. Katsaras, and G. W. Feigenson. 2017. Line Tension Controls Liquid-Disordered + Liquid-Ordered Domain Size Transition in Lipid Bilayers. Biophys. J. 112: 1431-1443.

183. Veatch, S. L., S. S. Leung, R. E. Hancock, and J. L. Thewalt. 2007. Fluorescent probes alter miscibility phase boundaries in ternary vesicles. J. Phys. Chem. B 111: 502-504.

184. Kreutzberger, M. A., E. Tejada, Y. Wang, and P. F. Almeida. 2015. GUVs melt like LUVs: the large heat capacity of MLVs is not due to large size or small curvature. Biophys. J. 108: 2619-2622.

185. Pokorny, A., L. E. Yandek, A. I. Elegbede, A. Hinderliter, and P. F. Almeida. 2006. Temperature and composition dependence of the interaction of delta-lysin with ternary mixtures of sphingomyelin/cholesterol/POPC. Biophys J. 91: 2184-2197.

186. Mason, J. T., A. V. Broccoli, and C. Huang. 1981. A method for the synthesis of isomerically pure saturated mixed-chain phosphatidylcholines. Anal Biochem 113: 96-101.

187. Fischer, R. T., F. A. Stephenson, A. Shafiee, and F. Schroeder. 1984. delta 5,7,9(11)-Cholestatrien-3 beta-ol: a fluorescent cholesterol analogue. Chem. Phys. Lipids 36: 1-14.

188. Kuklev, D. V., and W. L. Smith. 2004. Synthesis of four isomers of parinaric acid. Chem Phys Lipids 131: 215-222.

189. Björkqvist, Y. J., J. Brewer, L. A. Bagatolli, J. P. Slotte, and B. Westerlund. 2009. Thermotropic behavior and lateral distribution of very long chain sphingolipids. Biochim. Biophys. Acta 1788: 1310-1320.

190. Huang, C., and J. T. Mason. 1986. Structure and properties of mixed-chain phospholipid assemblies. Biochim Biophys Acta 864: 423-470.

191. Lakowicz, J. R. 1999. Principles of Fluorescence Spectroscopy. Kluwer Academic / Plenum Publishers, New York.

192. Davis, J. H. 1983. The description of membrane lipid conformation, order and dynamics by 2H-NMR. Biochim. Biophys. Acta 737: 117-171.

193. McCabe, M. A., and S. R. Wassail. 1997. Rapid deconvolution of NMR powder spectra by weighted fast Fourier transformation. Solid State Nuclear Magnetic Resonance 10: 53-61.

194. Gault, C. R., L. M. Obeid, and Y. A. Hannun. 2010. An overview of sphingolipid metabolism: from synthesis to breakdown. Adv. Exp. Med. Biol. 688: 1-23.

195. Westerlund, B., and J. P. Slotte. 2009. How the molecular features of glycosphingolipids affect domain formation in fluid membranes. Biochim. Biophys. Acta 1788: 194-201.

196. Castro, B. M., M. Prieto, and L. C. Silva. 2014. Ceramide: a simple sphingolipid with unique biophysical properties. Prog. Lipid Res. 54: 53-67.

197. Hsueh, Y. W., R. Giles, N. Kitson, and J. Thewalt. 2002. The effect of ceramide on phosphatidylcholine membranes: a deuterium NMR study. Biophys. J. 82: 3089-3095.

198. Silva, L. C., R. F. de Almeida, B. M. Castro, A. Fedorov, and M. J. Prieto. 2006. Ceramide-domain formation and collapse in lipid rafts: membrane reorganization by an apoptotic lipid. Biophys J. 92: 502-516.

199. Silva, L., R. F. de Almeida, A. Fedorov, A. P. Matos, and M. Prieto. 2006. Ceramide-platform formation and -induced biophysical changes in a fluid phospholipid membrane. Mol. Membr. Biol. 23: 137-148.

200. Welti, R., and D. F. Silbert. 1982. Partition of parinaroyl phospholipid probes between solid and fluid phosphatidylcholine phases. Biochemistry 21: 5685-5689.

201. Björkqvist, Y. J., S. Nybond, T. K. Nyholm, J. P. Slotte, and B. Ramstedt. 2008. N-palmitoyl-sulfatide participates in lateral domain formation in complex lipid bilayers. Biochim Biophys Acta 1778: 954-962.

202. Castro, B. M., R. F. de Almeida, L. C. Silva, A. Fedorov, and M. Prieto. 2007. Formation of ceramide/sphingomyelin gel domains in the presence of an unsaturated phospholipid. A quantitative multiprobe approach. Biophys J.

203. London, E., and G. W. Feigenson. 1981. Fluorescence quenching in model membranes. 1. Characterization of quenching caused by a spin-labeled phospholipid. Biochemistry 20: 1932-1938.

204. Yeagle, P. L., A. D. Albert, K. Boesze-Battaglia, J. Young, and J. Frye. 1990. Cholesterol dynamics in membranes. Biophys J 57: 413-24.

205. Rog, T., M. Pasenkiewicz-Gierula, I. Vattulainen, and M. Karttunen. 2009. Ordering effects of cholesterol and its analogues. Biochim. Biophys. Acta 1788: 97-121.

206. Baumgart, T., G. Hunt, E. R. Farkas, W. W. Webb, and G. W. Feigenson. 2007. Fluorescence probe partitioning between Lo/Ld phases in lipid membranes. Biochim. Biophys. Acta 1768: 2182-2194.

207. Bunge, A., P. Muller, M. Stockl, A. Herrmann, and D. Huster. 2008. Characterization of the ternary mixture of sphingomyelin, POPC, and cholesterol: support for an inhomogeneous lipid distribution at high temperatures. Biophys J. 94: 2680-2690.

208. Stillwell, W., and S. R. Wassall. 2003. Docosahexaenoic acid: membrane properties of a unique fatty acid. Chem. Phys. Lipids 126: 1-27.

209. Sklar, L. A., B. S. Hudson, and R. D. Simoni. 1977. Conjugated polyene fatty acids as fluorescent probes: synthetic phospholipid membrane studies. Biochemistry 16: 819-828.

210. Wassall, S. R., and W. Stillwell. 2009. Polyunsaturated fatty acid-cholesterol interactions: domain formation in membranes. Biochim. Biophys. Acta 1788: 24-32.

211. Shaikh, S. R., J. J. Kinnun, X. Leng, J. A. Williams, and S. R. Wassall. 2015. How polyunsaturated fatty acids modify molecular organization in membranes: insight from NMR studies of model systems. Biochim. Biophys. Acta 1848: 211-219.

212. Williams, J. A., S. E. Batten, M. Harris, B. D. Rockett, S. R. Shaikh, W. Stillwell, and S. R. Wassall. 2012. Docosahexaenoic and eicosapentaenoic acids segregate differently between raft and nonraft domains. Biophys J 103: 228-237.

213. Bartels, T., R. S. Lankalapalli, R. Bittman, K. Beyer, and M. F. Brown. 2008. Raftlike mixtures of sphingomyelin and cholesterol investigated by solid-state 2H NMR spectroscopy. J. Am. Chem. Soc. 130: 14521-14532.

214. Loura, L. M., A. Fedorov, and M. Prieto. 2000. Partition of membrane probes in a gel/fluid two-component lipid system: a fluorescence resonance energy transfer study. Biochim. Biophys Acta 1467: 101-112.

215. Klausner, R. D., and D. E. Wolf. 1980. Selectivity of fluorescent lipid analogues for lipid domains. Biochemistry 19: 6199-6203.

216. Pinto, S. N., F. Fernandes, A. Fedorov, A. H. Futerman, L. C. Silva, and M. Prieto. 2013. A combined fluorescence spectroscopy, confocal and 2-photon microscopy approach to re-evaluate the properties of sphingolipid domains. Biochim. Biophys. Acta 1828: 2099-2110.

217. Yasuda, T., N. MAtsumori, H. Tsuchikawa, M. Lönnfors, T. K. Nyholm, J. P. Slotte, and M. Murata. 2015. Formation of Gel-like Nanodomains in Cholesterol-Containing Sphingomyelin or Phosphatidylcholine Binary Membrane As Examined by Fluorescence Lifetimes and ^{2}H NMR Spectra. Langmuir 31: 13783-13792.

218. Huster, D., P. Muller, K. Arnold, and A. Herrmann. 2001. Dynamics of membrane penetration of the fluorescent 7-nitrobenz-2-oxa-1,3-diazol-4-yl (NBD) group attached to an acyl chain of phosphatidylcholine. Biophys. J. 80: 822-831.

219. Mesquita, R. M., E. Melo, T. E. Thompson, and W. L. Vaz. 2000. Partitioning of amphiphiles between coexisting ordered and disordered phases in two-phase lipid bilayer membranes. Biophys. J. 78: 3019-3025.

220. Sklar, L. A., G. P. Miljanich, and E. A. Dratz. 1979. Phospholipid lateral phase separation and the partition of cis-parinaric acid and trans-parinaric acid among aqueous, solid lipid, and fluid lipid phases. Biochemistry 18: 1707-1716.

221. Pinto, S. N., L. C. Silva, A. H. Futerman, and M. Prieto. 2011. Effect of ceramide structure on membrane biophysical properties: the role of acyl chain length and unsaturation. Biochim. Biophys. Acta 1808: 2753-2760.

222. Bergelson, L. D., J. G. Molotkovsky, and Y. M. Manevich. 1985. Lipid-specific fluorescent probes in studies of biological membranes. Chem. Phys. Lipids 37: 165-195.

223. Ramirez, D. M., W. W. Ogilvie, and L. J. Johnston. 2010. NBD-cholesterol probes to track cholesterol distribution in model membranes. Biochim. Biophys. Acta 1798: 558-568.

224. Loura, L. M., A. Fedorov, and M. Prieto. 2001. Exclusion of a cholesterol analog from the cholesterol-rich phase in model membranes. Biochim. Biophys Acta 1511: 236-243.

225. Milles, S., T. Meyer, H. A. Scheidt, R. Schwarzer, L. Thomas, M. Marek, L. Szente, R. Bittman, A. Herrmann, P. T. Gunther, D. Huster, and P. Muller. 2013. Organization of fluorescent cholesterol analogs in lipid bilayers - lessons from cyclodextrin extraction. Biochim. Biophys. Acta 1828: 1822-1828.

226. Heinemann, F., V. Betaneli, F. A. Thomas, and P. Schwille. 2012. Quantifying lipid diffusion by fluorescence correlation spectroscopy: a critical treatise. Langmuir 28: 13395-13404.

227. Heberle, F. A., and G. W. Feigenson. 2011. Phase separation in lipid membranes. Cold Spring Harb. Perspect. Biol.

228. Heerklotz, H., and A. Tsamaloukas. 2006. Gradual change or phase transition: characterizing fluid lipid-cholesterol membranes on the basis of thermal volume changes. Biophys. J. 91: 600-607.

229. Ionova, I. V., V. A. Livshits, and D. Marsh. 2012. Phase diagram of ternary cholesterol/palmitoylsphingomyelin/palmitoyloleoyl-phosphatidylcholine mixtures: spin-label EPR study of lipid-raft formation. Biophys. J 102: 1856-1865.

230. Pare, C., and M. Lafleur. 1998. Polymorphism of POPE/cholesterol system: a 2H nuclear magnetic resonance and infrared spectroscopic investigation. Biophys J 74: 899-909.

231. Bakht, O., P. Pathak, and E. London. 2007. Effect of the structure of lipids favoring disordered domain formation on the stability of cholesterol-containing ordered domains (lipid rafts): identification of multiple raft-stabilization mechanisms. Biophys. J. 93: 4307-4318.

232. McMullen, T. P., and R. N. McElhaney. 1997. Differential scanning calorimetric studies of the interaction of cholesterol with distearoyl and dielaidoyl molecular species of phosphatidylcholine, phosphatidylethanolamine, and phosphatidylserine. Biochemistry 36: 4979-86.

233. Maulik, P. R., and G. G. Shipley. 1996. N-palmitoyl sphingomyelin bilayers: structure and interactions with cholesterol and dipalmitoylphosphatidylcholine. Biochemistry 35: 8025-34.

234. Björkqvist, Y. J., T. K. Nyholm, J. P. Slotte, and B. Ramstedt. 2005. Domain formation and stability in complex lipid bilayers as reported by cholestatrienol. Biophys. J. 88: 4054-4063.

235. Sergelius, C., S. Yamaguchi, T. Yamamoto, O. Engberg, S. Katsumura, and J. P. Slotte. 2012. Cholesterol's interactions with serine phospholipids - A comparison of N-palmitoyl ceramide phosphoserine with dipalmitoyl phosphatidylserine. Biochim. Biophys. Acta 1828: 785-791

236. Jaikishan, S., A. Björkbom, and J. P. Slotte. 2010. Phosphatidyl alcohols: effect of head group size on domain forming properties and interactions with sterols. Biochim. Biophys. Acta 1798: 1615-1622.

237. Almeida, P. F. 2009. Thermodynamics of lipid interactions in complex bilayers. Biochim. Biophys. Acta 1788: 72-85.

238. Lopez, C. A., A. H. de Vries, and S. J. Marrink. 2013. Computational microscopy of cyclodextrin mediated cholesterol extraction from lipid model membranes. Sci. Rep. 3: 2071.

239. Davis, J. H., J. J. Clair, and J. Juhasz. 2009. Phase equilibria in DOPC/DPPC-d62/cholesterol mixtures. Biophys. J. 96: 521-539.

240. Marsan, M. P., I. Muller, C. Ramos, F. Rodriguez, E. J. Dufourc, J. Czaplicki, and A. Milon. 1999. Cholesterol orientation and dynamics in dimyristoylphosphatidylcholine bilayers: a solid state deuterium NMR analysis. Biophys. J. 76: 351-359.

241. Wang, C., Y. Yu, and S. L. Regen. 2017. Lipid Raft Formation: Key Role of Polyunsaturated Phospholipids. Angew. Chem. Int. Ed Engl. 56: 1639-1642.

242. Georgieva, R., C. Chachaty, R. Hazarosova, C. Tessier, P. Nuss, A. Momchilova, and G. Staneva. 2015. Docosahexaenoic acid promotes micron scale liquid-ordered domains. A comparison study of docosahexaenoic versus oleic acid containing phosphatidylcholine in raft-like mixtures. Biochim. Biophys. Acta 1848: 1424-1435.

243. Gerl, M. J., J. L. Sampaio, S. Urban, L. Kalvodova, J. M. Verbavatz, B. Binnington, D. Lindemann, C. A. Lingwood, A. Shevchenko, C. Schroeder, and K. Simons. 2012. Quantitative analysis of the lipidomes of the influenza virus envelope and MDCK cell apical membrane. J. Cell Biol. 196: 213-221.

244. Ahmed, S. N., D. A. Brown, and E. London. 1997. On the origin of sphingolipid/cholesterol-rich detergent-insoluble cell membranes: physiological concentrations of cholesterol and sphingolipid induce formation of a detergent-insoluble, liquid-ordered lipid phase in model membranes. Biochemistry 36: 10944-53.

245. Heberle, F. A., R. S. Petruzielo, J. Pan, P. Drazba, N. Kucerka, R. F. Standaert, G. W. Feigenson, and J. Katsaras. 2013. Bilayer thickness mismatch controls domain size in model membranes. J. Am. Chem. Soc. 135: 6853-6859.

246. Krause, M. R., T. A. Daly, P. F. Almeida, and S. L. Regen. 2014. Push-pull mechanism for lipid raft formation. Langmuir 30: 3285-3289.

247. Wang, C., M. R. Krause, and S. L. Regen. 2015. Push and pull forces in lipid raft formation: the push can be as important as the pull. J. Am. Chem. Soc. 137: 664-666.

248. Levental, K. R., J. H. Lorent, X. Lin, A. D. Skinkle, M. A. Surma, E. A. Stockenbojer, A. A. Gorfe, and I. Levental. 2016. Polyunsaturated Lipids Regulate Membrane Domain Stability by Tuning Membrane Order. Biophys. J. 110: 1800-1810.

249. Garcia-Saez, A. J., S. Chiantia, and P. Schwille. 2007. Effect of line tension on the lateral organization of lipid membranes. J. Biol. Chem. 282: 33537-33544.

250. Bleecker, J. V., P. A. Cox, and S. L. Keller. 2016. Mixing Temperatures of Bilayers Not Simply Related to Thickness Differences between Lo and Ld Phases. Biophys. J. 110: 2305-2308.

251. Levental, I., and S. L. Veatch. 2016. The Continuing Mystery of Lipid Rafts. J. Mol. Biol. 428: 4749-4764.

252. Sklar, L. A., B. S. Hudson, M. Petersen, and J. Diamond. 1977. Conjugated polyene fatty acids on fluorescent probes: spectroscopic characterization. Biochemistry 16: 813-819.

253. Marquardt, D., B. Geier, and G. Pabst. 2015. Asymmetric lipid membranes: towards more realistic model systems. Membranes. (Basel) 5: 180-196.

254. Steck, T. L., and Y. Lange. 2012. How slow is the transbilayer diffusion (flip-flop) of cholesterol? Biophys. J 102: 945-946.

255. Op den Kamp, J. A. 1979. Lipid asymmetry in membranes. Annu Rev Biochem 48: 47-71.

256. Cheng, H. T., and E. London. 2011. Preparation and properties of asymmetric large unilamellar vesicles: interleaflet coupling in asymmetric vesicles is dependent on temperature but not curvature. Biophys. J 100: 2671-2678.

257. Kiessling, V., C. Wan, and L. K. Tamm. 2009. Domain coupling in asymmetric lipid bilayers. Biochim. Biophys. Acta 1788: 64-71.

258. Polley, A., S. Vemparala, and M. Rao. 2012. Atomistic simulations of a multicomponent asymmetric lipid bilayer. J. Phys. Chem. B 116: 13403-13410.

259. Eicher, B., D. Marquardt, F. A. Heberle, I. Letofsky-Papst, G. N. Rechberger, M. S. Appavou, J. Katsaras, and G. Pabst. 2018. Intrinsic Curvature-Mediated Transbilayer Coupling in Asymmetric Lipid Vesicles. Biophys. J. 114: 146-157.

260. Lin, Q., and E. London. 2015. Ordered raft domains induced by outer leaflet sphingomyelin in cholesterol-rich asymmetric vesicles. Biophys. J. 108: 2212-2222.

261. Heberle, F. A., D. Marquardt, M. Doktorova, B. Geier, R. F. Standaert, P. Heftberger, B. Kollmitzer, J. D. Nickels, R. A. Dick, G. W. Feigenson, J. Katsaras, E. London, and G. Pabst. 2016. Subnanometer Structure of an Asymmetric Model Membrane: Interleaflet Coupling Influences Domain Properties. Langmuir 32: 5195-5200.

262. Lin, Q., and E. London. 2014. Preparation of artificial plasma membrane mimicking vesicles with lipid asymmetry. PLoS. One. 9: e87903.

263. Tulodziecka, K., B. B. Diaz-Rohrer, M. M. Farley, R. B. Chan, P. G. Di, K. R. Levental, M. N. Waxham, and I. Levental. 2016. Remodeling of the postsynaptic plasma membrane during neural development. Mol. Biol. Cell 27: 3480-3489.